ANALYSIS OF THE STRUCTURE OF WNTLESS PROTEIN AND ITS ROLE IN SUPPORTING WNT SECRETION AT THE ENDOPLASMIC RETICULUM COMPARTMENT

by

JIAXIN SUN

A Dissertation submitted to the
Graduate School-Newark
Rutgers, The State University of New Jersey
In partial fulfillment of the requirements
For the degree of
Doctor of Philosophy
Graduate Program in Biological Sciences
Written under the direction of
Advisor: Nan Gao
Co-advisor: Edward Bonder
And approved by

Newark, New Jersey

October 2017

©[2017]

JIAXIN SUN

ALL RIGHTS RESERVED

ABSTRACT OF THE DISSERTATION

ANALYSIS OF THE STRUCTURE OF WNTLESS PROTEIN AND ITS ROLE IN SUPPORTING WNT SECRETION AT THE ENDOPLASMIC RETICULUM

By JIAXIN SUN

Dissertation Director: Nan Gao, Ph.D.

Dissertation Co-Advisor: Edward M.Bonder, Ph.D.

Wnts are secreted glycolipoproteins fundamental for embryonic development and adult tissue homeostasis. Abnormal Wnt signal transduction is associated with human diseases, most notably colon cancers. Wnts act as extracellular ligands that bind specific surface receptors in Wnt-responding cells. In contrast to our comprehensive understanding of Wnt signal transduction in the ligand-responding cells, there is still a deficiency in the knowledge about the cellular mechanism that regulates Wnt secretion from the ligand-producing cells. A multi-pass transmembrane protein Wntless (Wls) binds and transports Wnt ligands for secretion, however the mechanism underlying the initial assembly of Wnt secretory vesicles has not been defined. Using proteomic and mutagenic analysis in mammalian cells and primary mouse intestinal organoids, we have delineated a sophisticated regulatory mechanism that controls the initial assembly of Wnt secretory vesicles at ER membrane. Binding of lipidated Wnt ligands to Wls in ER promotes an association between Wls and SEC12, an ER membrane-localized guanine nucleotide-exchanging factor (GEF) that activates the small GTPase SAR1. Compared with Wnt molecules that lack lipid modification, mature ligands drive a stronger Wls-SEC12 interaction that was biochemically mapped to cytosolic segments of both proteins. Remarkably, Wls utilizes a well conserved but separate protein motif in its C-terminus to engage with SAR1 for assembly of COPII ER-exiting vesicles. Mutating Wls at responsible amino acids or disrupting SAR1 activity accumulated Wls at ER exiting sites. Unlike the wild type Wls, mutant transporter failed to facilitate Wnt secretion and to support stem cell maintenance in mouse intestinal organoids.

Additional study suggests that GOLD domain-containing proteins may participate in subsequent transport of Wls/Wnt complex through COPII vesicles. Specifically, TMED10 binds Wnts and may act as a cargo adaptor to incorporate Wnt/Wls complex into the COPII vesicles. ACBD3, another GOLD domain containing protein, may contribute to selectively transport WNT7A for ER-to Golgi delivery. Our results suggest that Wnt exocytosis is carefully corroborated, at several distinct protein complex interfaces, from early steps of secretory pathway. These regulations may ensure effective export of mature and functional ligands. Due to the relatively simplified regulators, e.g., Wls, that control Wnt production, the molecular mechanism uncovered for Wnt secretion regulation may be useful to intervening Wnt production and signaling activity in certain cancers.

ACKNOWLEDGEMENTS

I would like to express my gratitude to Dr. Nan Gao, my thesis advisor, who has been a tremendous mentor for me. He always encouraged me to work hard in a smart way and allowed me to become an independent researcher. I want to thank him for supporting me in attending several conferences that broadened my scientific vision and helped me develop my technical and intellectual skills.

My sincere thanks also go to my co-advisor, Dr. Edward M. Bonder, for participating in every step of my scientific career- starting from establishing “neuron” for doing research to easing all the administrative hassles. He taught me that asking the right question is key to solve a scientific problem and helped me learn how to think critically. His passion and for basic Science greatly inspired me.

I would also like to thank my committee members- Dr. Wilma Friedman, Dr. Patrice Maurel, Dr. Radek Dobrowoski and Dr. Ronaldo P. Ferraris for being approachable and patient with me. They played a great role in making my doctoral journey an enjoyable one and helped me throughout with their useful suggestions. Thanks to Dr. Alexis Rodriguez, for providing scientific feedback and occasionally being an arbitrator for some of those heated discussions during lab meetings. I really appreciated his humorous scientific comments and the idea of “RE-search” that encouraged me to never give up.

Additionally, I want to thank all other (former and present) faculty and staff members of the Cell Molecular Biology community at Rutgers-Newark. Dr. Haesun Kim, who took me in as a rotation student and Dr. Greg Weber who gave me a lot of practical advice for both research and career development. Special thanks to Dr. Robert DeLotto and Dr. Yvonne DeLotto for their friendly support when I was new to the Department. Thanks to Dr. Morrison and Dr. Cervantes who taught me how to teach undergraduate students, and Dr. Nadim who shared his ideas in Critical Thinking with me. It would be remis of me not to thank our Department officers- Shandell, Neermala, Sheronda and Maty, who always helped with administrative work.

Most importantly, thanks to all former and present members of Life Science Center. Ryo taught me the first experiment I ran in LSC; my lovely colleagues in Gao Lab, Richard, Qiang, Luca, Soumya, Xiao, Juan, Iyshwarya, Sheila and Ivor for their cooperation and constant support; Chaitali, Rucha, Shalaka, Kavya, Jhiyun, Hyosung, Ming, Juan, Laura, Lissette, Justin, Brian, Huri and Subhashini for being the wonderful people they are; the talented Masters and undergraduate students- Catherine Capac, Timothy Daudelin, Michelle Aligbe, Conrad R.Trojanowski, for all their help in my project.

Last but not the least, I would like to thank my family, my parents and my brother for their continuous love and support.

TABLE OF CONTENT

ABSTRACT OF THE DISSERTATION..ii

ACKNOWLEDGEMENTS...iv

TABLE OF CONTENT vi

LIST OF ABBREVIATIONS...xi

LIST OF ILLUSTRATION xiii

LIST OF TABLE...xvi

CHAPTER 1 1

BACKGROUND AND INTRODUCTION..1

1.1 Overview of the intracellular compartment.....................................2

1.2 Introduction to protein sorting and traffic.......................................3

1.3 Introduction to the vesicle 6

1.4 Introduction to vesicle sorting 8

1.5 Introduction to the Wnt signaling 11

1.6 WNT secretion in development, homeostasis and diseases.......18

1.7 Significance of understanding the molecular regulation of Wls-mediated Wnt delivery...22

CHAPTER 2 .... **27**

MATERIALS AND METHODS **27**

Mouse and Cell lines **28**

Retroviral production and establishment of stable cell lines **29**

Plasmids and siRNA **30**

Antibodies **32**

Confocal live cell imaging **34**

Wnt3a-Gluc secretion assay **34**

OptiPrep density gradient centrifugation and cellular fractionation **35**

Organoid culture and retroviral infection **36**

Quantifications and statistical analysis **37**

CHAPTER 3 .... **39**

WLS TRAFFICS THROUGH COPII COMPLEX TO ENTER SECRETORY PATHWAY **39**

3.1 Introduction **40**

3.1.1 Porcupine-mediated lipidation of Wnts 40

3.1.2 Wls is a unique transmembrane protein specifically transporting Wnt for secretion 42

3.1.3 The kinetics of Sar1 GTPase activity is critical to maintain the regular function of COPII vesicles 45

3.2 Results 46

3.2.1 Proteomic analysis uncovers the involvement of COPII machinery in Wls traffic...46

3.2.2 Export of Wls into COPII vesicle depends on SAR1 activity 48

3.2.3 Recruitment of SAR1 by SEC12 promotes Wls association with COPII complex 50

3.2.4 Wls-SEC12 interaction is mediated by specific motifs: Wls$^{377-431}$ and SEC12$^{301-388}$ 52

3.2.5 Wls-SEC12 complex is critical for Wnt secretion 55

3.3 Discussion 56

3.3.1 Wls transports Wnt in a GTPase dependent manner....................56

3.3.2 Wls transporter carries Wnt ligands initially from the ER 57

3.3.3 Speculation on how Sec12 reaches the ER exit sites 58

CHAPTER 4 96

MULTI-PROTEIN COMPLEX MODULATES ER EXIT OF WNT-WLS FOR SECRETION...96

4.1 Introduction 97

4.1.1 Sar1 GTPase activity is crucial for the assembly and fission of COPII vesicles 97

4.1.2 P24 family proteins are potential regulators of Wnt secretion at ER..98

4.1.3 Additional factors might regulate the ER export of Wnt-Wls via modulating Wls-Sec12 complex 99

4.2 Results 100

4.2.1 Wls-SAR1 association is dependent on the structural integrity of Wls carboxyl terminus 100

4.2.2 The proline-serine motif (494-495) is critical for Wls's Exit from the ER..101

4.2.3 The hexapeptide and proline 494 are critical for Wls-SAR1 interaction 103

4.2.4 The Gold-domain containing protein TMED10 facilitates Wnt secretion..104

4.2.5 Wnt-Wls interaction within ER lumen is independent of the COPII vesicles assembly 105

4.2.6 WNT7A and ACBD3 are in the same protein complex................106

4.2.7 Wls-SEC12 complex responds to mature Wnt binding to Wls in the ER..106

4.3 Discussion 108

4.3.1 The hexapeptide of Wls may contribute to Sar1 activation 108
4.3.2 A potential role of GOLD-domain containing proteins in supporting Wnt secretion...110
4.3.3 A ready-to-go Wls-Sec12 complex on ER membrane supports Wnt secretion...112
CHAPTER 5 149
DISCUSSION AND FUTURE PROSPETCTUS 149
5.1 A sophisticated mechanism controlling the entry of Wnt ligands into the early secretory pathway 150
5.2 Potential regulation on size of Wnt/Wls-containing COPII vesicle 152
5.3 Potential strategies to modulate Wnt secretion for cancer therapy 153
5.4 The hypothetical contribution of TMED10 and ACBD3 to WNT7A secretion 154
5.5 The potential application and pitfall in utilizing the *ex vivo* organoid culture 156
5.6 Conclusion...159
References 168

LIST OF ABBREVIATIONS

ACBD	Acyl-CoA Binding Domain
AP	Adaptor Proteins
APC	Product of the adenomatous polyposis coli gene
CCV	Clathrin-Coated Vesicles
CGN	*Cis*-Golgi Network
CL	Cytosolic Loop
COPI	Coat Protein complex I
COPII	Coat Protein complex II
CRD	Cysteine-rich Domain
DSH	Drosophila Dishevelled
EGFP	Enhanced Green Fluorescence Protein
EE	Early Endosome
ER	Endoplasmic Reticulum
ERGIC	ER to Golgi intermediate compartment
FBS	Fetal Bovine Serum
GAP	GTPase-activiting protein
GDP	Guanosine Diphosphate
GEF	Guanine nucleotide Exchange Factor
GOLD	Golgi Dynamics
GOLGI	Golgi Apparatus
GPCR	G protein-coupled receptor
GSK-3β	Glycogen synthase kinase-3β
GTP	Guanosine Triphosphate
HA	Hemagglutinin antigen
HEK	Human Embryonic Kidney
LEF	Lymphoid enhancer-binding factor
LL	Luminal Loop
LE	Late Endosome
LRP	Low-density lipoprotein receproe-related protein
M6P	Mannose 6-phosphate
MEF	Mouse Embryonic Fibroblast
MVB	Multivesicle bodies
p24	Protein 24
SDS	Sodium dodecyl sulfate
SDS-PAGE	Sodium dodecyl sulfate-polyacrylamide gel electrophoresis
SEC	Secretory protein

siRNA	Small interfering RNA
SNARE	Soluble NAF Attachment Protein Receptor
SNX	Sorting nexin
SRFP	Solubile Frizzled-related proteins
TCF	T-cell factor
TGN	*Trans*-Golgi Network
TM	Transmembrane
TMED	Transmembrane emp24 domain-containing protein
VAPA	Vesicle-associated protein A
VPS	Vacuolar protein sorting-associated protein
WBD	Wnt-binding domain
βGC	β-Glucocerebrosidase

LIST OF ILLUSTRATIONS

Figure **Page**

1.1 Overview of the intracellular compartment ………………………… 23

1.2 The dynamic of Sar1 GT Pase activities is crucial for the initiation, assembly and fission of COPII vesicles …………………………. 25

3.1 Current understanding in the molecular regulation of Wnt secretion. 62

3.2 Wls is associated with COPII components……………………………. 64

3.3 Sar1 GTPase activities is essential for Wls-Sar1 association………. 67

3.4 Inhibition of SAR1 activities impairs Wls's vesicular traffic …………. 69

3.5 Inhibition of SAR1 activities leads to Wls aggregation near the SEC16-positive ER exit site …………………………………….... 71

3.6 SAR1^{T39N} interferes the secretion of Wnt 3a and Shh secretion…..... 73

3.7 Two hypothetical models about the recruitment of SEC12 and SAR1 onto the ER membrane via associating with Wls ……………………..75

3.8 Recruitment of SAR1 by SEC12 promotes the association of Wls with the COPII complex……………………………………………..77

3.9 Wls interacts with SEC12 endogenously…………………………….... 79

3.10 Wls-SEC12 interaction is mediated by specific domain: Wls$^{377-431}$ ... 81

3.11 Wls-SEC12 interaction is mediated by specific domain:

SEC12$^{301-388}$ ………………………………………………………... 83

3.12 Truncated Wls$^{1-431}$ and Wls$^{1-376}$ do not show vesicular pattern….. 86

3.13 SEC12 modulates Wnt secretion…………………………………… 88

3.14 SEC12 modulates Wls's subcellular distribution………………….. 90

3.15 Wls$^{1-376}$, lacking the defined SEC12-binding domain, fails to support WNT secretion……………………………………………… 92

4.1 Sequence alignment of Wntless across multiple animal species…. 114

4.2 The hexapeptide of Wls are critical for ER exit of Wls………………116

4.3 Lacking the hexapeptide prevents Wls trafficking to membrane ….119

4.4 The proline 494 and serine 495 of Wls are critical for Wls's vesicular distribution……………………………………………………………121

4.5 Wls^{P494A} did not affect the vesicular traffic of Wls wild type ………..123

4.6 Wls^{P494A}, a vesicle-deficient mutant, loses association with COPII vesicle componens, but remains interaction to WNT3A and SEC12 ……………………………………………………………………. 125

4.7 Mutation on the proline 494 accumulates Wls within ER …………..127

4.8 The hexapeptide and proline 494 is critical for Wls-SAR1 interaction ……………………………………………………….. 129

4.9 TMED10 modulates WNT3A secretion…………………………….... 131

4.10 TMED10 did not affect the Wnt3a-Wls interaction ……………….. 133

4.11 WNT3A^{S209A}, a lipid-deficient mutant, is less associated with TMED10……………………………………………………………… 135

4.12 The association of TMED10 and ACBD3 is triggered by the over-expression of WNT7A ligand………………………………..… 137

4.13 Overexpressing WNT3A-V5 increases SEC12 association with Wls ……………………………………………………………………… 139

4.14 Overexpressing WNT3A-V5 did not increases SEC12 association with Wls$^{\Delta WBD}$……………………………………………………………141

4.15 Addition of C59 in cell culture reverses the Wnt-triggered Wls-Sec12 association……………………………………………………………..143

4.16 Addition of C59 in cell culture causes an ER accumulation of wild type Wls ………………………………………………………….145

4.17 Wnt3a^{S209A} induces less Wls-SEC12 association.……………….. 147

5.1 A schematic diagram illustrating COPII-dependent ER export of Wls-Wnt ………………………………………………………………160

5.2 Organoids were infected by lentivirus expression mCherry-Wls ..162

5.3 The hexapeptide-regulated Wls's ER export is essential for Wnt secretion and intestinal stem cell maintenance in organoid culture ………………………………………………………………164

5.4 Survived Organoids were validated by EdU labeling ……………166

LIST OF TABLES

Page

Table 3.1 Proteomic identification of protein targets in wild type Wls and Wls$^{1-491}$ immunoprecipitates ……………………………… 61

Table 3.2 Primers for protein recombination ……………………………..… 94

CHAPTER 1

BACKGROUND AND INTRODUCTION

1.1 Overview of the intracellular compartment

Each cell is surrounded by a membrane, which protects the inside of a cell from its surrounding environment (Singleton, 1999). Most of the prokaryotic cells contain only one plasma membrane, where different cellular processes occur, e.g., DNA replication or respiration (Alberts, 2002). In the advanced prokaryotes cells, certain patches of the plasma membrane was known and identified by its specific functions (Alberts, 2002). For example, the specific lipid monolayer is formed within the plasma membrane in some Archaea to allow the Archaea living in the boiling water (Lewalter and Muller, 2006). The specialized functions is more advanced and differentiated by various membrane-bound intracellular compartments in eukaryotic cells. For example, DNA replication occurs in the nucleus and respiration is mainly in mitochondria in eukaryote (Alberts, 2002).

Materials were shuttled outward or inward within the cells through different intracellular compartments for their own needs **(Figure 1.1)**. In the exocytic pathway (outward flows), Endoplasmic Reticulum (ER) is the site where synthesis of all secreted proteins and resident proteins for other subcellular compartments occurs (Segev, 2009). Then the nascent proteins are trans-located into the Golgi apparatus. The Golgi apparatus is the major sorting compartment of the cells as the protein destined for secretion is sorted to the plasma membrane

(Wu, 2012); resident proteins for endosomes or lysosomes are transported to their destined compartment (Nolan and Sly, 1987); and the escaped ER resident proteins are caught within the Golgi and delivered back to the ER (Segev, 2009; Yamamoto et al., 2001). In the endocytic pathway (inward flows), proteins are internalized with a portion of plasma membrane and intracellular delivered via early and late endosomes to lysosome for degradation. Since the lysosome is also the major degradation site for cellular proteins, they can get into lysosome directly from the cytoplasm as well (Ghosh et al., 2003; Wang and Klionsky, 2003). Lastly, multivesicular bodies (MVBs), also referred as late endosomes, are known to fuse with the plasma membrane for secreting macromolecules (Dreyer and Baur, 2016; Stoorvogel et al., 2002). Although the unique contribution of different subcellular compartments in the eukaryotic cells help in better pursuing cell functions, this advanced compartmentalization creates a new problem that communication between the different cellular compartments is required. To our knowledge, the major communication between the subcellular compartments in the cells is achieved by vesicular transport, which will be discussed in the later section.

1.2 Introduction to protein sorting and traffic

During the past decades, there has been developing and innovative understanding of the mechanisms that underlie intracellular protein sorting and vesicular traffic along the exocytic pathway. We now know that the newly synthesized proteins in the endoplasmic reticulum (ER) need to go through an elaborate quality control process (Hurtley and Helenius, 1989), which ensures that only the properly folded proteins and correctly assembled protein complexes exit from the ER (Benedetti et al., 2000; Hampton, 2000). In contrast, ER resident proteins are normally retained in ER. Even though some ER resident proteins happen to escape from ER (Andres et al., 1990; Yamamoto et al., 2001), they can be captured and retrieved by receptors in the *cis*-Golgi network, a stack of Golgi apparatus as a collection of fused and flattened membrane-enclosed disks (Day et al., 2013). In addition, there is a distinct ER to Golgi intermediate compartment (ERGIC) with specific morphology and biochemical features (Schweizer et al., 1988). In mammalian cells, cargoes are transported from ER to ERGIC via the COPII vesicles (refers as the specific coat protein complex II) (Hammond and Glick, 2000); while cargoes are delivered from ERGIC to *cis*-Golgi network via COPI vesicles (Bonifacino and Glick, 2004). In 1980s, it was hypothesized that cargo exiting from ER is not selective and follows the so-called “bulk-flow” process (Fine, 1989; Renkin, 1980). However, growing evidences in recent years suggest that proteins are carefully selected for ER export via a specific recognition of cargoes by their adaptors, receptors, or even the COPII coat protein components themselves (Barlowe and Helenius, 2016).

Along the exocytic pathway, especially in Golgi apparatus, cargo can be modified in transit by glycosylation (Kelleher and Gilmore, 2006), phosphorylation (Capasso et al., 1985), sulfation (Capasso and Hirschberg, 1984). Starting from the *trans*-Golgi (TGN, the final cisternal structure of Golgi apparatus), the newly modified proteins are selectively packaged into different cargo containers - secretory granules (Arvan and Castle, 1998; Tooze, 1998), apical or basolateral cognate constitutive secretory vesicles (Kroschewski et al., 1999; Okamoto et al., 2002) or clathrin-coated vesicles (CCV, as discussed in next section) for transporting cargoes to lysosome (Ni et al., 2006). Soring proteins into secretory granules or vesicles is considered to occur by aggregation or by sorting signals from protein itself. The current view of the lysosomal sorting pathway is mainly established by understanding a typical mannose 6-phosphate (M6P)-modified acid hydrolase and the non-M6P-modified β-glucocerebrosidase (βGC) (Braulke and Bonifacino, 2009). Lysosomal hydrolases are always marked with one of the members belonging to M6P group and captured by the trans-membrane M6P receptor proteins, waiting in the TGN. Then M6P receptor, together with adaptor proteins, facilitate the assembly of CCVs that later bud from the TGN. The CCVs deliver their contents, mostly lysosomal proteins, to lysosome for maintaining the normal lysosome function (Ni et al., 2006). Most of the molecules are transported in a form of vesicles between the subcellular compartments. Attention has been drawn to understand how the traffic is regulated and how signals are transduced from one cellular compartment to the other.

1.3 Introduction to the vesicle

Most molecules, due to the size or their different characters, are difficult to pass directly through the intracellular membranes. Alternatively, those molecules are loaded into the membrane-wrapped container, termed vesicle. Vesicles are assembled mostly on the ER, the Golgi apparatus, and the plasma membrane. Once properly formed, the entire vesicle pinches off from the membrane, travels with their contents to the intracellular or intercellular destinations and then merges with the other membrane to release their cargoes. In such a way, proteins or other large molecules are allowed to transport through the membrane without directly crossing it.

Most of the transport vesicles form with the help of cytosolic coat proteins. Typical coat proteins can either bind to each other, associate with membrane of a specific compartment or directly interact with cargoes. Clathrin-coated vesicle (CCV), COPII and COPI (referred to as the specific coat protein complex I and II) vesicle are the three types of well-characterized coated vesicles involving in different intracellular trafficking routes.

Clathrin plays a major role in forming the coated vesicles that serve at the late secretory pathway (Bao et al., 2005; Hao et al., 1999) and the endocytic pathway (Carpentier et al., 1982; Neutra et al., 1985). Three clathrin heavy chains and three light chains form a triskelion-shape structure; and the triskelias interact with each other to form a polyhedral lattice later surrounded the vesicle (Kirchhausen and Harrison, 1981). The Clathrin-associated adaptor proteins (AP), the major adaptors contributing to the CCV formation, connect the clathrin lattice and the lipid or protein components of the membrane (Bao et al., 2005; Beck et al., 1992; Dell'Angelica et al., 1998; Dell'Angelica et al., 1999; Traub et al., 1995).

COPII-coated vesicles transport proteins from the ER **(Figure 1.2)**. The typical COPII vesicle consists of the inner coat proteins/adaptors SEC23/24 (SEC refers as secretory protein), outer coat protein SEC13/31 (Aridor et al., 1998). The assembly of COPII vesicle involves p24 protein, another group of adaptors (Blum et al., 1999; Rojo et al., 2000). p24 protein group is a family of small integral membrane proteins weighted approximately 24 kDa, which is primarily found in the ER membrane (Carney and Bowen, 2004; Strating and Martens, 2009). COPI-coated vesicles shuttle proteins back to the ER from the Golgi. The adaptor and the cage complexes of COPI vesicle are associated as a single heptametrical complex (Cosson and Letourneur, 1997). Despite having the specificities in travel destination and different structural components, the above vesicles are assembled following a similar molecular mechanism. In the beginning, activation of a co-recruitment GTPase initiates the vesicle formation. SAR1 is the typical small GTPase for COPII vesicles (Sato and Nakano, 2005). ARF small GTPases are for COPI vesicle (Rein et al., 2002) and clathrin vesicle from the Golgi (Puertollano et al., 2001). These GTPases expose an N-terminal amphipathic helix inserted onto the outer leaflet of the membrane for anchoring (Lee et al., 2005). Then the adaptors and cage complex are further recruited. Alternatively, a specific GTPase is not required for the initiation of Clathrin-coated vesicle for endocytosis but the phosphatidylinositol phosphates (PIPs) is essential for the recruitment of AP2 complex (Gaidarov et al., 1996). After the budding complex is properly formed, the vesicle scission at the neck of the bud is induced by either the hydrolysis of the GTPase stimulated by the coat proteins or through the recruitment of coat protein itself (Beck et al., 2011; Bielli et al., 2005; Lee et al., 2005). Thus, the geometrical arrangement of GTPase/adaptor/coat complex on the surface of membrane helps in cargo collection, vesicle assembly and membrane scission.

1.4 Introduction to vesicle sorting

During the last decade, information gained from the study of ER or Golgi transport *in vitro* and from studying various traffic-defective mutants has uncovered that vesicular transport at different steps along the exocytic pathway shares common features (Barlowe and Helenius, 2016). Most vesicles have coats, of which there are several types as we have discussed in the prior section. Assembly of the protein coats is believed to be the first steps for initiating the vesicle budding. The latter triggers further assembly of elaborate membrane and cytosolic protein complexes (Antonny and Schekman, 2001). These cytosolic protein complexes are usually unique for specific vesicle population, facilitating the budding, fission, and docking of vesicles (Bi et al., 2007; Sohn et al., 1996; Stamnes et al., 1995). Of notes, the cell uses an extensive network of Rab GTPases (belong to Ras GTPase superfamily for cellular signal transduction) and SNARE proteins to organize and regulate the vesicle travel (Colicelli, 2004).

Rab GTPase was name for Ras-like proteins from rat brain (Touchot et al., 1987). They have been numbered according to their sequences obtained. Eventually, 11 Rab members were discovered in yeast and over 60 identified as mammalian homologues (Colicelli, 2004). Numerous researches have linked specific Rab GTPase to the endocytic traffic of molecules from one cellular compartment to the other.

The majority of Rab1 located at the ERGIC and a portion of Rab1 protein has also been found at ER exit site (Sannerud et al., 2006). The proposed role of Rab1 is to mediate the ER-Golgi trafficking (Batoko et al., 2000; Pind et al., 1994). Rab2, located at the ERGIC, might also be regulating the retrograde traffic from Golgi to ER (Cheung et al., 2002; Dong and Wu, 2007; Tisdale and Balch, 1996). The Golgi-localized Rab6, Rab33 and Rab40 play their roles in helping intra-Golgi trafficking (Amaya et al., 2016; Martinez et al., 1994; White et al., 1999). Rab33 and Rab24 work together to regulate the formation of autophagosomes (Egami et al., 2005; Yla-Anttila et al., 2015). Rab8 contributes the trafficking the secretory granules and the constitutive secretory vesicles from the *trans*-Golgi network

(TGN) (Ang et al., 2003; Huber et al., 1993; Juarez et al., 2000; Sato et al., 2007). Rab8, together with Rab10 and Rab14, also participates in GLUT4 vesicle translocation (Patrussi and Baldari, 2016) and helps in ciliogenesis with Rab17 and Rab23 (Patrussi and Baldari, 2016). Rab3, Rab26, Rab27 and Rab37 work as a group or individual in mediating various types of regulated exocytic events (Bustos et al., 2012; Ljubicic et al., 2013; Schluter et al., 2002; Tian et al., 2010). When Rab32 alone controls the mitochondrial fission (Li et al., 2016; Wang et al., 2012), Rab32, when partnered with Rab38, regulates the biogenesis of melanosomes (Bultema et al., 2014; Park et al., 2007). Rab18 carefully regulates the formation of lipid droplets (Martin et al., 2005). Rab22 shuttles proteins between TGN and early endosomes (Johnson et al., 2017; Kauppi et al., 2002; Maldonado-Baez and Donaldson, 2013).

As the typical action of GTPase, Rabs switch between two conformations, a GDP (guanosine diphosphate)-bound inactive form and a GTP (guanosine triphosphate) -bound active form. A guanine nucleotide exchange factor (GEF) regulates the GTP loading and activation of Rab proteins. Rab protein‘s inherent GTP hydrolysis activity is triggered by the GTPase-activating protein (GAP), resulting in Rab inactivation. The downstream effectors of Rab small GTPases only bind to the active Rab; recruitment of these effectors facilitates Rab functions. For example, active form of certain Rab GTPases recruit the effectors such as the group of tethering factors named Soluble NAF Attachment Protein receptor

(SNARE) and facilitate downstream membrane traffic events (Stenbeck, 1998).

SNARE protein family consists at least 24 members in yeast and more than 60 members in mammal (Burri and Lithgow, 2004). SNARE proteins mostly involve in the membrane fusion during exocytosis. In most of the case, pairs of integral vesicle and target membrane proteins (v-SNARES and t-SNARES), with further specific sub-family members assigned to different stations, assure the docking to the appropriate membrane receptor. This is the fusion of vesicles with their target membrane bond compartments.

1.5 Introduction to the Wnt signaling

The protein structure and posttranslational modifications of Wnt

Wnt (originally known as Wingless-Type MMTV Integration Site Family Member) proteins belong to a family of secreted lipid-modified glycoproteins (Nusse et al., 1984). As extracellular growth factors, Wnts transduce signals from Wnt-producing cells to Wnt-receiving cells by binding to its cell surface receptor Frizzled (a separate group of ten G-protein couple receptors categorized as the receptor of Wnt family) (Nusse and Varmus, 1992). The lipid modification, mainly palmitoylation, involves the covalent attachment of the palmitoleic acid on the highly conserved serine residue (Komekado et al., 2007; Kurayoshi et al., 2007). The palmitoylation of Wnt5a is essential to its binding to the Frizzled receptor and the initiation of downstream pathway, but not to Wnt5a secretion. Only the glycosylated Wnt5a proteins are secreted out from the producing cells (Kurayoshi et al., 2007). In the case of Wnt3a, both glycosylation and palmitoylation are required for the secretion of Wnt3a (Komekado et al., 2007). Moreover, the lipid modification renders the hydrophobic Wnt ligands, which need to be chaperoned by the plasma membrane-bound heparin sulphate proteoglycans (Fuerer et al., 2010); otherwise lipid-modified Wnt would form cluster *in vitro* (Takada et al., 2006; Willert et al., 2003).

Canonical versus non-canonical Wnt signaling

Wnt signaling is activated by one of the 19 Wnt ligands bind to the extracellular cysteine-rich domain (CRD) of Frizzled receptors (Nusse et al., 1991). Then Frizzled receptor binds to LRP 5/6 (low-density lipoprotein receptor-related protein 5/6) (Williams and Insogna, 2009) for canonical pathway or Tyrosine-protein kinase trans-membrane receptor (ROR) for non-canonical pathway (Li et al., 2008). Both Frizzled-LRP5/6 and Frizzled-ROR complexes pass their own biological signals to the Dishevelled protein (Dsh, first discovered in flies) via the regulatory process on the intracellular PDZ (Psd-95/dics large/ZO1)-binding domain of Frizzled receptor (MacDonald et al., 2009). Of note, Dsh, a family of cytoplasmic phosphoprotein acting downstream of Frizzled receptor, involve in both canonical and non-canonical Wnt signaling pathways

(Penton et al., 2002). In the canonical Wnt pathway, upon the activation of Dsh, the conventional destruction complex composed of AXIN (originally discovers as the protein product of the mouse gene called Fused) (Reed, 1937), Protein Phosphatase 2A (the PPP2CA gene encoding protein in human) (Jones et al., 1993), Adenomatosis Polyposis Coli (APC, also known as deleted in polyposis 2.5) (Nishisho et al., 1991), Glycogen Synthase Kinase 3 (GSK3, first reported in June 1980 as a regulatory kinase for Glycogen synthase) (Hemmings and Cohen, 1983) is recruited to plasma membrane. The translocation of destruction complex prevents β-catenin (CTNNB1 encoded protein, first known as a component of a mammalian cell adhesion complex) (McCrea et al., 1991) from a continuous ubiquitination for degradation (Peifer et al., 1991). Thus, β-catenin accumulates in the cytoplasm and eventually trans-locates into the nucleus, where it serves as a transcriptional activator of T-cell factor/lymphoid enhancer-binding factor (TCF/LEF) proteins (Kim et al., 2013). TCF/LEF proteins, members of the high mobility group (HMG) box family, act as transcription factors to drive expression of Wnt target genes (Molenaar et al., 1996).

Beside the β-catenin dependent canonical Wnt pathway, there are two well-understood β-catenin independent pathways, known as the planar cell polarity (PCP) pathway and the Wnt/Ca^{2+} pathway. Both of these two non-canonical pathways inhibit the canonical Wnt pathway. The PCP pathway is activated via the binding of Wnt ligands (typically Wnt 5a, 5b and 11a) to Frizzled and its specific co-receptor ROR1/2 (Gordon and Nusse, 2006). Then the Frizzled-ROR receptor complex recruits Dsh to form a larger complex with Dishevelled-associated activator of morphogenesis 1 or 2 (DAAM 1/2) (Sato et al., 2006). Later Daam proteins can activate the small G-protein Rho GTPase through the guanine exchange factor, and hence Rho-associated kinase (ROCK) is activated for the regulation of cytoskeleton (Habas et al., 2001). On the other hand, Dsh can also associate with Rac1 GTPase or c-Jun N-terminal kinase (JNK), which together regulate cell motility and tissue polarity, so-called Planer Cell Polarity pathway (Lapebie et al., 2011). The Wnt-Ca^{2+} pathway is a classical G-protein-coupled signaling pathway (Kuhl et al., 2000a). The Phospholipase C-beta (PLC-beta) is activated by the Frizzled-Wnt interaction on the plasma membrane (Shojaie and Ghaffari, 2016) and cleaves phosphatidylinositol 4,5-bisphosphate (PIP2) into 1,2-diacylglycerol (DAG) and inositol 1,4,5-triphosphate (IP3) (Han et al., 2001). IP3 diffuses throughout the cytosol and interacts with the calcium channels on the ER membrane, and hence the calcium ions are released from the ER in order to control the intracellular calcium level (Niu et al., 2012). Calcium ions along with calmodulin (ubiquitously expressed eukaryotic protein) activate calcium calmodulin-dependent protein kinase II (CaMKII) and lead to downstream activation of TGF-beta-activated kinase 1 (TAK1), Nemo-like kinase (NLK) and Calcineurin phosphatase (Ishitani et al., 2003). The above regulator together dephosphorylates and activates the

Nuclear Factor Associated with T cells (NFAT) (Gregory et al., 2010; Zhang et al., 2015), which serves as the transcription factor to initiate the transcription of Wnt/Ca^{2+} pathway target genes, such as interleukin 4 (referred as IL4, cytokine in adaptive immunity) (Winslow et al., 2006). Those genes responding to Wnt/Ca^{2+} pathway are known in regulating cell fate and cell migration.

Based on the biological signaling induced, Wnt ligands are previously subdivided into two classes, the canonical and noncanonical Wnts, and the classification holds the same for Frizzled receptors (Kuhl et al., 2000b). For example, the Wnt isoforms 1, 3a or 8 usually activate the β-catenin dependent canonical pathway (Chong et al., 2007; Si et al., 2006; Wikramanayake et al., 2004), whereas Wnt 5a or 11 are considered to trigger noncanonical Wnt canonical Wnt signaling (Cheng et al., 2008; Hardy et al., 2008). However, the above-mentioned classification has been challenged by several recent finding that the canonical Wnt ligands can activate the noncanonical Wnt signaling incorporating with appropriate Frizzled receptors and vice versa. The “Canonical” Wnt3a molecule can induce the Wnt/JNK pathway in human bone marrow stromal (mesenchymal) stem cells (Qiu et al., 2011) and the “noncanonical” Wnt5a modulates the Wnt/β-catenin signaling during embryonic development (van Amerongen et al., 2012). Wnt7a-Fzd5 couples to Wnt/β-catenin signaling and increases proliferation. Conversely, Wnt7a-Fzd10 complex is shown to induce a β-catenin independent pathway (Carmon and Loose, 2008). On the other hand, the concentrations of Wnt ligands are considered to regulate signaling controversially. For example, high concentration of Wnt3a blocks T-cell development at the early stage *in vitro*; an intermediate level of Wnt3a can accelerate the development of T cell (Famili et al., 2015). These data suggest the differences in the affinities of Wnt ligands and Frizzled receptors and their local concentrations can branch Wnt down-stream signaling. However, the above findings also indicate the challenging questions: How does Wnt molecule arrive at the plasma membrane to interact with a particular Frizzled receptor? And how is the specificity achieved?

Short and long range Wnt signaling

Wnt is a family of secreted ligands produced by a defined set of cells so-called Wnt-producing cells and forms a concentration gradient by spreading through the tissue (Logan and Nusse, 2004). Wnt-receiving cells responding in a ligand-specific concentration-dependent manner as discussed above are usually found in the vicinity of the Wnt-producing cells (Wang et al., 2014). Signaling activation in Wnt-receiving cells close to the Wnt-producing cells are called “short-range transduction”, whereas the signaling activated at a longer distances from the source of Wnt production are considered as “long-range transduction” (Bartscherer and Boutros, 2008). Therefore, the gradient formation of the extracellular Wnt molecules is a critical feature in the Wnt signaling transduction

(Port and Basler, 2010). However, how Wnt extracellular gradients are formed is not yet well understood. The collected experimental evidences regarding Wnt secretion highlight the specialized machinery for the intracellular transport of Wnt molecules, rather than a passive flow of them through the secretory pathway. Remarkably, almost all secreted Wnt detected in the extracellular space are highly hydrophobic due to the lipid-modification by the acyl-transferase Porcupine (PORCN in human, an ER resident enzyme for Wnt lipidation) (Tanaka et al., 2000). Then an evolutionary conserved multi pass transmembrane transporter called Wntless/Evenness interrupted/Sprinter interacts with lipid modified Wnts and delivers them to the plasma membrane (Banziger et al., 2006; Bartscherer et al., 2006; Goodman et al., 2006). Because of the hydrophobicity of Wnt molecules, they are strongly insoluble and retain on the plasma membrane upon secretion. These membrane-associated Wnts are considered to facilitate the “short-range transduction” (Pfeiffer et al., 2002). Taken together, the above observations suggest that the free Wnt diffusion is unlikely the major player in the formation of gradient concentration. On the other hand, the extracellular microvesicles so-called exosomes that have endosomal origin are gaining recognition for their roles in the “long-range transduction” of Wnt signaling (Gross et al., 2012; Stoorvogel et al., 2002), most probably since Wnts can be less hydrophobic if their lipid chains are imbedded into exosome membrane (Dreyer and Baur, 2016).

1.6 WNT secretion in embryonic development, tissue homeostasis and diseases

WNT secretion in embryonic development

Loss-of-function of Evi in *Drosophila* showed embryonic defects, which phenocopied the Wnt-depletion (Banziger et al., 2006). Global knockout of Wls in mice results in a disruption of axial patterning, which leads to embryonic lethality (Fu et al., 2009). Germ cell-specific Wls knockout mice shows abnormal spermatogenesis in an age-dependent manner, as there are elevated ROS levels and increased apoptosis in Wls-deficient germ cell (Chen et al., 2016).

During early embryonic development, Wls is detected at the isthmic organizer (ISO) in brain, mainly mediating the Wnt1 secretion (Fu et al., 2011). ISO tissue-specific deletion of Wls leads to the loss of the cerebellar structure (Carpenter et al., 2010; Fu et al., 2011), which phenocopied Wnt1 null abnormalities in the mid brain (McMahon and Bradley, 1990; Thomas and Capecchi, 1990). In the later stage of cerebellar development, Wls is primarily found in the cells in the interior face of the rhombic lip (iRL) (Yeung et al., 2014), which implicated in the orchestration of cerebellar development (Yeung and Goldowitz, 2017). Wls is also found in the epidermis in mice and contributes to the embryonic hair follicle (HF) induction (Huang et al., 2012), postnatal HF morphogenesis (Huang et al., 2015) and adult HF growth and regeneration in skin tissue (Myung et al., 2013). Wls plays an important role in limb bud development. Loss of the mesenchymal Wls disrupts the differentiation of distal mesenchyma and prevents the limb outgrowth, most likely due to the indispensible role of Wls in secreting the non-canonical Wnt5a (Zhu et al., 2012).

WNT secretion in supporting various tissue morphology

Mutations in the human PORCN gene have been reported in patients suffering from focal dermal hypoplasia (FDH, Goltz syndrome), a rare genetic disease disorder (Fernandes et al., 2010; Grzeschik et al., 2007; Wang et al., 2007). Mouse with ectoderm-specific depletion of Porcn recapitulates FDH phenotypes that showed the abnormalities in the skin, teeth, skeleton and digestive system (Barrott et al., 2011).

The typical mouse model to assess the function of endogenous Wnt secretion in craniofacial tissue is the $Ocn^{Cre/+}; Wls^{fl/fl}$ mouse, which deletes Wls in osteoblasts, odontoblasts, ameloblasts, and cementoblasts (Lim et al., 2014a; Lim et al., 2014b; Lim et al., 2014c). The deficiency of Wls in Ocn-expressing cells lead to a dramatic loss in cementum (Yin et al., 2015) and the specific reduction in alveolar bone volume and density (Lim et al., 2014b; Lim et al., 2014c). Above results suggested that Wls-mediated Wnt secretion is required to maintain cementum volume. As the acellular cementum presumably represents the mineralized part of the periodontal ligament closest to the tooth surface (Yin et al., 2015), does the periodontal ligaments cells require Wnt secretion? In fact, the adult periodontal ligament is the Wnt-responsive tissue as Wnt secretion is critical to support the homeostasis of mineralized tissues of the craniofacial complex (Lim et al., 2014a). When Wnt secretion is restricted in the cells in osteoblasts, odontoblasts, ameloblasts, and cementoblasts, the periodontal ligament space is pathologically widened in the $Ocn^{Cre/+}; Wls^{fl/fl}$ mouse (Lim et al., 2014b). These data suggested the importance of Wnt secretion in maintaining the morphology of periodontal ligament.

A number of Wnts, including Wnt2a, Wnt4, Wnt5a and Wnt7b, are detected during the development of pancreas (Heller et al., 2002). When only Wnt5a mutant shows some defects in islet formation, however, none of the aforementioned Wnt-isoform mutants present a loss-of-function phenotype in pancreas (Kim et al., 2005). These results hint the possibility of the complexity and the overlapping Wnt-isoforms in supporting the homeostasis of pancreas. Mice with a conditional deletion of the Wls in pancreatic precursor cells exhibit extreme pancreatic hypoplasia (Carpenter et al., 2010).

WNT secretion in maintaining gut homeostasis

The renewal stem cell compartment, sitting at the bottom of the crypt, either gives rise to the committed progenitor cells that proliferate rapidly or produces the diverse differentiated progeny that migrate up the villi, being shed into the lumen eventually. This continuous self-renewal of epithelial cells partially underscores gut homeostasis. Wnt signaling supports gut homeostasis by regulating proliferation in the crypt. In a screening of RNA expression for Wnt ligands, Wnt3, Wnt6 and Wnt9b are detected in crypt epithelial cells, when Wnt2b, Wnt4, Wnt5a and Wnt5b are in differentiated epithelial and mesenchymal cells of the small intestine and colon (Gregorieff et al., 2005). The role of Paneth cells, a specific cell population producing Wnt3 ligands in the crypt base, have been later confirmed in supporting intestinal stem cell homeostasis as ablation of Paneth cell in organoids, an epithelial-only *ex vivo* system, results in the death of the organoids (Sato et al., 2011). In addition, genetic ablation of Porcn enzyme (Kabiri et al., 2014), Wls transporter (Valenta et al., 2016) or Vps35 retromer protein (de Groot et al., 2013) that is essential for the secretory activity of all vertebrate Wnts results in the disassembly of intestine organoids. These results demonstrate the role of intestinal epithelial Wnts in supporting the survival of organoids in the ex vivo culture system. The addition of recombinant Wnt2b in the culture medium, a specific Wnt isoform secreted from mesenchymal cells, can restore the growth of intestinal organoids derived from Wls-deficient mouse (Valenta et al., 2016). Unexpectedly, mice lacking epithelial Wnt activity, however, exhibit normal intestinal proliferation, differentiation or recovery from radiation injury, indicating that the epithelial Wnts are not vital for these processes. On the other hand, full inhibition of PORCN activity in both epithelium and stroma of the intestine by high-dose C59 treatment blocks proliferation and increases sensitivity to radiation stress in the intestine (Kabiri et al., 2014). Taken together, stromal Wnts do play a crucial role in the maintenance of small intestine homeostasis *in vivo*.

1.7 Significance of understanding the molecular regulation of Wls-mediated Wnt delivery

Wnts are a group of secreted growth factors that facilitated signaling in regulating embryonic development and adult tissue homeostasis (Herr et al., 2012). Mis-regulating Wnts and their downstream signaling cascades are observed in various human diseases (Clevers and Nusse, 2012), and inhibiting Wnt secretion level can reverse abnormal tumor cell growth (Voloshanenko et al., 2013). The secretion of Wnt proteins requires Porcupine (Kadowaki et al., 1996; van den Heuvel et al., 1993) and Evenness interrupted/Wntless/G protein-coupled receptor 177 (Banziger et al., 2006; Bartscherer et al., 2006; Fu et al., 2009) in various species. Wls, the conserved Wnt transporter, has been shown its indispensable role for Wnt secretion in *C.Elegans* (Bartscherer et al., 2006), *Drosophila* (Banziger et al., 2006), mouse and human cells (Fu et al., 2009; Yu et al., 2010). Understanding the molecular regulation of Wnt secretion with respect to the unique transporter Wls is a major interest in generating therapeutics targeting aberrant Wnt signaling.

Figure 1.1

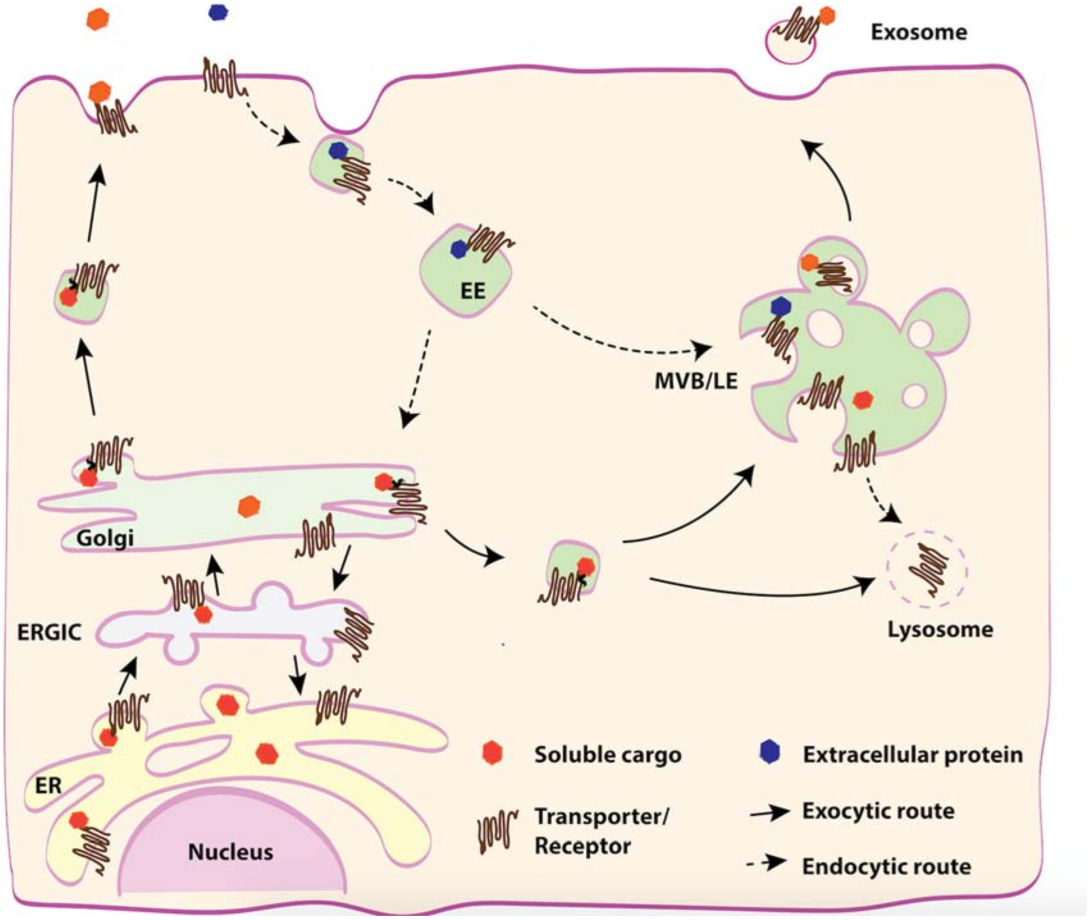
Exosome
EE
MVB/LE
Golgi
ERGIC
ER
Nucleus
Lysosome
Soluble cargo
Extracellular protein
Transporter/
Receptor
Exocytic route
Endocytic route

Figure 1.1 Overview of the intracellular compartment

In the exocytic pathway (solid arrows), trans-membrane transporter carries nascent soluble cargos from the ER and shuttles them between ER, ERGIC and Golgi compartments. Cargos are selected into secretory vesicles and delivered to the plasma membrane for secretion; other resident proteins for subcellular compartment, e.g. late endosome (LE) and lysosome, are packaged into different vesicles for their unique destination. In the endocytic pathway (dotted arrows), extracellular proteins are recognized by their trans membrane receptors and are internalized to early endosome (EE) through endocytosis. Certain secretory proteins are delivered to multivesicle body (MVB) and packaged into exosome for long distance delivery.

Figure 1.2

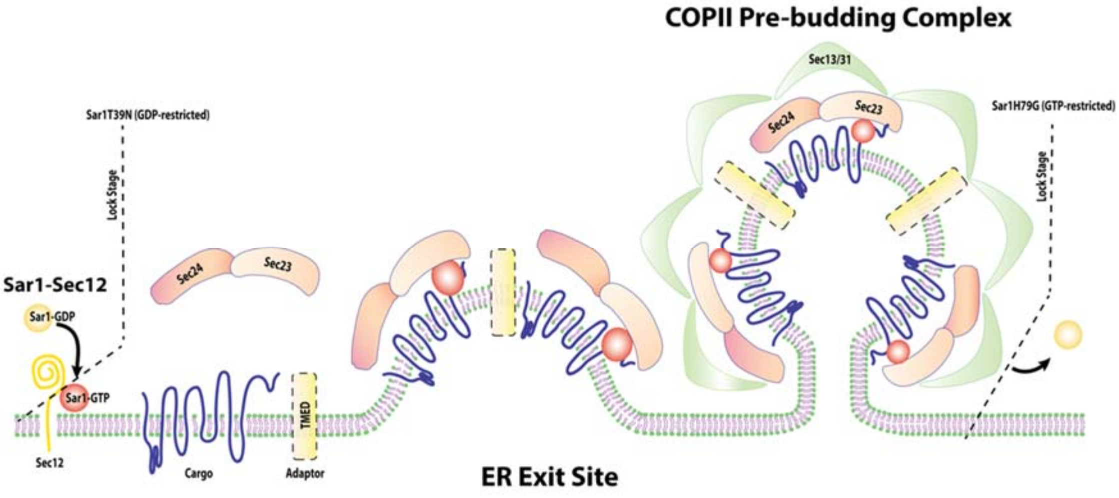
COPII Pre-budding Complex
Sec13/31
Sar1T39N (GDP-restricted)
Lock Stage
Sec24
Sec23
Sar1H79G (GTP-restricted)
Lock Stage
Sar1-Sec12
Sar1-GDP
Sar1-GTP
Sec12
Cargo
TMED
Adaptor
ER Exit Site

Figure 1.2 The dynamic of Sar1 GTPase activities is crucial for the initiation, assembly and fission of COPII vesicles.

Sec12, a Guanine nucleotide Exchange Factor (GEF) of Sar1, initiates the assembly of COPII vesicle on the ER membrane. After catalyzed by the exchange of GDP for GTP at ER exit sites (ERES), specific ribosome-free locations on ER membrane, the small GTPase Sar1 inserts its N-terminus into the outer leaflet of the ER membrane and then recruits the Sec23/24 inner-coat complexes. The Sec23/24 complex is considered to assist incorporating the cargo proteins into the nascent COPII-coated buds and recruiting the Sec13/31 outer-coat complexes, resulting in the formation of the COPII vesicles. Then the deactivation of Sar1 by the hydrolysis of GTP mediates fission of the COPII-coated vesicles, leading the release of the cargo-carrying COPII-coated vesicles from the ER membrane. Note that the GTP-restricted form of Sar1 allows the assembly of COPII pre-budding complex but prevents the vesicles budding from the ER membrane. The GDP-restricted form of SAR1 blocks the assemblies of the COPII components from initiation hence no pre-budding complex will be form, respectably.

CHAPTER 2

MATERIALS AND METHODS

(Information included in this chapter is partially taken from Sun et al. Journal of Cell Science (2017) 130, 2159-2171.

Mouse and Cell lines

The Wls$^{fl/fl}$ mice have been described previously (Fu et al., 2011). In brief, loxP sites have been inserted to flank exon 3 of Wls in the presence of Cre recombinase. The removal of Wls's exon 3 resulted in a frame-shift mutation leading to introduction of a stop codon and a null phenotype. Villin is a tissue-specific actin binding protein that is associated with the brush border and is detected mainly in renal and gastrointestinal epithelial cell populations (Friederich et al., 1999). In the Wls$^{fl/fl}$, VillinCreERT2 mice, CreERT2 is expressed under the control of Villin promoter and the CreERT2 protein translocates into the nuclear to delete Wls upon injection of Tamoxifen (el Marjou et al., 2004). After Tamoxifen addition into the culture medium, intestinal organoids that grew from Wls$^{fl/fl}$, VillinCreERT2 mice will lose Wls expression (Valenta et al., 2016).

To obtain Wls $^{fl/fl}$ mouse embryonic fibroblasts (MEFs), the trunk of E12.5-13.5 Wls $^{fl/fl}$ embryo was diced into multiple small pieces and incubated with Trypsin-EDTA at 37 °C for 20 mins. The tissue remnants were mechanical dissociated via vigorously shaking and centrifuged at 1,000 rpm for 3 mins. Pellets were carefully collected and plated with culture medium containing 1× Dulbecco's Minimal Essential Media (DMEM) with 10% FBS, 5% Penicillin/Streptomycin and 10 μg/mL Gentamycin. To derive Wls deficient MEFs, Wls$^{fl/fl}$ MEFs were infected with retroviral CMV-Cre and selected by Hygromycin B

(500 μg/ml) over 3 weeks. The procedure of retroviral production is described below.

HeLa, HEK293T and Gp2-293 cells were purchased from the American Type Culture Collection (ATCC). MEFs, HeLa, HEK293T and Gp2-293 cells were grown and passaged in Dulbecco's Modified Eagle's Medium (DMEM) (Corning) supplied with 10% Fetal Bovine Serum (FBS) (GIBCO) and Penicillin/Streptavidin (P/S).

C59, 4-(2-Methyl-4-pyridinyl)-N-[4-(3-pyridinyl)phenyl] benzeneacetamide, was purchased from CellagenTech (C7641-2s) and dissolved in DMSO (100mM Stock) and administrated into culture media with indicated concentrations and treatment duration. Cells were treated with same volumes of DMSO in control groups.

Retroviral production and establishment of stable cell lines

GP2-293 cells were grown in 10-cm culture dishes until 90% confluence and then transfected with Flag-, EGFP-, or mCherry-tagged wild type or mutant Wls in a pQCXIP vector backbone with pVSVG. DNA usages together with transfection procedures follow the manufacturer’s instruction for transfection using Lipofectamine 3000 (Life Technologies). Six hours after transfection, viral harvest medium (DMEM, 10% FBS plus 100 ng/ml BSA) was applied to maximize the retroviral production. After two additional days, retrovirus-containing medium was collected, centrifuged at 1,000 g to remove cell debris and ultra-centrifuged at 15,000 g at 4°C for 2 hrs (Optima^{TM} L-100XP Ultracentrifuge; SW41 rotor, serial no. 105E2961; Beckman Coulter). After ultracentrifugation, the supernatant was discarded and the viral pellet re-suspended in DMEM medium for infecting the culturing cells or in the infection medium for the intestinal organoids. The ingredient of infection medium is described below.

For culture cell infection, MEFs or HeLa Cells of 80% confluence in a 10-cm dish were incubated with viral-DMEM medium for 6 hours and continued to be cultured in fresh DMEM medium with 10% FBS supplement for another 24 hours. Stable clones were selected by treating cultures with puromycin (2 μg/ml) for 7 days (for HeLa cells) or Hygromycin B (500 μg/ml) for 3 weeks (for MEFs). The expression of the recombinant Wls protein in HeLa cells or Wls deletion efficiency in MEFs were assessed by the Western blot and fluorescent microscopic assays.

Plasmids and siRNA

cDNA for mCherry or EGFP or three copies of Flag sequence (this should be nucleic acid sequence) were inserted into Not I/Age I sites of pQCXIP vector (Clontech), referred to as pQCXIP-mCherry, pQCXIP-EGFP or pQCXIP-3×Flag vectors. Full-length or truncated Wls sequences were amplified from a mouse Wls (UniProtKB - Q6DID7) cDNA clone (Fu et al., 2009). cDNA fragments of Wls

(1-541), Wls (1-491), Wls (1-497), Wls (1-431), and Wls (1-376) were subcloned into the Xho I/EcoR I sites of the pQCXIP-3×Flag vector to generate Flag-tagged recombinant fusion constructs. A non-tagged full-length Wls cDNA was cloned into the Xho I/EcoR I sites of pQCXIP expression vector and used in Wnt secretion assays. Site-directed mutagenesis was used to generate mutant constructs, including Wnt3a^{S209A}, Sar1aT39N and Sar1a^{H79G} following manufacturer's protocol (New England Biolabs). In order to avoid introducing additional oligonucleotides between fusion proteins, truncated forms of Wls (Δ101-232, Δ233-301, Δ302-376) were created using NEBuilder HiFi DNA assembly methods (New England Biolabs). Human SEC12 cDNA clone (SC319881) and human SAR1A-myc-Flag cDNA ORF clone (RC201450) were purchased from Origene. SEC12 (1-417), SEC12 (80-417), SEC12 (80-408), SEC12 (201- 408), SEC12 (301-417), and SEC12 (80-388) were then amplified from the cDNA clone and cloned into pCS2-6×Myc vector (Myc tag: EQKLISEEDL) between EcoR I and Xho I sites.

Using NEBuilder HiFi DNA assembly methods, EGFP-SEC12$^{389-417}$ was generated by inserting cDNA of EGFP between Myc tag and a.a. 389 of SEC12. SEC12$^{301-388}$-VAPA^{TM} was generated by fusing oligonucleotides encoding the transmembrane region (LPSLLVVIAAIFIGFFLGKFI) of human VAPA after a.a. 388 of SEC12. Plasmids of pEF.myc.ER-E2-Crimson (#38770) for labeling ER in the far-red channel, pcDNA-WNT3AV5 (#34927), pmGFP-SEC16A (#15776) and pcDNA3-Shh-Renilla (#37677) were purchased from Addgene. Metridia luciferase constructs were from Clontech (#631704). pmEGFP was generated by inserting oligonucleotides encoding the first 10 amino acids (MGCVCSSNPE) of mouse LCK into Xho I/EcoR I sites of the pEGFP N1 vector to attach the plasma membrane-targeting motif to EGFP at its N terminus, to label plasma membrane. Human TGN38 encoding sequences was cloned in frame into pEGFP-N1 vector to generate a C-terminal EGFP tagged TGN38 plasmid pTGN38-EGFP. pEGFPKDEL was a gift from Dr. Nihal Altan-Bonnet (National Heart, Lung and Blood Institute, USA). Human PREB (M-017655-00-0020) siGENOME siRNAs SMART pool and ON Human SAR1A (L-016756-00-0020) TARGETplus SMARTpool were purchased from Dharmacon.

Antibodies

Horseradish peroxidase (HRP) conjugated anti-V5 and anti-Myc antibodies were purchased from Thermo Fisher. Mouse polyclonal anti-FLAG and HRP conjugated anti-FLAG antibodies were purchased from Sigma. Rabbit polyclonal anti-SEC12, anti-SAR1A and anti-TMED10 antibodies were from Proteintech Inc, and rabbit anti-Sec24B and anti-Calnexin from Cell Signaling. HRP conjugated anti-rabbit IgG was purchased from GE Healthcare. Anti-FLAG M2 agarose beads were purchased from Sigma and c-Myc Monoclonal Antibody-Agarose Beads were from Clontech Inc.

Co-immunoprecipitation and proteomic analysis

Stable and transiently transfected cells were washed once with PBS and the lysed with 600 μl per plate (for 10 cm plate) of lysis buffer (50 mM Tris HCL, pH7.4, 150 mM NaCl, 1 mM EDTA, 1×Roche Proteinase Inhibitor cocktail, and 0.25% Triton X-100). Cells were lysed and sonicated at 4 °C. Two milligrams of protein were mixed with 40 μl wet volume of anti-Flag M2 affinity gel (A2220, Sigma) and incubated at 4 °C for 6 hrs. The suspension was pelleted by centrifugation at 1,000 g for 1 min and washed three times with washing buffer (50 mM Tris HCL, pH 7.4, and 150 mM NaCl). Bound proteins were eluted with 50 μl 3×Flag peptides (150 ng/μl), mixed with SDS sample buffer (NP0007, Life Technology), denatured at 95 °C for 5 mins and analyzed by SDS-PAGE and immunoblotting as previously described (Yu et al., 2014b). For proteomic analysis of wild type and a traffic-defective Wls, immunoprecipitation of Flag-Wls or Flag-Wls$^{1-491}$ was performed using anti-FLAG M2 agarose beads on stable HeLa cell lines expressing above proteins. Identical concentrations of precipitates were resolved by SDS-PAGE, followed by Ruby Red protein staining. Bands at 50 kDa corresponding to the antibody heavy chains were excised and excluded from analysis. The remaining lane of gel for each sample was subjected to in-gel digestion and mass spectrometry identifications. For IP of endogenous Wls, the YJ5 antibody (EMD Millipore) was used (Coombs et al., 2010).

Confocal live cell imaging

Cell cultures were prepared for confocal immunofluorescent microscopy according to previously published procedures from the Gao lab (Sakamori et al., 2012; Sakamori et al., 2014). Briefly, HeLa cells were cultured in glass bottom chambers (LabTek Corporation, Catalog # 155383) with 90% confluence. Then Hela cells were imaged by a Zeiss LSM510META laser scanning confocal microscope (Carl Zeiss, USA) using high-magnification, high numerical aperture objective (Plan-Apochromat 63×/1.4 Oil DIC). Live cells were maintained on the microscope at 37°C and 5% CO_2 using a Zeiss stage mounted environmental chamber. Live cells images were taken within 3 hours since the cells were first placed on the microscope. All images were later processed with LSM Image Browser (Zeiss).

Wnt3a-Gluc secretion assay

Wnt3a-Gluc secretory activities were measured from culture medium with cells seeded in 24-well plate. HEK293T or MEF Cells were grown until 85 - 90% confluence and transiently transfected with 0.1 ng Wnt3a-Gluc or Shh-Ren plasmid DNA and 0.01 ng firefly luciferase plasmid DNA serving as the transfection control. Six hours after transfection, fresh medium was exchanged to limit the effects of the initial secretory activity of Wnt. Depending on the experimental design, supernatant and cell lysates were simultaneously collected after 2, 4, 12 or 24 Hrs and subjected to dual luciferase assay (Promega, E1980), using the Glomax multi-detection system (Promega).

For detection of each reaction, 50 μl pellet-clear media or 10 μl pellet-clear cell lysates were used for detection. Fifty μl of the luciferase assay substrate and 50 μl of Stop-and-Glo reagent from the dual luciferase assay were added into the reaction well. Fluorescent units were determined sequentially by the multi-detection system. For quantitative analysis, luminescence units from Guassia luciferase (Wnt3a-Gluc) and Renilla luciferase (Shh-Ren) in the culture medium were normalized against the units from the intracellular Firefly luciferase. Assays were performed at least 3 independent times with 3 technical replicates for individual experiment condition.

OptiPrep density gradient centrifugation and cellular fractionation

Iodixanol gradients for ultracentrifugation and fractionation were performed using an ER isolation kit (ER0100, Sigma). HeLa cells grown to 90% confluence on 10 cm plates were detached by Trypsin-EDTA, collected by centrifugation at 600 g for 5 minutes and washed twice with cold PBS. Pelleted cells from one 10-cm plate were suspended in three volumes of 1× hypotonic extraction buffer (10 mM HEPES, pH 7.8, 25 mM potassium chloride and 1 mM EGTA) and incubated at 4°C for 20 mins. The resulting suspension was centrifuged at 600 g for 5 mins and the supernatant discarded. The pellet was re-suspended with two volume of 1× Isotonic Extraction Buffer (10 mM HEPES, pH 7.8, with 250 mM sucrose, 1 mM EGTA, and 25 mM potassium chloride) and disrupted using a 1ml Dounce homogenizer (Wheaton; USA). The nuclear fraction and unbroken cells were pelleted by centrifugation at 1,000 g for 10 mins at 4°C, the supernatant was collected and mixed with 1 ml 20% iodixanol (OptiPrep density gradient medium; Sigma) followed by overlaying onto 1ml 30% iodixanol layer. One ml of each of the iodixanol steps, 17.5%, 15%, 12.5%, 10% to 8% were sequentially overlaid. Sample-loaded gradients were centrifuged at 50,000×g for 18 hrs in a SW41 rotor using a Beckman ultracentrifuge (Optima^{TM} L-100XP Ultracentrifuge; serial no. 105E2961; Beckman Coulter). The top 250 µl of the resulting gradient was removed. The remainder was collected as 500 µl of each fraction (total 13 fractions) and all fractions were prepared for SDS-PAGE analysis.

Organoid culture and retroviral infection

Small intestinal crypts were freshly isolated from adult *Wls$^{fl/fl}$, Villin-CreERT2* mice and maintained in ENR intestinal organoid culture medium containing 50 ng/ml mouse epidermal growth factor, 100 ng/ml Noggin and 500 ng/ml mouse R-Spondin1 (Sakamori et al., 2014; Sato et al., 2009). Two days before retroviral infection, 100 ng/ml Wnt3a and 10 mM nicotinamide were added into ENR medium. Retrovirus was prepared as described above in section of “Retroviral production and establishment of stable cell lines”.

The viral pellet was re-suspended in 250 ul infection medium: ENR medium supplemented by 100 ng/ml murine Wnt3a (Peprotech), 10 mM nicotinamide (Sigma), 10 µM Y27632 (Sigma), and 8 µg/ml Polybrene (Sigma). Organoid infection with mCherry-Wls expressing retroviruses was performed according to (Koo et al., 2012) using glass bottom chamber slides for subsequent fluorescence live cell imaging. Infected organoids were kept in ENR medium with Wnt3a and nicotinamide for additional 48 hrs after infection. ENR medium, without Wnt3a, was then replaced for additional 3 to 5 days before tamoxifen administration. 4-Hydroxytamoxifen (4-OHT, Sigma) was added into culture media at a final concentration of 500 nM for 48 hrs. Organoid morphology was monitored daily using differential interference contrast (DIC) and fluorescence imaging using a ZEISS VivaTome microscope system with the following objectives: 10× NA 0.25 and 20× NA 0.75 at room temperature. Digital images were recorded using an AxioCam MRm (Zeiss) and processed by AxioVision software (Zeiss).

Quantifications and statistical analysis

All data were analyzed from independent experiments. Co-IP and Western blot experiments were repeated at least 2 times. Bands were quantitated using NIH Image J software (ver 2.0.0-rc-43/1.51j)(Schneider et al., 2012). In brief, western bolt films are scanned at 300 dpi in TIFF format using EPSON PERFECTION V750 PRO scanner. TIFF images are opened in ImageJ software. The Region of Interest (ROI) containing individual band is selected by the “rectangle” tool under the main menu and taken into measurement under the analyze menu. Data were collected and plotted into graphs using Graph Pad Prism 5; mean values are shown with error bars representing S.E.M.

To quantify the co-localization between two fluorescent molecules, a 2 color channel image was opened in ImageJ and the two channels were split into two separate images. The freehand ROI selection tool can manually select the cytoplasmic area for an individual cell. Then the Manders’ coefficient values were automatically computed from confocal cellular images of the ROI area using the Coloc2 plugin for ImageJ (Fiji) (Schindelin et al., 2012). To assess percentage of red signals co-localizing with green signals, yellow signals were captured by Co-localization Highlighter plugin. The total pixel numbers corresponding to signal channel or yellow particles (size equal or above 10 pixels) were obtained using Nucleus Counter Plugin for ImageJ. Data were plotted as Tukey box-and-whisker plot with outliners shown as dots or column bar graph. Statistical analysis was performed using one-way ANOVA on the basis of experimental setups and graphs were constructed by Graph Pad Prism 5. *, **, and *** represent $p < 0.05$, 0.01, and 0.001, respectively.

CHAPTER 3

WLS TRAFFICS THROUGH COPII COMPLEX TO ENTER SECRETORY PATHWAY

Information included in this chapter is partially taken from Sun et al. Journal of Cell Science (2017) 130, 2159-2171.

3.1 Introduction

Recent studies investigating Wnt secretion suggests that vesicles carrying Wnt-Wls cargo may require the critical actions of several regulatory molecules. In endoplasmic reticulum (ER), newly synthesized Wnt proteins are lipid-modified by an ER membrane-bound O-acyltransferase: Porcupine (Gao and Hannoush, 2014; Kurayoshi et al., 2007). Porcupine lipidates Wnt proteins at conserved cysteine and serine residues (Coombs et al., 2010; Herr and Basler, 2012; Janda et al., 2012; Takada et al., 2006; Willert et al., 2003). These lipid modifications are necessary for Wnt recognition and binding by Wls (Herr and Basler, 2012), and may play a role in initiating Wnt-Wls interaction in ER (Sun et al., 2017b). Serving as an unique cargo transporter for all Wnts, Wls shuttles Wnt molecules from the ER to the plasma membrane (Das et al., 2015; Sun et al., 2017b), where they act in autocrine or paracrine manner to transduce Wnt-signaling in ligand-receiving cells **(Figure 3.1)** (Augustin et al., 2017; Zhu et al., 2012).

3.1.1 Porcupine-mediated lipidation of Wnts

The fatty acid modification of Wnt was first reported in 2003 via experiments with radioactive [^{3}H] palmitic acid (C16:0) and *in vivo* metabolic labeling (Willert et al., 2003). Subsequently, palmitoleate (C16:1n-7), a mono-unstaturated fatty acid that contains 16 carbons with one *cis* double bond at the seventh carbon was suggested as the dominant fatty acyl chain attached to Ser209 of Wnt3a (Rios-Esteves and Resh, 2013; Takada et al., 2006). Additionally, studies identified that other fatty acyl chains with the length ranging from 13 to 16 carbons might also be linked to Ser209 of Wnt3a (Niehrs, 2012).

In Wnt-secreting cells, newly synthesized Wnt ligands are initially palmitoylated by porcupine, the ER membrane-bound O-acyltransferase (MBOAT) (Grzeschik et al., 2007; Hofmann, 2000; Kurayoshi et al., 2007; Wang et al., 2007). Porcupine is a Protein-serine O-palmitoleoyltransferase responsible for transferring the 14- to16-carbon-chain fatty acyl group onto the conserved serine residues of Wnts (Gao and Hannoush, 2014; Rios-Esteves and Resh, 2013). 13- and 18-carbon chain can be incorporated with the serine residues in certain cases but in a much lower efficiency manner (Gao and Hannoush, 2014). Typically, porcupine recognizes a disulfide-constrained region on Wnt comprising ~21 amino acids (Miranda et al., 2014).

Multiple studies found that human and mouse Porcupine specifically lipidates Wnt3a at serine 209 (Coombs et al., 2010; Herr and Basler, 2012; Janda et al., 2012; MacDonald et al., 2014; Takada et al., 2006; Willert et al., 2003). Without palmitoylation by Porcupine, non-lipidated Wnts cannot bind to Wls (Proffitt et al., 2013), and are retained in ER (Herr and Basler, 2012). Given the importance of lipidation to Wnt secretion and functionality, targeting porcupine may become a useful approach to modulate Wnt secretion and functionality.

3.1.2 Wls is a unique transmembrane protein specifically transporting Wnt for secretion

Lipidated Wnts are transported by an evolutionarily conserved multi-pass transmembrane protein Wls **(Figure 3.1)**; Wls is also referred to as MIG-14 in *C. elegans* and putative G-protein coupled receptor 177 (Gpr177) in mice. Loss of function studies affirmed the indispensible role of Wls for secretion of virtually all Wnts across the animal kingdom (Banziger et al., 2006; Bartscherer et al., 2006; Fu et al., 2009). Wls has been shown to carry Wnts from Golgi to plasma membrane via Rab8a GTPase associated secretory vesicles. Physiologically, loss of Rab8a leads to the impairment of Paneth cell maturation, a specific cell type located in intestinal crypts that secrets Wnts ligand to maintain the stem cell niche (Das et al., 2015). The acidic environment of secretory vesicles (pH 5.5) also appears to play an important role in facilitating Wnt secretion, possibly inducing dissociation of Wnt from Wls in post-Golgi secretory vesicles (Coombs et al., 2010). However, the precise role of the environmental or intracellular pH in Wnt secretory pathway remains to be explored.

After Wnts are released from the secreting cells to extracellular matrix, Wls can be internalized from plasma membrane via AP2- and clathrin-dependent endocytosis followed by routing to endosomes (Gasnereau et al., 2011; Pan et al., 2008), where Wls is retrieved by retromer in a vacuolar protein sorting-associated protein 35 (Vps35)- and sorting nexin 3 (SNX3)-dependent fashion back to the Golgi compartment (Belenkaya et al., 2008b; Franch-Marro et al., 2008; Harterink et al., 2011a; Port et al., 2008; Rojas et al., 2008; Yang et al., 2008). Sorting of ligand-bound Wls from endosome to multivesicular body (MVB) has also been shown to export unsecreted Wnts that remain complexing with Wls, in a form known as exosome (Gross et al., 2012). Recent studies illustrated the involvement of ARF/ERGIC2 and COPI vesicles in regulating a Golgi-to-ER retrograde transport of Wls for Wnt secretion (Yu et al., 2014). These studies highlight a sophisticated regulatory process of anterograde and retrograde Wls trafficking, which is presumably designed for efficient Wnt export.

The functional role of Wg/Evi-containing membranous vesicles during Wnt signal transduction in the *Drosophila* neural-muscular junctions has been previously reported (Korkut et al., 2009). These membranous vesicles were later demonstrated as exosomes via electron microscopy and proteomic profiling analysis (Koles et al., 2012). The presence of exosomal Wg/Wnt in *Drosophila* and human cell was later confirmed by independent studies (Beckett et al., 2013; Gross et al., 2012). The consensus is that some Wnts can be delivered into the multivesicular bodies (MVBs) by Wls from early endosomes, and packaged into exosomes for secretion. Blocking the MVB-to-exosome secretory pathway reduced approximately 40% of Wnt secretion (Gross et al., 2012). Fractionated exosomal Wg/Wnt proteins from conditioned medium of *Drosophila* or mammalian cell culture remain their activities in inducing downstream signaling (Gross et al., 2012; Luga et al., 2012). In addition, *Drosophila* Wg is colocalized with two exosomal proteins, CD63 (known as a member of tetraspan transmembrane protein family) and Rab4 (Gross et al., 2012). The mammalian WNT11 was found in CD81-positive exosomes (Luga et al., 2012). Exosome-mediated Wnt secretion is thought to favor Wnt signal transduction in a long distance.

Multiple domains of Wls serve as sorting motifs in regulating the intracellular traffic of Wnt-Wls complex between different subcellular compartments. For example, Wnt-binding domain has been found in the first luminal loop, from amino acid (a.a.) 101 to a.a. 232 (Fu et al., 2009). During the retrograde traffic, Wls utilizes its specific regulatory motif (a.a. 425-428) to communicate with AP2/clathrin for endocytosis (Gasnereau et al., 2011). Retromer complexes recycle the ligand-free Wls from early endosome to the Trans-Golgi Network (TGN) (Belenkaya et al., 2008a) and the retromer regulatory motif is located at 429-431 a.a. (Harterink et al., 2011b). In 2014, Virshup group reported their observation that Wls is further recycled back to the ER via the cooperation of the Wls motif (537-541 a.a.) and ARF-COPI vesicles (Yu et al., 2014). Above reports suggested Wls mostly utilizes different internal sorting motifs to facilitate precise intracellular delivery and potentially efficient Wnt secretion.

Das et al. (2015) previously showed that a C-terminally truncated mouse

Wls failed to interact with Rab8a (the GTPase carrying Wls from Golgi) and hence speculated the C-terminus of Wls is critical for its exocytotic traffic. In addition, Wls$^{1\text{-}491}$, a mutant with a complete deletion of C-terminus presented a trafficking defect (Fu et al., 2009). Taking advantage of the discovered of trafficking defective Wls$^{1\text{-}491}$ mutants, we will explore whether and how the sorting events mediated by the C-terminus of Wls may affect its ability to transport Wnts, which eventually contributes to the molecular regulation of Wnt secretion.

3.1.3 The kinetics of Sar1 GTPase activity is critical to maintain the regular function of COPII vesicles

Formation and release of COPII vesicles from ER membrane are driven by the GTP/GDP exchanging dynamics of SAR1 (Sato and Nakano, 2005). In general, SEC16 recruits SEC12 to ER exit sites (Montegna et al., 2012). SEC12 resides in ER membrane as a single-pass transmembrane protein, which recruits and stimulates SAR1 activity as a specific guanine nucleotide exchanging factor (GEF) (Barlowe and Schekman, 1993). GTP-loaded active SAR1 attaches to ER membrane (Aridor et al., 2001), initiating a sequential assembly of inner (SEC23/SEC24) and outer (SEC13/SEC31) coats of COPII vesicle that encapsulates the cargo (Aridor et al., 1998). Upon proper formation of pre-budding COPII complex, SEC13/SEC31 stimulates the GTPase activating protein (GAP) activities of SEC23 toward SAR1 (Bi et al., 2007; Sato and Nakano, 2005; Yoshihisa et al., 1993). GTP hydrolysis of SAR1 results in the detachment of COPII vesicles from ER membrane (Sato and Nakano, 2005). A serial formation of COPII pre-budding complex is shown in **Figure 1.2** previously.

3.2 Results

3.2.1 Proteomic analysis uncovers the involvement of COPII machinery in Wls traffic

According to the information discussed in a prior introduction section **(3.1.2 Wls is a unique transmembrane protein specifically transporting Wnt for secretion)**, we hypothesized that proteomic analysis comparing wild type Wls and traffic-defective Wls$^{1\text{-}491}$ might shed light on the cellular machinery required for Wls trafficking. Jin et al. (2010) demonstrated that an N-terminally Flag-tagged full-length Wls retains biochemical and functional Wnt secretion when transfected into cultured cells. Extracts from HeLa cells stably expressing 3xFlag-tagged wild type Wls or Wls$^{1\text{-}491}$ were subjected to immune-precipitation using anti-FLAG antibodies. Proteins collected by immune-precipitation were resolved on SDS-PAGE, and subjected to in-gel digestion followed by mass spectrometry.

Proteomic analysis for wild type Wls affirmed a number of previously reported regulators of Wls trafficking, including Rab8a GTPase for post-Golgi secretory vesicles (Das et al., 2015), adaptor protein (AP) 2 (Pan et al., 2008a) and Clathrin (Gasnereau et al., 2011) for endocytosis from the plasma membrane, and retromer components (VPS26, VPS29, VPS35) (Port et al., 2008b) for Wls's recycle route from the early endosome to Golgi **(Table 3.1)**. In contrast, proteomic analysis of Wls$^{1-491}$ showed an almost complete loss of the above factors, consistent with the defective vesicular traffic in Wls$^{1-491}$ expressing cells. However, ER resident proteins, as well as Wls itself, were detected in Flag-Wls$^{1-491}$ proteomic analysis **(Table 3.1)**, suggesting that a lack of detected vesicular trafficking regulators in Wls$^{1-491}$ precipitates was not simply due to protein degradation. Importantly, proteomic analysis of wild type Wls uncovered several major components of the COPII machinery, including the COPII specific small GTPase (SAR1), the inner coat protein (SEC23, SEC24), the outer coat protein (SEC31), and COPII specific adaptors (TMED7, TMED9, and TMED10). Interestingly, none of these COPII-associated proteins were detected in Wls$^{1-491}$ precipitates. The above potential regulators are shown in **Figure 3.1** with their corresponding cellular compartments. Independent Co-IP analysis verified specific associations of wild type Flag-Wls, but not Wls$^{1-491}$, with SAR1, SEC24B, and TMED10 (**Figure 3.2A**). In addition, we observed an interaction between Wls and Wls$^{1-491}$ SEC12, a known specific GEF for SAR1. These data speculated that Wls might travel with the estimated COPII vesicles for Wnt export (**Figure 3.2B**) and the loss of cytosolic tail in Wls$^{1-491}$ most likely prevented its incorporation into COPII vesicles due to a potential mis-folding or lack of association with COPII machinery. To date, Wls is associated with multiple COPII components and the

C-terminus of Wls seems to involve in its intracellular vesicular traffic.

3.2.2 Export of Wls into COPII vesicle depends on SAR1 activity

To examine whether Wls indeed travels through COPII vesicles for ER exit, COPII pre-budding complexes were isolated by immune-precipitation of lysates prepared from cells overexpressing SAR1^{H79G} that remains in the GTP-restricted form (Aridor et al., 1995) or SAR1^{T39N} that remains in the GDP-bound form (**Figure 3.3A).** The change on the amino acid of the wild type, GTP-restricted form or GDP-restricted form of SAR1 is indicated in **Figure 3.3A**. As shown in the illustration of COPII pre-budding complex, Wls was abundantly detected in isolated wild type SAR1 or SAR1^{H79G} complexes. In contrast, almost no Wls was detected in SAR1^{T39N} precipitates, reflecting the incapability of attaching to ER membrane by this GDP-restricted SAR1 mutant **(Figure 3.3B, C)** (Bielli et al., 2005). Wild type SAR1 and SAR1^{H79G}, but not Sar1^{T39N}, recruited coat (Sec24B) and adaptor (TMED10) proteins **(Figure. 3.3B),** consistent with the notion that active SAR1 stimulates COPII complex assembly. In addition, associations of SEC12 with wild type SAR1 and SAR1^{T39N} (GDP-restricted) were detected, but not with SAR1^{H79G} **(Figure 3.3B)**. These results were in agreement with published reports that SEC12 has high affinity towards GDP-bound SAR1 (Barlowe and Schekman, 1993). Above observations affirmed the incorporation of Wls into COPII vesicles and suggested this incorporation may be related to the dynamics of Sar1 GTPase activity.

As SAR1^{T39N} binds to SEC12 but cannot be activated, it is proposed that overexpression of SAR1^{T39N} might interfere with SEC12 function and prevent Wls from trafficking into COPII vesicles. Imaging of HeLa cells expressing mCherry-tagged Wls and overexpressing SAR1^{T39N} detected a decrease in vesicular-type localization Wls when compared to cells transfected with empty vector **(**red in **Figure 3.4)**. The Golgi apparatus marked by TGN38 was intact in SAR1^{T39N} cells **(**green in **Figure 3.4)**, suggesting that the blockage of Wls traffic by SAR1^{T39N} was not due to impairment of Golgi compartment, but potentially occurred at ER level ($p<0.05$ based on colocalization of Wls and KDEL, **Figure 3.4**). We then used a GFP-tagged SEC16 (Bhattacharyya and Glick, 2007) to label ER exit sites in mCherry-Wls expressing live cells. We observed localizations of the cellular Wls adjacent to SEC16-marked exit sites (arrowheads in **Figure 3.5**), potentially reflecting a highly rapid and transient ER-exiting process (Wilhelmi et al., 2016). Overexpressing a GDP-restricted SAR1^{T39N} dispersed Wls throughout the cells and away from SEC16-positive exit sites ($p<0.05$ based on colocalization of Wls and SEC16, **Figure 3.5)**. Of note, large SEC16-positive puncta appeared in SAR1^{T39N} expressing cells with Wls proteins aggregated near these SEC16 punctate, a phenomenon previously associated with disrupted SAR1 activities (Watson et al., 2006). Above results indicated the SAR1 GTPase activity contributed to the vesicular distribution of Wls.

We then assessed the role of Sar1 GTPase activities on Wnt secretion using a luciferase assay that monitored the amount of secreted Wnt3a-Gluc or Sonic Hedgehog (Shh)-Renilla in the culture medium (Chen et al., 2009; Das et al., 2015). Shh is a secreted protein found in secretory vesicles and exosomes (Vyas et al., 2014), a similar scenario for Wnt secretion. Transient expression of SAR1 wildtype increased Wnt3a secretion and the presence of GDP form of SAR1^{T39N}, on the contrary, interfered Wnt3a delivery (**Figure 3.6A**). The similar regulation depending on Sar1 GTPase activity also applied to the secretion of Shh proteins (**Figure 3.6B**). Above results suggests that SAR1 activities might be contributing the global ER exiting as well as Wls trafficking dynamics.

3.2.3 Recruitment of SAR1 by SEC12 promotes Wls association with COPII complex

SEC12 is a specific GEF activator for SAR1. It is not clear whether Wls-SAR1 association depends on SEC12 binding to Wls. Two hypothetical models are provided in **Figure 3.7**: (A) Wls interacts independently with SEC12 and Sar1 and the binding leads to formation of a platform for the GTPase activation; and (B) Wls interacts with SEC12, followed by SAR1 recruitment by SEC12. We accessed these hypotheses by knocking down the levels of endogenous SEC12, or SAR1 using siRNAs in HeLa cells stably expressing Flag-Wls. Compared to cells treated with the scrambled control siRNA, knockdown of SEC12 by approximately 43% led to a proportional reduction of Wls-SAR1 (by 55%) and Wls-SEC12 (by 58%) associations **(Figure 3.8A)**. In contrast, silencing SAR1 by 80% only reduced the level of Wls-SAR1 association, but slightly enhanced Wls-SEC12 association by 12% **(Figure 3.8A)**, suggesting that Wls-SAR1 association depended on SEC12 whereas Wls-SEC12 association was not affected by SAR1.

To further test whether Wls-SEC12 complex formation might increase SAR1 recruitment to Wls complex on ER, 6×Myc-tagged Sec12 was transiently introduced into HeLa cells that stably expressed wild type Wls. Both the endogenous SEC12 (filled arrowhead, **Figure 3.8B**) and the transfected 6×Myc-Sec12 proteins (open arrowhead, **Figure 3.8B**) were co-immunopreciated with Wls. This forced Sec12 overexpression increased the level of Wls-SAR1 association approximately 4-fold **(**normalized against Wls, **Figure 3.8B),** suggesting that increased Wls-SEC12 complex formation could promote Wls-SAR1 association. Quantification for the relative bands intensity is individually shown under each band **(Figure 3.8 A-B)**. To this end, we concluded that Wls interacted with SEC12 and Sec12 recruited Sar1 for the association with COPII vesicle.

3.2.4 Wls-SEC12 interaction is mediated by specific motifs: Wls$^{377\text{-}431}$ and SEC12$^{301\text{-}388}$

Above results suggested a relatively stable and constant complex formation between Wls and SEC12, even when the truncated Wls retained in ER **(Figure 3.2A)**. Importantly, using a previously reported antibody against the endogenous WLS (Coombs et al., 2010; Yu et al., 2014), SEC12 co-immunoprecipitated with WLS in HeLa cell lysates, indicating that there is an endogenous SEC12-WLS interaction **(Figure 3.9)**. Wls is a putative eight-pass transmembrane protein. In order to systematically map out the responsible motif(s) that mediate Wls-SEC12 interaction, five additional Flag-tagged Wls fusion proteins with various deletions (Wls$^{\Delta 101\text{-}232}$, Wls$^{\Delta 233\text{-}301}$, or Wls$^{\Delta 302\text{-}376}$, Wls$^{1\text{-}376}$, Wls$^{1\text{-}431}$) were prepared **(Figure 3.10A).** The topology of Wls protein is acquired from Ensembl Genome Browser. Wls$^{\Delta 101\text{-}232}$ is the Wnt-binding domain-deficient mutant; Wls$^{\Delta 233\text{-}301}$ lacks the first trans-membrane (TM) region (a.a. 233-251), the first cytosolic loop (CL1) (a.a. 252-264), the second TM (a.a. 265-287) and second luminal loop (LL2) (a.a. 288-301); Wls$^{\Delta 302\text{-}376}$ lacks the TM4 (a.a. 302-319), the CL2 (a.a. 320-331), the TM5 (a.a. 332-354) and the LL3 (a.a. 355-376); Wls$^{1\text{-}376}$ is the shortest truncation form lacking the TM6 (a.a. 377-401), the CL3 (a.a. 402-428), the TM7 (a.a 429-450aa), the LL4 (a.a 451-469), the TM8 (a.a. 470-491) and C-terminus (a.a. 492-541); Wls$^{1\text{-}431}$ is truncate with the deletion of the TM7 through the C-terminus. In co-IP analysis, both Wls$^{\Delta 302\text{-}376}$ and Wls$^{1\text{-}431}$ were able to bind SEC12, however Wls$^{1\text{-}376}$ failed to bind **(**red asterisk, **Figure 3.10B)**, suggesting that SEC12-interacting motif resides between amino acids 377 and 431, a fragment predicted to contain a TM6 domain and a CL3 domain **(Figure 3.10A, B)**. Of note, Wls$^{\Delta 101\text{-}232}$ that lacked the Wnt-binding domain (WBD) retained its SEC12 association, however with lower affinity **(**black asterisk, **Figure 3.10B)**. Interestingly, only full-length Wls, while none of the truncated forms, associated with SAR1, indicating that, at this level of structural resolution, only the full-length Wls has the correct conformation capable of assembling into COPII ER-exiting machinery.

We performed reciprocal mapping for the Wls-interacting domain in SEC12 using a similar strategy. SEC12 is a single-pass type-II ER transmembrane protein consisting 417 amino acids (a.a.). Seven tryptophan-aspartic acid (WD) 40 motifs (Neer et al., 1994) are suggested at the cytosolic portion of SEC12 (Chardin and Callebaut, 2002). Since the WD motifs are always used as scaffolding sites for protein-protein interaction (Stirnimann et al., 2010), we generated 5 different Myc-tagged truncates (SEC12$^{80\text{-}417}$, $^{80\text{-}408}$, $^{201\text{-}408}$, $^{301\text{-}417}$, and $^{80\text{-}388}$) preserving the intact WD motifs for potential functional binding site to Wls, respectively **(Figure 3.11A)**. The truncated SEC12 constructs covered specific portions of the protein: N-terminal putative GEF domain (McMahon et al., 2012), cytosolic region, transmembrane domain and the ER lumen-residing C-terminal tail. Surprisingly, neither the GEF domain (a.a. 1-79) nor the ER luminal domain (a.a. 408-417) was required for Wls interaction **(Figure 3.11A, B)**. A truncated SEC12 (a.a. 201-408) containing only a partial cytosolic region plus the transmembrane domain was sufficient to bind Wls **(Figure 3.11A, B)**. Deletion of the transmembrane domain only weakened but did not abolish Wls interaction (please see SEC12$^{80\text{-}388}$, **Figure 3.11B**), suggesting that the cytosolic domain corresponding to a.a. 301-388 might be responsible for Wls binding. Above conclusions were suggested by the co-IP assay of Flag-Wls with various Myc-tagged truncated Sec12 proteins illustrated in **Figure 3.11A.**

However, due to the weakened Wls binding upon removal of the transmembrane domain, it was not clear whether the transmembrane domain also contributed to the interaction. We then generated two chimeric SEC12 proteins: one (EGFP-SEC12$^{389\text{-}417}$) with the entire cytosolic portion replaced by an EGFP while preserving SEC12's transmembrane and ER luminal domains; and the other (SEC12$^{301\text{-}388}$-VAPA^{TM}) with the suspected Wls-interacting cytosolic motif (a.a. 301-388) fused to the transmembrane domain of Vesicle-associated protein A (VAPA) (Skehel et al., 2000), an unrelated type II ER membrane protein **(Figure 3.11A)**. Flag-Wls bound to SEC12$^{301\text{-}388}$-VAPA^{TM}, but not EGFP-SEC12$^{389\text{-}417}$ **(Figure 3.11B)**. Finally, Wls$^{1\text{-}431}$ was able to bind SEC12$^{301\text{-}417}$ but not EGFP-SEC12$^{389\text{-}417}$ **(Figure 3.11C)**, suggesting that a.a. 301-388 of SEC12 was sufficient to mediate Wls-SEC12 interaction **(**red box, **Figure 3.11A).** However, Wls$^{1-431}$, a C-terminal truncation mutant containing the SEC12-binding domain (377-431aa), is accumulated around the perinuclear region **(Figure 3.12).** These puncta-like subcellular distributions (vesicle-defect phenotype) of Wls$^{1-431}$ suggested the interaction of Wls-Sec12 alone was not sufficient to support Wls exiting from the ER. Additional regulation step(s) in the ER export of Wls need to be further investigated.

3.2.5 Wls-SEC12 complex is critical for Wnt secretion

We next assessed the impact of SEC12 on Wnt secretion using a luciferase assay that monitored the amount of secreted Wnt3a-Gluc in culture medium (Chen et al., 2009; Das et al., 2015). Transient overexpression of wild type SEC12 enhanced Wnt3a-Gluc secretion by 40% while knocking down SEC12 by only 20% was sufficient to decrease Wnt secretion by 24% **(Figure 3.13A, B)**. These observations suggested SEC12 indeed regulated Wnt3a secretion. Likewise, overexpression of SEC12 truncates lacking GEF domain but capable of Wls-binding inhibited secretion by 62-74%. These inhibitory effects of truncated SEC12 were corroborated by an increased ER retention of endogenous WLS illustrated by antibody co-staining of CALNEXIN **(Figure 3.14A-D)**. These results suggested the SEC12 truncates lacking GEF domain behaved as the dominant-negative mutant regarding its role in supporting Wnt secretion. As overexpression of SEC12 fragments might alter the global ER exit processes, we further performed Wnt3a-Gluc secretion rescue experiments in Wls-deficient MEFs that are defective in Wnt secretion **(Figure 3.15A)** (Das et al., 2015). Transient transfection of a full-length Wls (untagged or Flag-tagged) into these Wls-deficient MEFs significantly increased their secreted Wnt3a-Gluc levels in the medium **(Figure 3.15B)**. This rescuing effect was not seen with the transfection of Wls$^{1\text{-}376}$ that was deficient in SEC12-binding **(Figure 3.10A, 15B)**. Note that the observed enhancement of Wnt secretion by transiently transfected Wls was obtained on an approximately 8% transfection efficiency. These data suggested that influencing the amount and function of Wls-SEC12 complex might affect Wnt secretion.

Remarkably, Wls utilizes COPII complex to exit from the ER. Wls interacts with Sec12 and then recruits Sar1 for its activation. The Wls-Sec12-Sar1 complex controls the initial assembly of Wls-containing secretory vesicles at ER membrane and hence regulates Wnt secretion.

3.3 Discussion

3.3.1 Wls transports Wnt in a GTPase dependent manner

Rab8a GTPase, AP2/Clathrin complex, VPS26/29/35 retromer complex, a group of previously identified Wls interacting proteins, have been found in our proteomic analysis of Wls-immunoprecipitates **(Table 3.1)**. These observations affirmed the efficiency and sensitivity of our proteomic approach. 15 different Rab GTPases were identified as potential interactors with Wls **(Table 3.1)**. These Rab GTPases serve as coordinators in sorting the intracellular vesicles between various subcellular compartments, respectively (Stenmark, 2009). To date, our study suggests that the transport of Wls within the Wnt-secreting cells may largely depend on the function of specific Rab small GTPase family.

3.3.2 Wls transporter carries Wnt ligands initially from the ER

Unlike the proposed role of Wls in shuttling Wnts along the post-Golgi exocytic delivery and the endocytic recycling pathway, the potential role of Wls in mediating the ER to Golgi delivery of Wnts has been ignored until recently. Yu et al. (2014) reported Wls is primarily located in ER and undergoes the Golgi-to-ER retrograde traffic for supporting the effective Wnt secretion. Das et al. (2015) afterwards reported the majority of Wls-positive immunogold particles were detected within the ER in the normal mouse intestinal tissue. Above subcellular ER distribution of Wls raised the question about the role of Wls proteins in ER: whether Wls transports Wnt from the ER. The observation that Wls is immunoprecipitated with ER resident Porcupine enzyme (Galli et al., 2016) further supported the hypothesis that Wls and Porcupine may synergically mediate the ER export of Wnt molecules.

To our knowledge, the results discussed here represent the first to define

Wls-SEC12 and Wls-COPII interaction. Activated SAR1 by SEC12 GEF initiates the formation of COPII-coated vesicles and triggers the release of the cargo-bearing vesicles from the ER. Wls appears to use the same machinery for ER exit as reported for other growth factors, including collagen type I (Jin et al., 2012), type VII (Saito et al., 2009) and the G-protein-coupled receptors, AT1R, β2-AR, α2B-AR and hCaR (Dong et al., 2008; Zhuang et al., 2010). However, the molecular basis of Wls–COPII communication differs from mechanisms proposed for other cargos utilizing the ER-to-Golgi intermediate complex (ERGIC) (discussed in the introduction section **1.1 Introduction to protein sorting and traffic**). Our proteomic study did not identify any components of the ERGIC that regulate an alternative ER-to-Golgi transport pathway, suggesting that Wls may selectively utilize COPII vesicles for ER exit.

3.3.3 Speculation on how Sec12 reaches the ER exit sites

In all eukaryotes studied to date, COPII vesicles are assembled at the ER exit site (ERES), but the onset of the COPII vesicles formation on the ERES is still in debate. In cultured mammalian cells, ERESs are usually dispersed in the cytoplasmic ER network but concentrated in specific ERES regions for cargo exiting (Brandizzi and Barlowe, 2013). ERES is usually shown as subcellular puncta by the immuno-fluorescence staining SEC16, the ERES resident protein (Hughes et al., 2009; Liu et al., 2017; Wang et al., 2015). In the budding yeast

Pichia Pastoris, Sec12 also presents a puncta-like distribution. This is consistent with the fact that Sec12 activates SAR1 GTPase at those specific ERESs for ER export (Montegna et al., 2012; Soderholm et al., 2004). However, Sec12 is found throughout the ER in *Saccharomyces Cerevisiae*, presenting as a smear-like distribution (Shindiapina and Barlowe, 2010). The variability of SEC12's subcellular localization suggests that Sec12 might be recruited onto the ERES rather than playing a role in establishing the nascent ERES.

Sec16, a large peripheral ER membrane protein, has been proposed as a Sec12 binding partner recruiting Sec12 onto ERES (Montegna et al., 2012). In mammalian and *Drosophila* cells, Sec16 plays a key role in organizing the ER exit site (Piao et al., 2017; Zanetti et al., 2012). In mammalian cells, over-expression of Sec12 delocalized itself from ERES throughout the ER network, when co-overexpression of Sec16 can retain more Sec12 proteins at the ER exit site (Montegna et al., 2012). These observations hint the possibility that Sec12 is recruited onto ERES via its interaction with Sec16. On the other hand, the cargo protein may directly recruit Sec12 onto the ERES as suggested by the study of collagen ER export (see below).

A concentration of Sec12 at ER exit sites in human cells has been shown its indispensable role for collagen VII export. During the collagen VII secretion, the recruitment of Sec12 to ER exit sites is driven by a direct interaction between

Sec12 and cTAGE5 (Saito et al., 2014; Tanabe et al., 2016), a previously characterized collagen cargo transporter component (Saito et al., 2009). Thus, in the case of Wls mediated ER exports of Wnt, it remains the possibility that Sec12 is recruited via the transporter Wls on the ERESs to support Wnt secretion.

Table 3.1 Proteomic identification of protein targets in wild type Wls and Wls$^{1-491}$ immunoprecipitates

Cellular compartment and identified proteins		Spectra counts (Number of unique peptides)	
		Wild type Wls	Wls$^{1-491}$
	Wls	17 (7)	19 (7)
ER	CALL	9 (4)	13 (5)
	HSP 90	32 (7)	19 (8)
	HSP70C	57 (28)	33 (25)
Lysosome	LAMP1	5 (4)	5 (4)
	LAMP2	6 (3)	5 (2)
Golgi	AP1	10 (7)	2 (2)
	p115	2 (2)	0
	GOGA4	1	0
	ACBD3	2 (2)	0
COPII Complex	SEC23B	4 (3)	0
	SEC24C	6 (4)	0
	SEC31A	1	0
	SAR1	1	0
	TMED7	1	0
	TMED9	3 (2)	0
	TMED10	2 (2)	0
Rab Small GTPase	RAB18	1	0
	RAB21	1	0
	RAB38	2 (2)	0
	RAB25	3 (2)	0
	RAB5C	5 (2)	0
	RAB3D	4 (1)	0
	RAB5A	6 (4)	1
	RAB2A	6 (6)	0
	RAB11A	7 (5)	0
	RAB10	7 (1)	0
	RAB1B	8 (4)	0
	RAB14	9 (6)	0
	RAB7A	10 (6)	0
	RAB9A	1	0
Known Wls Interacting Proteins	RAB8A	7 (1)	0
	AP2M1	2 (2)	0
	AP2A1	1	0
	VPS29	1	0
	VPS26A	1	0
	VPS35	5 (5)	0
	Clathrin	56 (39)	1

Note that protein band corresponding to antibody heavy chain (approximately 50 kDa), detected by Ruby protein stain, were excised and excluded from the analysis.

Figure 3.1

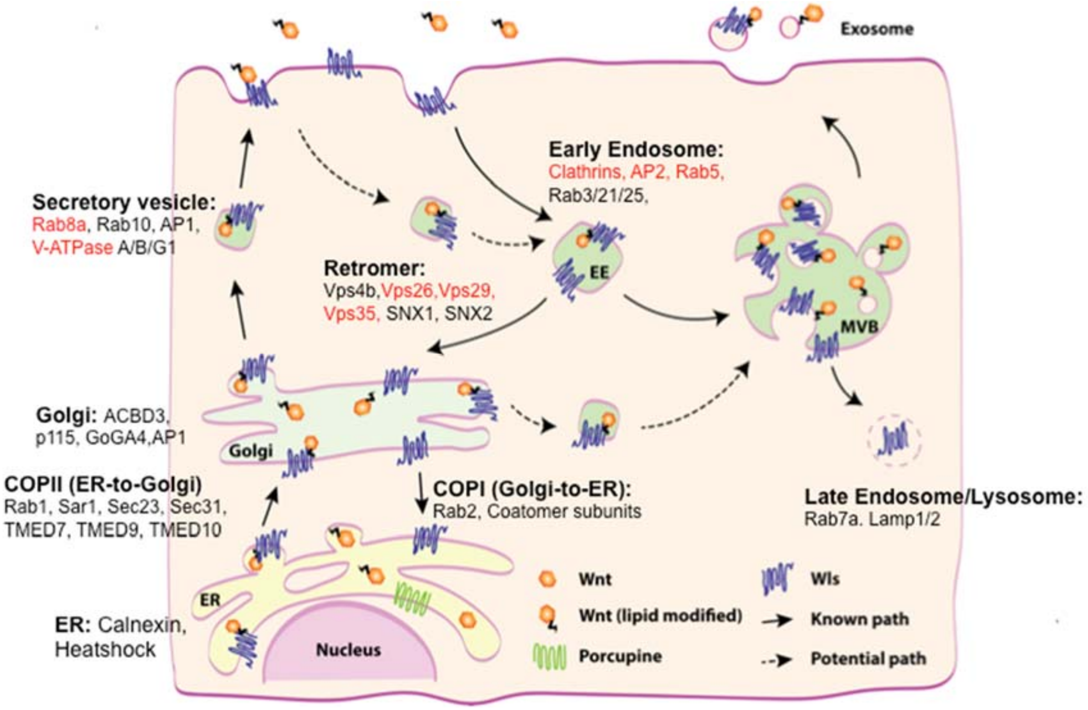
Exosome
Early Endosome:
Clathrins, AP2, Rab5,
Rab3/21/25,
Secretory vesicle:
Rab8a, Rab10, AP1,
V-ATPase A/B/G1
Retromer:
Vps4b, Vps26, Vps29,
Vps35, SNX1, SNX2
EE
MVB
Golgi: ACBD3,
p115, GoGA4, AP1
Golgi
COPII (ER-to-Golgi)
Rab1, Sar1, Sec23, Sec31,
TMED7, TMED9, TMED10
COPI (Golgi-to-ER):
Rab2, Coatomer subunits
Late Endosome/Lysosome:
Rab7a. Lamp1/2
ER
ER: Calnexin,
Heatshock
Nucleus
Wnt
Wnt (lipid modified)
Porcupine
Wls
Known path
Potential path

Figure 3.1 Current understanding in the molecular regulation of Wnt secretion

In the secreting cells, nascent Wnt molecules are translated in the endoplasmic reticulum (ER) where it is bound and modified with lipids by the ER membrane bounded acyltransferase Porcupine. The Wls transporter binds and transports the lipidated mature Wnt molecules to the plasma membrane. After releasing Wnt molecules to the extrecellular space, Wls undergoes endocytosis and reaches early endosome. At the early endosome, the Wnt-free Wls is recycled back to *trans* Golgi network by retromer and further transported to the ER compartment for carrying Wnt; the Wls-Wls complex in early endosome is sorted to multivesicle body and packaged into exosome for long distance secretion. After finishing its functions in supporting Wnt secretion, Wls transporter is degraded in lysosome. The potential regulators identified by the proteomic analysis following by the Wls pull-down assay are shown in the figure with the corresponding subcellular compartment. The known factors involving in Wls traffic are highlighted with RED color.

Figure 3.2

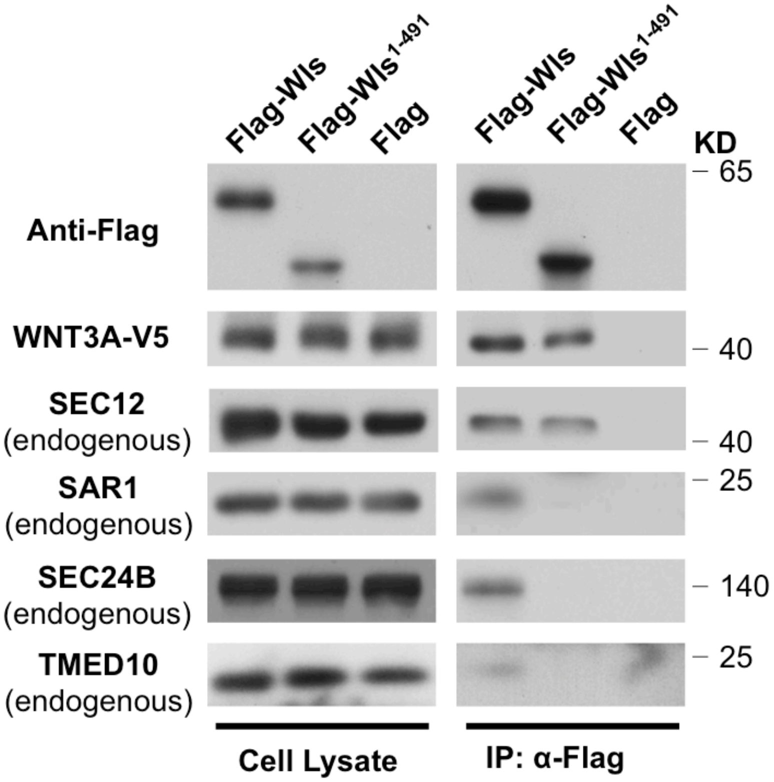
Flag-Wls
Flag-Wls$^{1-491}$
Flag
Flag-Wls
Flag-Wls$^{1-491}$
Flag
KD
65
Anti-Flag
WNT3A-V5
40
SEC12
(endogenous)
40
SAR1
(endogenous)
25
SEC24B
(endogenous)
140
TMED10
(endogenous)
25
Cell Lysate
IP: α-Flag

B

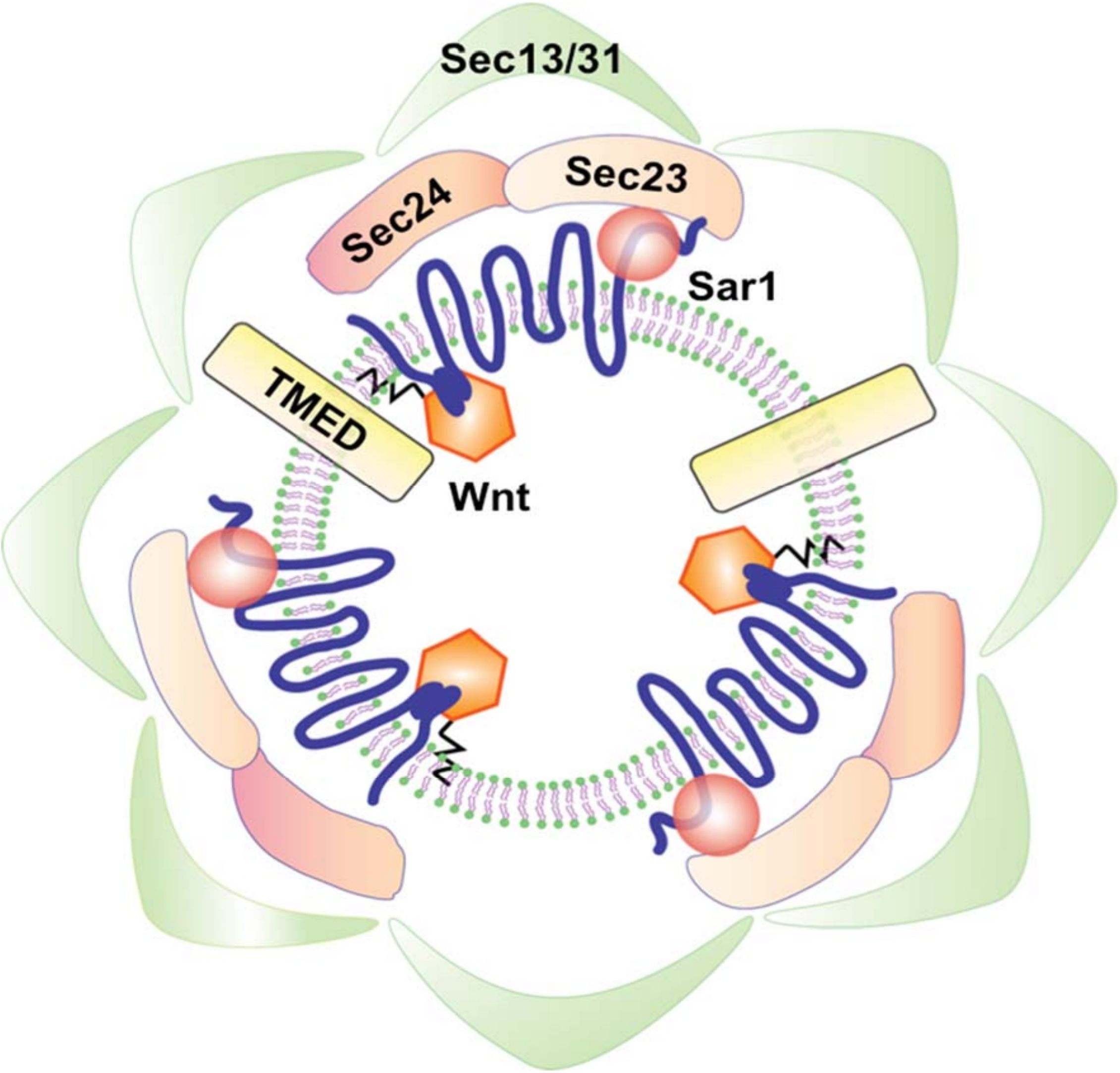
WIs-Wnt in COPII Vesicle
Sec13/31
Sec23
Sec24
Sar1
TMED
Wnt

Figure 3.2 Wls is associated with COPII components.

(A) Co-IP assays by anti-FLAG antibody were performed on HeLa cells stably expressing 3×Flag, 3×Flag-Wls or 3×Flag-Wls$^{1\text{-}491}$. WNT3A-V5 and endogenous SEC12 showed interaction with Flag-Wls and Flag-Wls$^{1\text{-}491}$, while SAR1, SEC24B, and TMED10 showed interaction with Flag-Wls but not with Flag-Wls$^{1\text{-}491}$ or Flag alone.

(B) A schematic diagram showed a hypothetic COPII vesicle for Wls-Wnt export on the basis of proteomic and Co-IP analyses, based on proteomic results and results in panel A. The Wls-Wnt complex-carrying COPII vesicle contains TMED adaptors, SAR1 GTPase, the inner coat proteins Sec23/Sec24 and the outer coat proteins Sec13/Sec31.

Figure 3.3

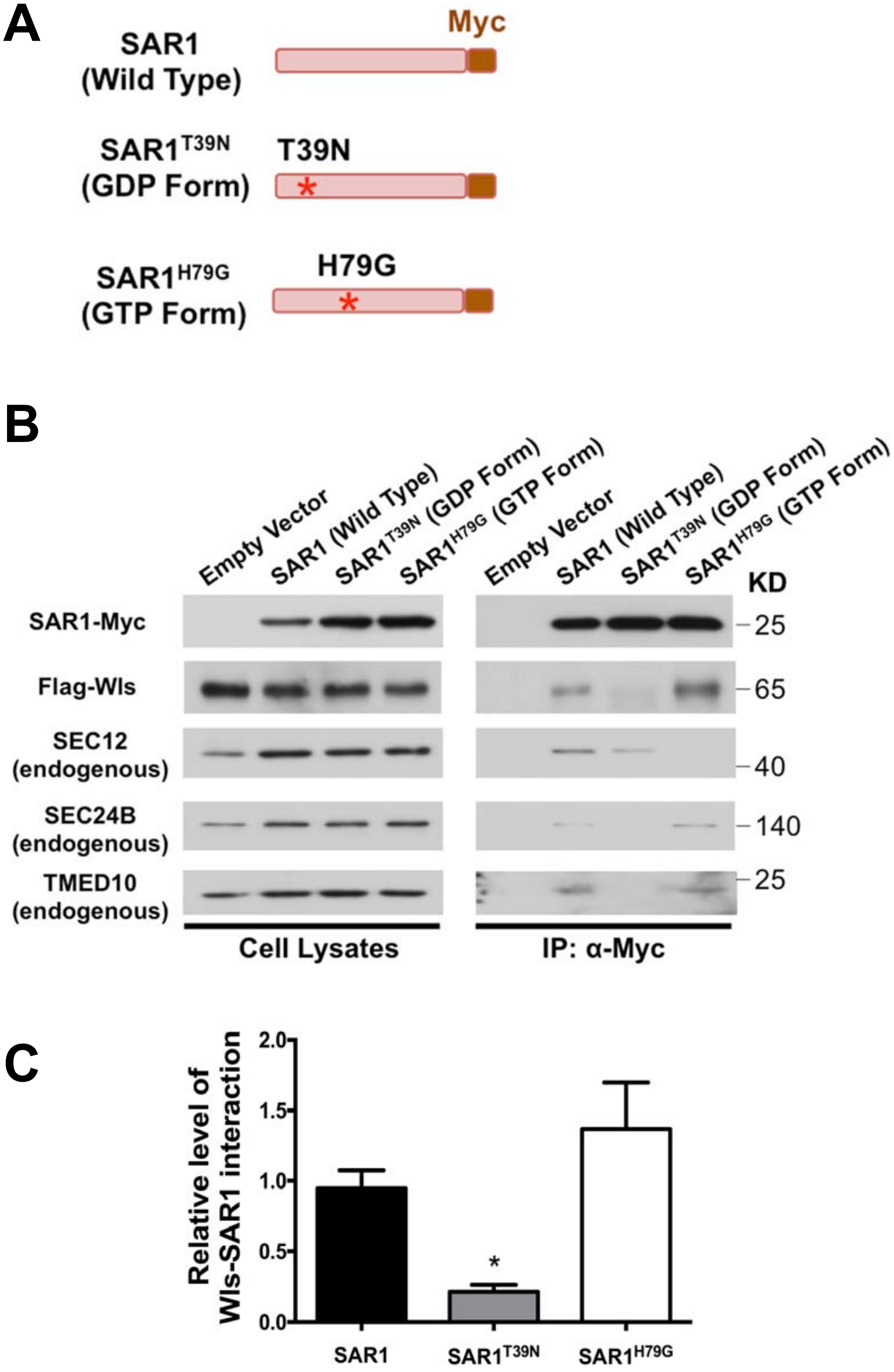
A
SAR1 (Wild Type)
Myc
SAR1T39N (GDP Form)
T39N
SAR1H79G (GTP Form)
H79G
B
Empty Vector
SAR1 (Wild Type)
SAR1T39N (GDP Form)
SAR1H79G (GTP Form)
Empty Vector
SAR1 (Wild Type)
SAR1T39N (GDP Form)
SAR1H79G (GTP Form)
KD
SAR1-Myc
25
Flag-Wls
65
SEC12 (endogenous)
40
SEC24B (endogenous)
140
TMED10 (endogenous)
25
Cell Lysates
IP: α-Myc
C
Relative level of Wls-SAR1 interaction
2.0
1.5
1.0
0.5
0.0
*
SAR1
SAR1T39N
SAR1H79G

Figure 3.3 Sar1 GTPase activities is essential for Wls-Sar1 association

(A) Protein structures of Sar1 Wild type, Sar1^{T39N} (GDP restricted form) and Sar1^{H79G} (GTP restricted form).

(B) Co-IP of Myc-tagged wild type or mutant SAR1 (T39N and H79G) showed a reduced Wls association with SAR1^{T39N} (GDP restricted). Cell lysates and α-Myc immunoprecipitants were resolved on SDS-PAGE and subject to Western blotting with Flag, Sec24B, Sec12, and TMED10 antibodies. Both wild type SAR1 and SAR1^{T39N} are associated with SEC24B and TMED10, indicating the α-Myc immunoprecipitants includes the COPII pre-budding complexes.

(C) Western blot quantification of panel B. Intensity of individual bands in α-Myc immunoprecipitants was quantified using ImageJ software, and expressed relative to Sar1-Flag signal, as a measure of protein relative abundance in different samples. * represents $p<0.05$

Figure 3.4

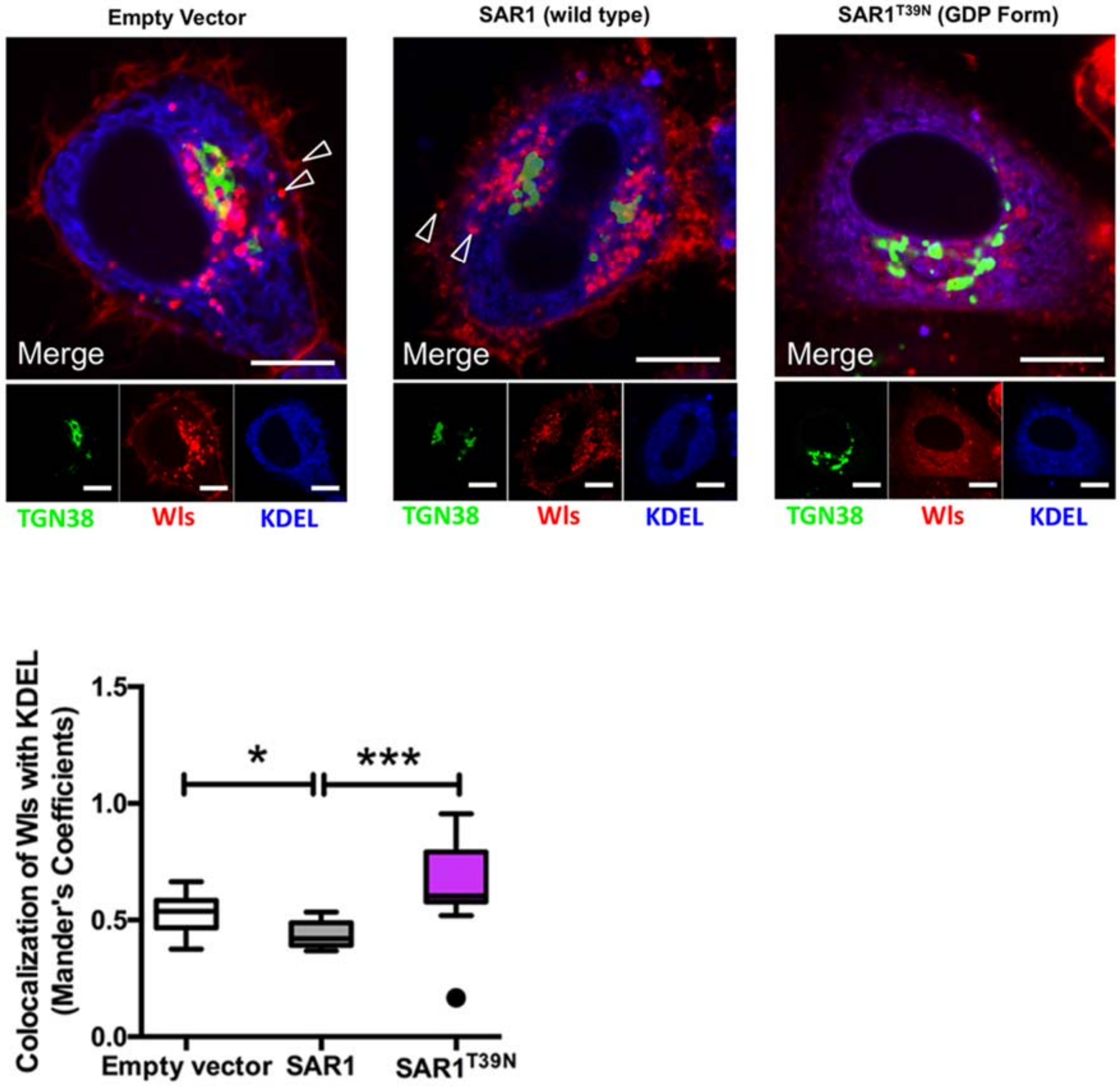
Empty Vector
SAR1 (wild type)
SAR1T39N (GDP Form)
Merge
Merge
Merge
TGN38
Wls
KDEL
TGN38
Wls
KDEL
TGN38
Wls
KDEL
Colocalization of Wls with KDEL (Mander's Coefficients)
1.5
1.0
0.5
0.0
*
***
Empty vector
SAR1
SAR1T39N

Figure 3.4 Inhibition of SAR1 activities impairs Wls's vesicular traffic.

Live cell images of control (with endogenous SAR1) (n=23), SAR1 wild type-overexpressing (n=9) and SAR1^{T39N}-overexpressing (n=16) mCherry-Wls (red) HeLa cells transiently transfected E2-Crimson-KDEL (blue, for ER) and TGN38-GFP (green, for Golgi), showed that SAR1^{T39N} impaired the vesicular pattern of wild type Wls. The cell with endogenous SAR1or SAR1-overexpression allows the vesicular distribution of wild type Wls. Arrowheads point to peripheral vesicle and plasma membrane localization. Tukey box-and-whisker plot illustrates colocalization values by Manders' coeffieient analysis, with outliners shown as dots. *, $p < 0.05$; ***, $p < 0.001$.

Scale bars: 5 μm.

Figure 3.5

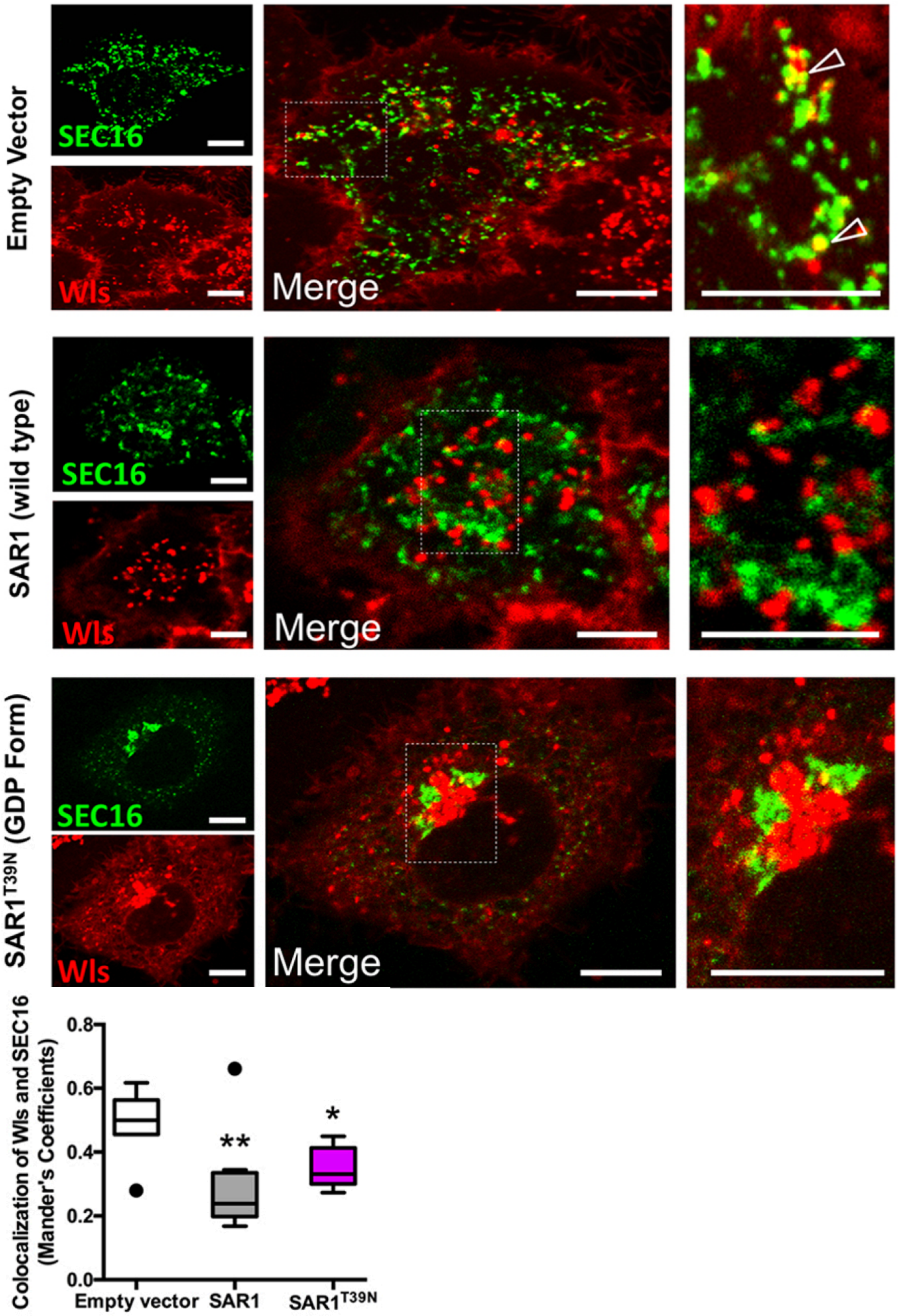
Empty Vector
SEC16
Wls
Merge
SAR1 (wild type)
SEC16
Wls
Merge
SAR1T39N (GDP Form)
SEC16
Wls
Merge
Colocalization of Wls and SEC16 (Mander's Coefficients)
0.0
0.2
0.4
0.6
0.8
**
*
Empty vector
SAR1
SAR1T39N

Figure 3.5 Inhibition of SAR1 activity leads to Wls aggregation near the SEC16-positive ER exit site.

Live-cell images of control (empty vector, n=8), SAR1-overexpressing (n=9) or SAR1T39N-expressing (n=12) mCherry–Wls (red) HeLa cells transiently transfected with EGFP–SEC16 (green, to mark ER exit sites) showing that SAR1T39N altered the wild-type Wls vesicular pattern at exit sites. Arrowheads point to Wls at exit sites in HeLa cells. *P<0.05; **P<0.01.

Scale bars: 5 μm.

Figure 3.6

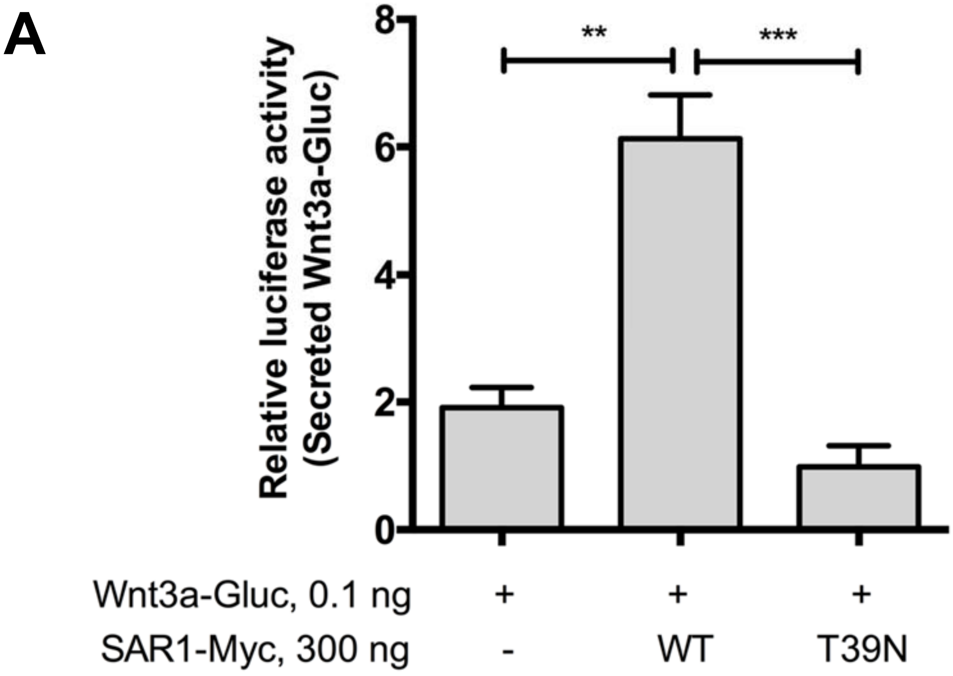
A
Relative luciferase activity
(Secreted Wnt3a-Gluc)
0
2
4
6
8
**
***
Wnt3a-Gluc, 0.1 ng
+
+
+
SAR1-Myc, 300 ng
-
WT
T39N

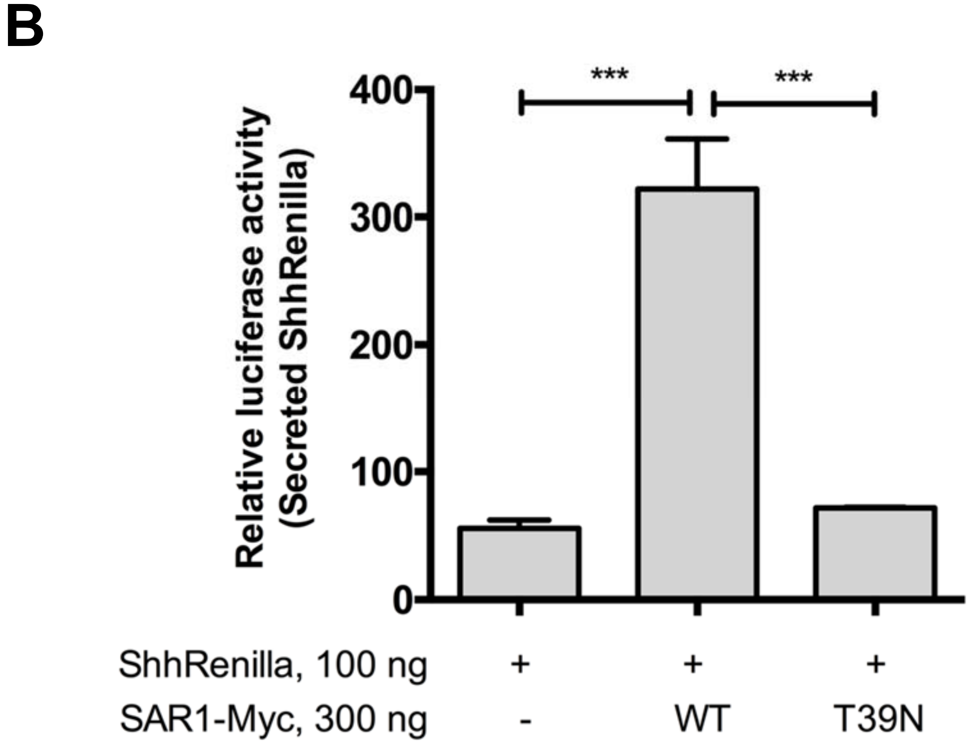
B
Relative luciferase activity
(Secreted ShhRenilla)
0
100
200
300
400
***
***
ShhRenilla, 100 ng
+
+
+
SAR1-Myc, 300 ng
-
WT
T39N

Figure 3.6 SAR1^{T39N} interferes the secretion of Wnt 3a and Shh secretion.

(A) Wnt secretion measured by dual-luciferase methods showed the Wnt3a secretory activity in Hela cells was increased by transient overexpression of a full-length SAR1, but not by a GDP-restricted form of SAR1^{T39N}. **P<0.01; ***P<0.001.

(B) The dual-luciferase assay measuring the ShhRenilla secretion showed a severe Shh secretion defect in SAR1^{T39N} expressing HeLa cells, compared to wild type Sar1 overexpressing cells. ***P<0.001.

Graph is generated from two independent experiments and each experiment contains three technical replicates.

Figure 3.7

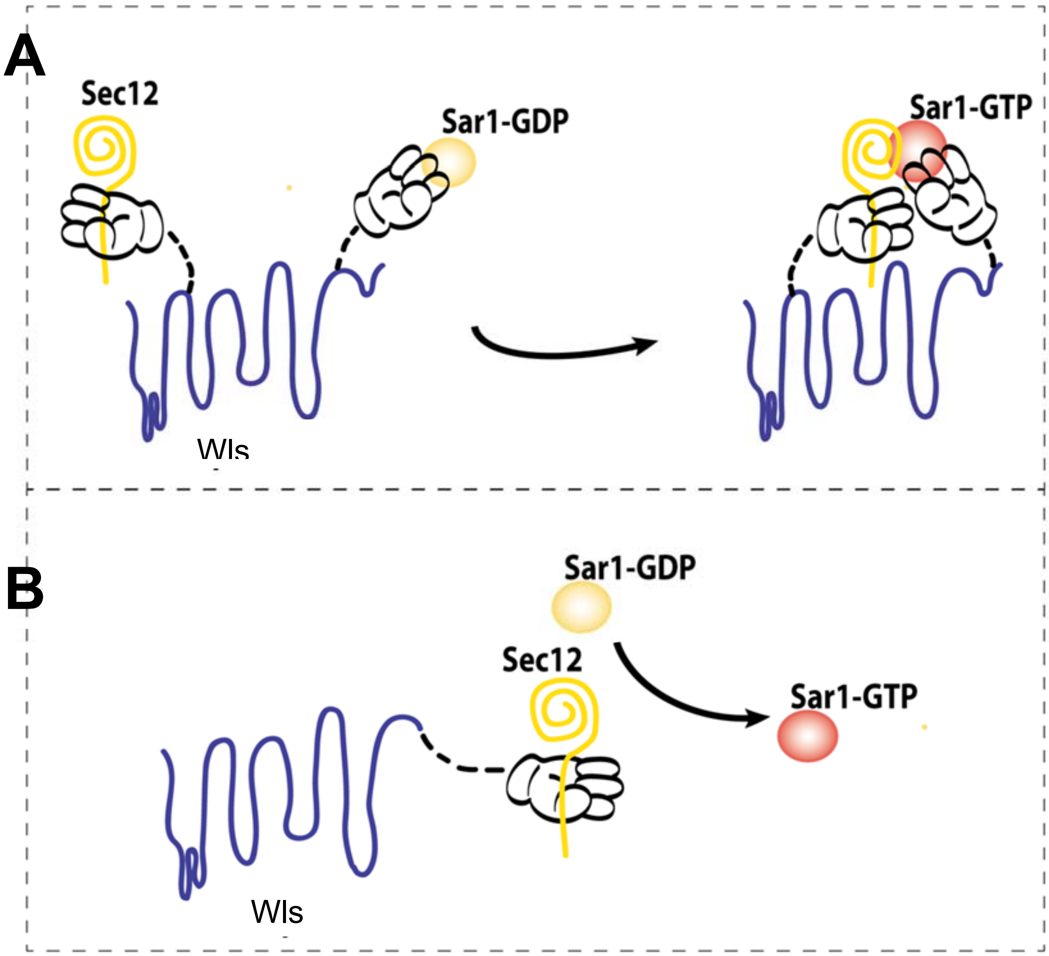
A
Sec12
Sar1-GDP
Sar1-GTP
Wls
B
Sar1-GDP
Sec12
Sar1-GTP
Wls

Figure 3.7 Two hypothetical models about the recruitment of SEC12 and SAR1 onto the ER membrane via associating with Wls

(A) Wls interacts independently with Sec12 and Sar1-GDP. The separate binding to Sec12 and Sar1 leads to the formation of a platform for activating Sar1 GTPase.

(B) Wnt interacts with Sec12, followed by Sar1 recruitment by Sec12. The recruitment of Sar1 GTPase to Wls depends Sec12, the unique GEF of Sar1.

Figure 3.8

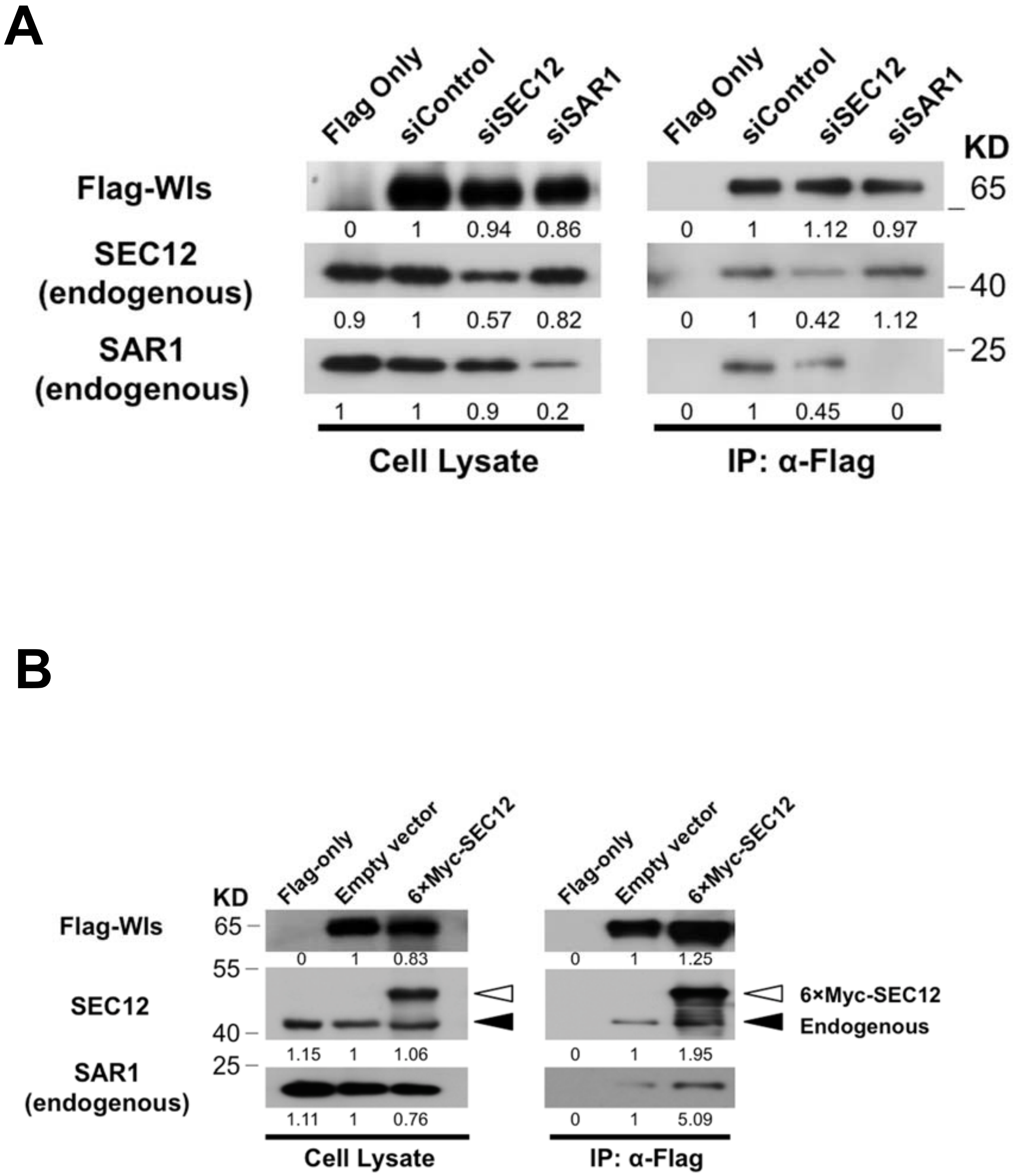
A
Flag Only
siControl
siSEC12
siSAR1
Flag Only
siControl
siSEC12
siSAR1
KD
Flag-Wls
65
0 1 0.94 0.86
0 1 1.12 0.97
SEC12 (endogenous)
40
0.9 1 0.57 0.82
0 1 0.42 1.12
SAR1 (endogenous)
25
1 1 0.9 0.2
0 1 0.45 0
Cell Lysate
IP: α-Flag
B
KD
Flag-only
Empty vector
6×Myc-SEC12
Flag-only
Empty vector
6×Myc-SEC12
Flag-Wls
65
0 1 0.83
0 1 1.25
55
SEC12
40
6×Myc-SEC12
Endogenous
1.15 1 1.06
0 1 1.95
25
SAR1 (endogenous)
1.11 1 0.76
0 1 5.09
Cell Lysate
IP: α-Flag

Figure 3.8 Recruitment of SAR1 by SEC12 promotes the association of Wls with the COPII complex

(A) Co-IP assays using anti-FLAG antibody in SEC12-knockdown or SAR1-knockdown HeLa cells lysates (stably expressing Flag-Wls) showed that SEC12 reduction affected Wls-SAR1 association, however SAR1 depletion did not affect Wls-SEC12 association. Data represent two independent experiments.

(B) Co-IP assays using anti-FLAG antibody in SEC12-overexpressing Hela cells showed that overexpression of a 6×Myc-SEC12 promoted Wls-SAR1 association. Empty and solid arrowheads pointed to 6×Myc-SEC12 and the endogenous SEC12, respectively. Data represent two independent experiments.

Figure 3.9

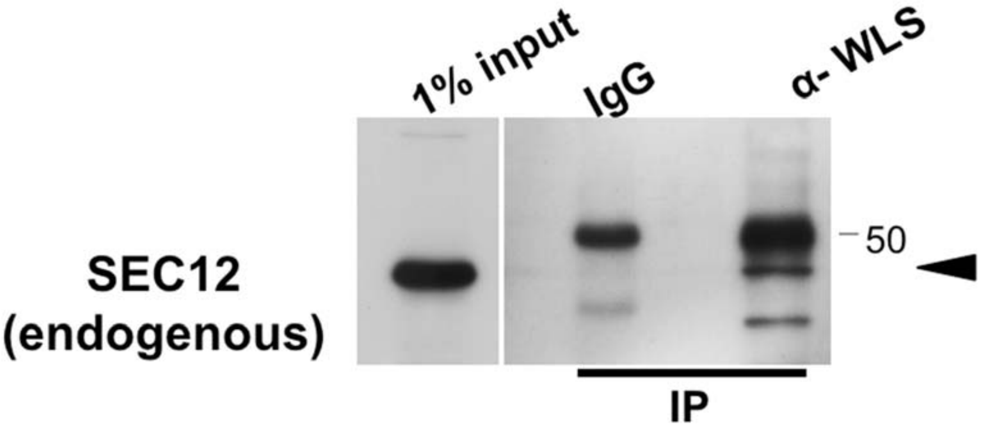
1% input
IgG
α- WLS
SEC12
(endogenous)
50
IP

Figure 3.9 Wls interacts with SEC12 endogenously.

SEC12 is co-immunopreciated with WLS in HeLa lysates by an antibody against endogenous WLS. Arrowhead pointed to endogenous SEC12. Data represent two independent experiments.

Figure 3.10

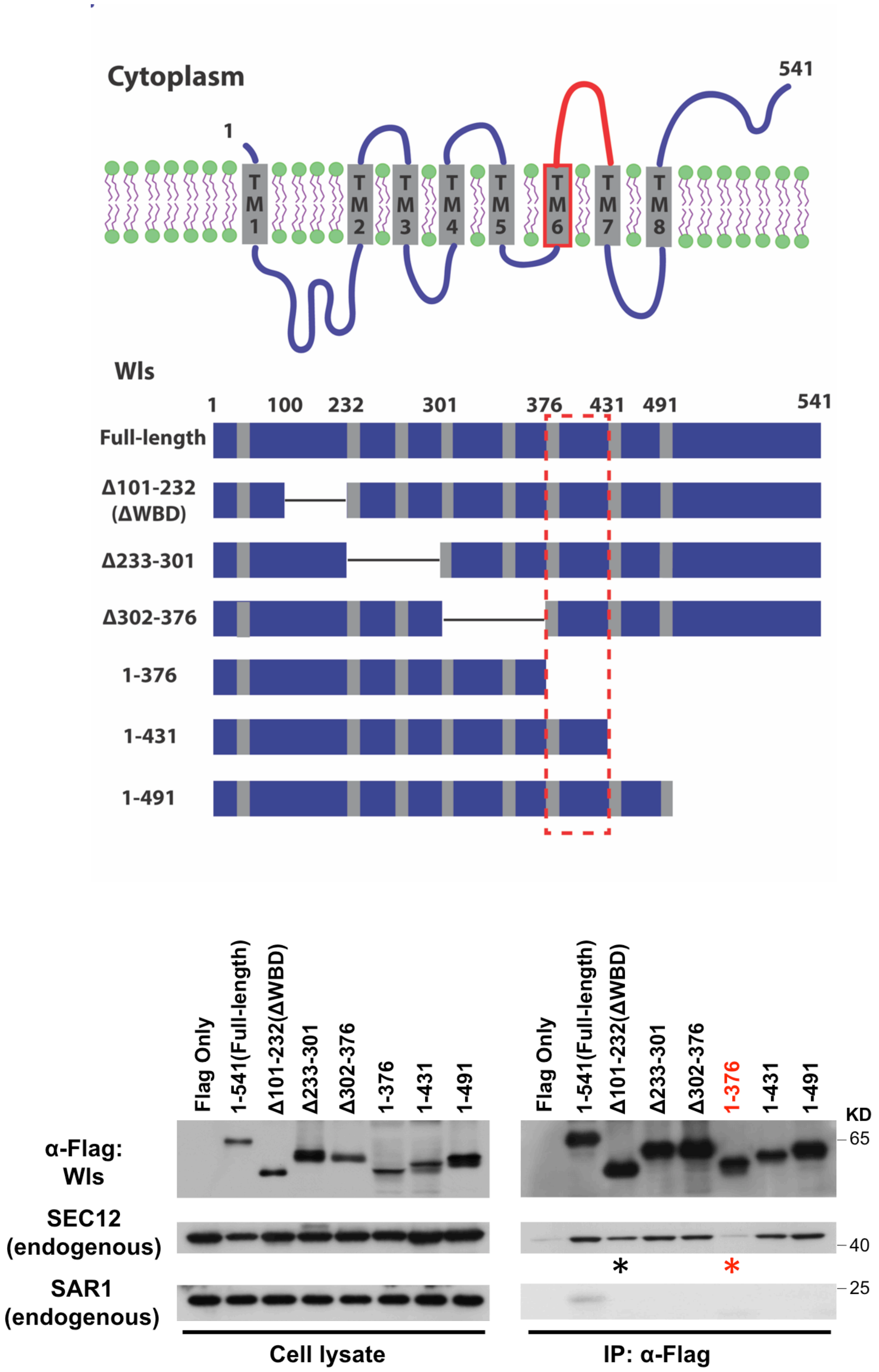
Cytoplasm
1
541
TM1
TM2
TM3
TM4
TM5
TM6
TM7
TM8
Wls
1
100
232
301
376
431
491
541
Full-length
Δ101-232 (ΔWBD)
Δ233-301
Δ302-376
1-376
1-431
1-491
Flag Only
1-541(Full-length)
Δ101-232(ΔWBD)
Δ233-301
Δ302-376
1-376
1-431
1-491
Flag Only
1-541(Full-length)
Δ101-232(ΔWBD)
Δ233-301
Δ302-376
1-376
1-431
1-491
KD
65
40
25
α-Flag: Wls
SEC12 (endogenous)
SAR1 (endogenous)
*
*
Cell lysate
IP: α-Flag

Figure 3.10 Wls-SEC12 interaction is mediated by specific domain: Wls$^{377\text{-}431}$.

(A-B) SEC12-interacting protein domain mapping in Wls was carried out using co-IP analyses (Flag antibody) with various Flag-tagged truncated Wls proteins illustrated in diagram. All mutants are generated based on the topology information of Wls protein from Ensembl Genome Browser. Wls$^{\Delta 101\text{-}232}$ is the Wnt-binding domain-deficient mutant; Wls$^{\Delta 233\text{-}301}$ lacks the first trans-membrane (TM) region (a.a. 233-251), the first cytosolic loop (CL1) (a.a. 252-264), the second TM (a.a. 265-287) and second luminal loop (LL2) (a.a. 288-301); Wls$^{\Delta 302\text{-}376}$ lacks the TM4 (a.a. 302-319), the CL2 (a.a. 320-331), the TM5 (a.a. 332-354) and the LL3 (a.a. 355-376); Wls$^{1\text{-}376}$ is the shortest truncation form lacking the TM6 (a.a. 377-401), the CL3 (a.a. 402-428), the TM7 (a.a 429-450aa), the LL4 (a.a 451-469), the TM8 (a.a. 470-491) and C-terminus (a.a. 492-541); Wls$^{1\text{-}431}$ is truncate with the deletion of the TM7 through the C-terminus. Red asterisk denoted the lost interaction between Wls$^{1\text{-}376}$ and SEC12. Red box illustrated the SEC12-interacting motif (a.a. 377-431) in a predicted cytosolic loop of Wls. Note that Wls$^{\Delta 101\text{-}232}$ lacking WBD showed a reduced SEC12 binding (black asterisk).

Figure 3.11

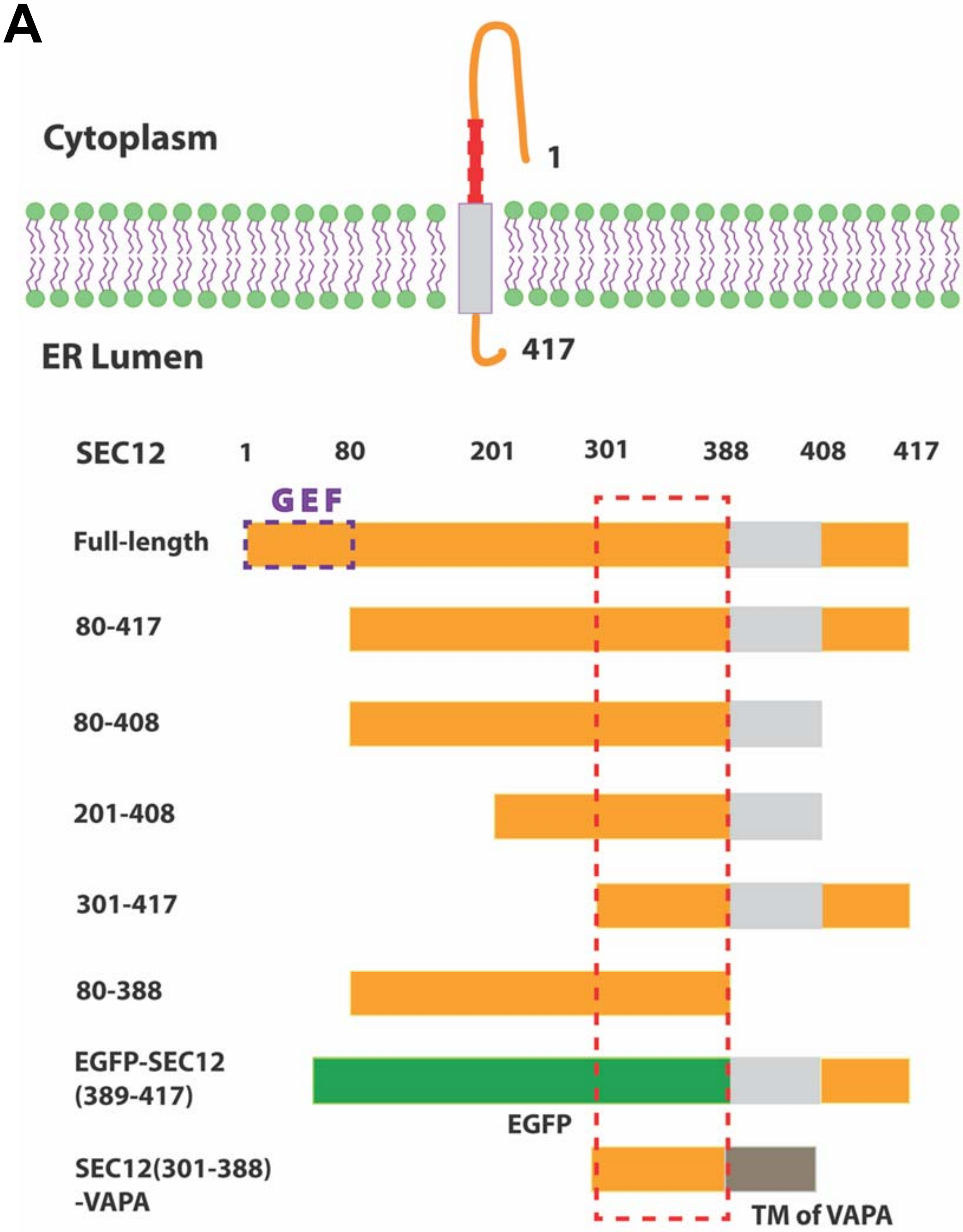
A
Cytoplasm
1
ER Lumen
417
SEC12
1
80
201
301
388
408
417
GEF
Full-length
80-417
80-408
201-408
301-417
80-388
EGFP-SEC12
(389-417)
EGFP
SEC12(301-388)
-VAPA
TM of VAPA

B

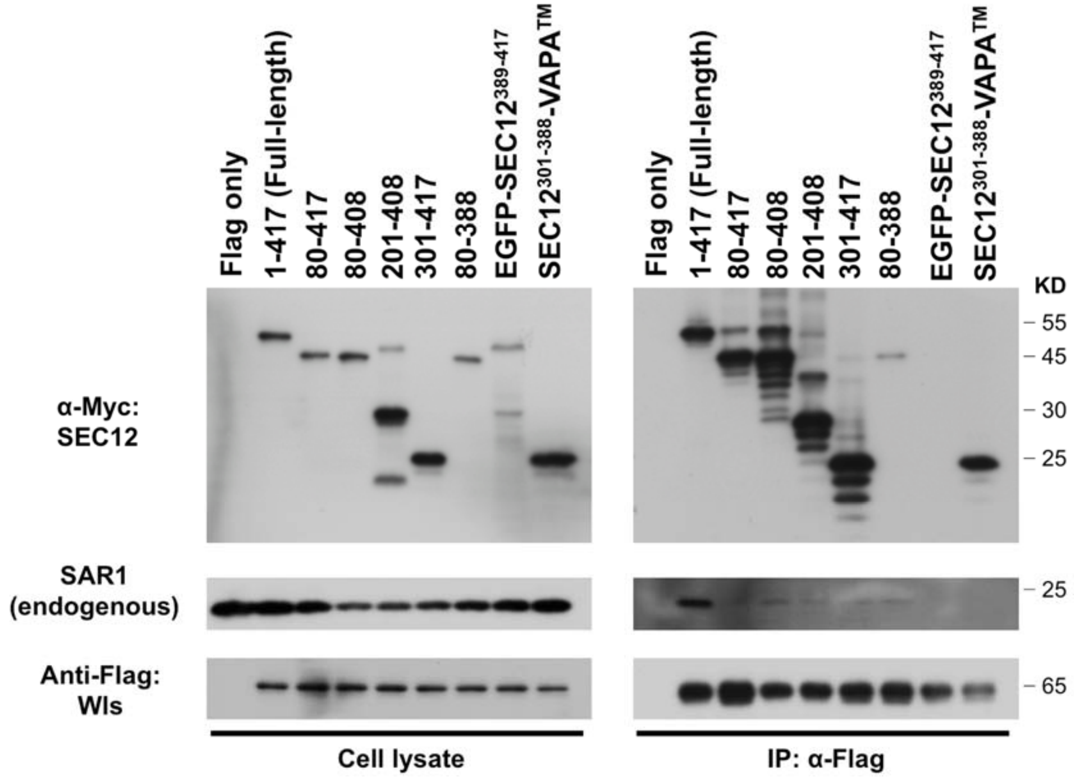
Flag only
1-417 (Full-length)
80-417
80-408
201-408
301-417
80-388
EGFP-SEC12389-417
SEC12301-388-VAPATM
Flag only
1-417 (Full-length)
80-417
80-408
201-408
301-417
80-388
EGFP-SEC12389-417
SEC12301-388-VAPATM
KD
55
45
30
25
25
65
α-Myc:
SEC12
SAR1
(endogenous)
Anti-Flag:
Wls
Cell lysate
IP: α-Flag

C

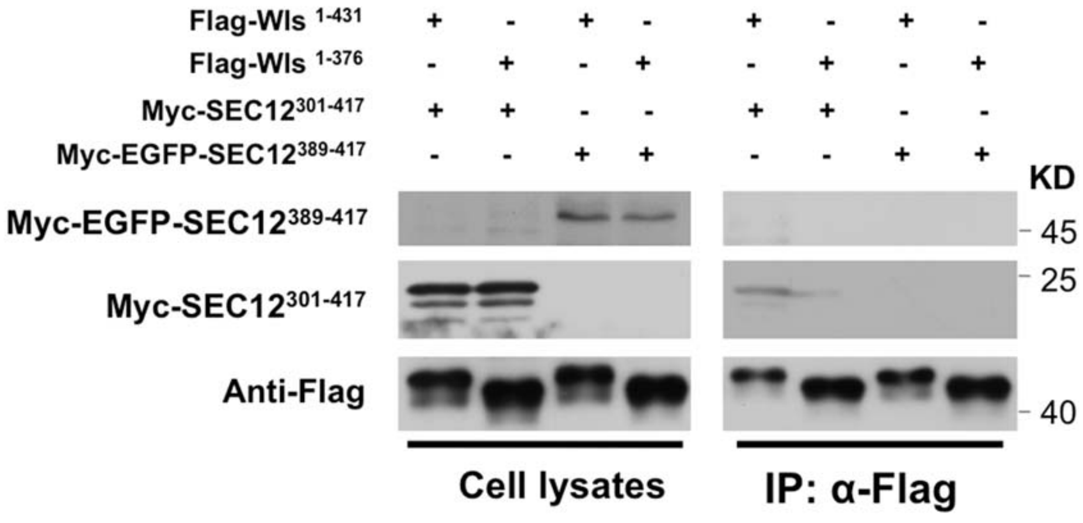
Flag-Wls 1-431
Flag-Wls 1-376
Myc-SEC12301-417
Myc-EGFP-SEC12389-417
+ - + - + - + -
- + - + - + - +
+ + - - + + - -
- - + + - - + +
KD
Myc-EGFP-SEC12389-417
Myc-SEC12301-417
Anti-Flag
45
25
40
Cell lysates
IP: α-Flag

Figure 3.11 Wls-SEC12 interaction is mediated by specific domain: SEC12$^{301-388}$.

(A-B) Similar strategy for mapping Wls-interacting SEC12 domains identified a cytosolic motif (a.a. 301-388) that is responsible for Wls association. The truncated Sec12 proteins are illustrated in diagram A. The truncated SEC12 constructs covered specific portions of the protein: N-terminal putative GEF domain cytosolic region, transmembrane domain and the ER lumen-residing C-terminal tail. Of specific note, Sec12 contains seven tryptophan-aspartic acid (WD) domains, which usually serve as scaffold sites for protein-protein interaction. Sec12 truncates (SEC12$^{80-417}$, $^{80-408}$, $^{201-408}$, $^{301-417}$, and $^{80-388}$) preserving the intact WD motifs for potential functional binding site to Wls, respectively. Note that a chimeric protein (SEC12$^{301-388}$-VAPA^{TM}) carrying the cytosolic motif (a.a. 301-388) motif fused to an independent ER transmembrane domain of VAPA (Vesicle-associated membrane protein-associated protein A) showed association with Wls.

(C) Co-IP assays using anti-MYC antibody in HeLa cells lysate showed Wls$^{1-431}$ was sufficient to bind SEC12$^{301-417}$. Data represent two independent experiments.

Figure 3.12

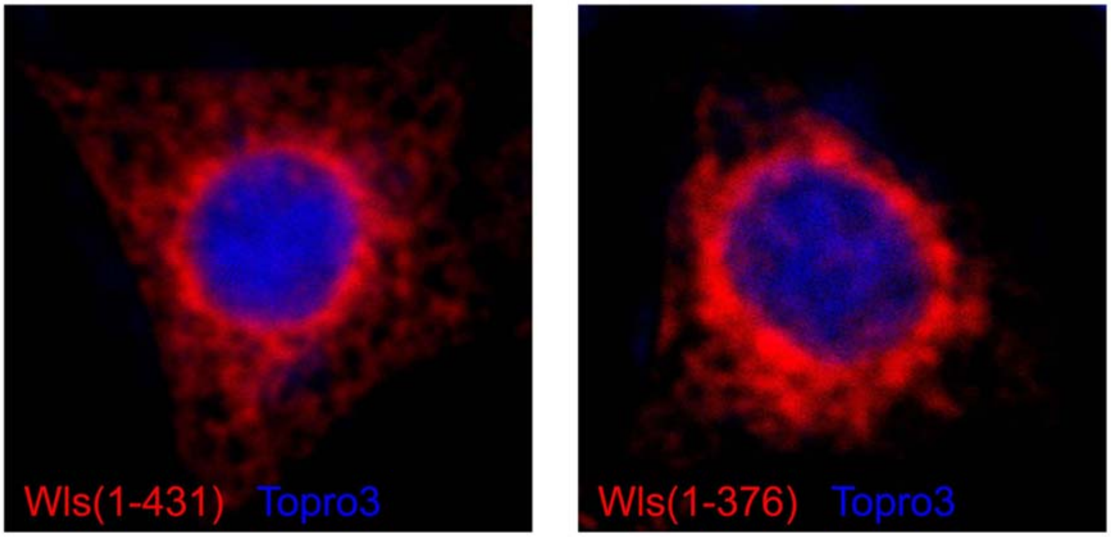
Wls(1-431) Topro3
Wls(1-376) Topro3

Figure 3.12 Truncated Wls$^{1\text{-}431}$ and Wls$^{1\text{-}376}$ (in red) do not show vesicular pattern.

Anti-FLAG immunofluorescence staining on Hela cell expressing Wls$^{1\text{-}431}$ and Wls$^{1\text{-}376}$ mutants showed both the truncated Wls$^{1\text{-}431}$ and Wls$^{1\text{-}376}$ mutants lost the vesicular distribution and appeared to be aggregated in Hela cells. Nucleus is labeled by Topro3 dye.

Figure 3.13

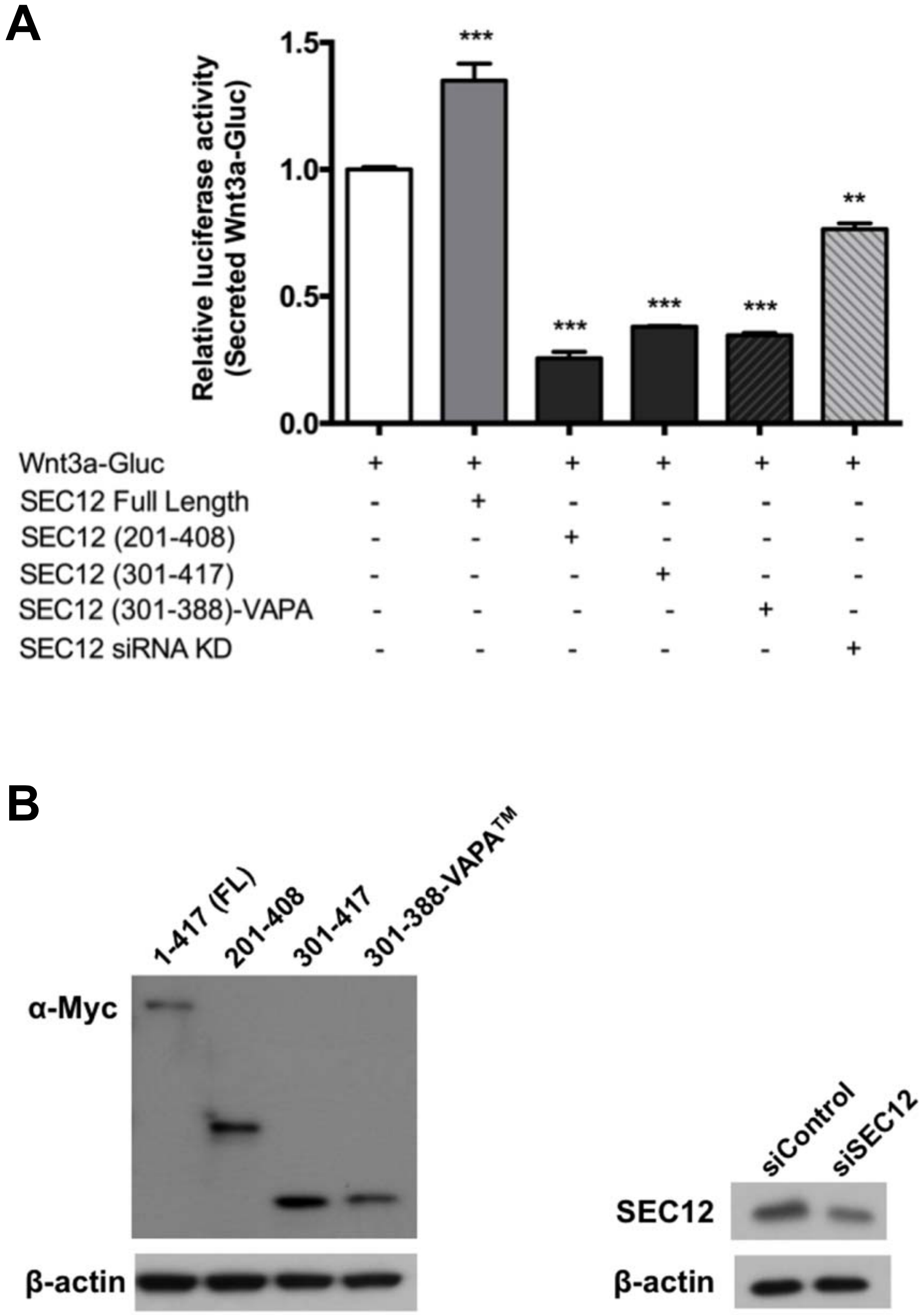
A
Relative luciferase activity (Secreted Wnt3a-Gluc)
1.5
1.0
0.5
0.0
***
***
***
***
**
Wnt3a-Gluc + + + + + +
SEC12 Full Length - + - - - -
SEC12 (201-408) - - + - - -
SEC12 (301-417) - - - + - -
SEC12 (301-388)-VAPA - - - - + -
SEC12 siRNA KD - - - - - +
B
1-417 (FL)
201-408
301-417
301-388-VAPA™
α-Myc
β-actin
siControl
siSEC12
SEC12
β-actin

Figure 3.13 SEC12 modulates Wnt secretion

(A) Inhibiting Sec12 activity impairs Wnt secretion in HEK293T cells. HEK293T cells were co-transfected with Wnt3a-Gluc and firefly luciferase, along with wild type or truncated SEC12, or SEC12-specific siRNA. Enhanced Sec12 full-length protein level increased Wnt secretion. Overexpression of Sec12 truncates (SEC12 $^{201\text{-}408}$, $^{301\text{-}417}$, $^{301\text{-}388\text{-VAPA(TM)}}$ resulted in the inhibitory effect on Wnt secretion. Knockdown Sec12 by its specific siRNA leads to a reduction of Wnt secretion. Luciferase activities were measured from culture media simultaneously harvested 4 hrs after a change of fresh medium. Data represent 2 independent experiments, each with 3 replicates. $^{**}P<0.01$; $^{***}P<0.001$.

(B) The corresponding lysates for panel A were subjected to SDS-PAGE gel and immunoblotted with anti-Sec12 antibody for the detection of overexpressed or depleted SEC12 proteins.

Figure 3.14

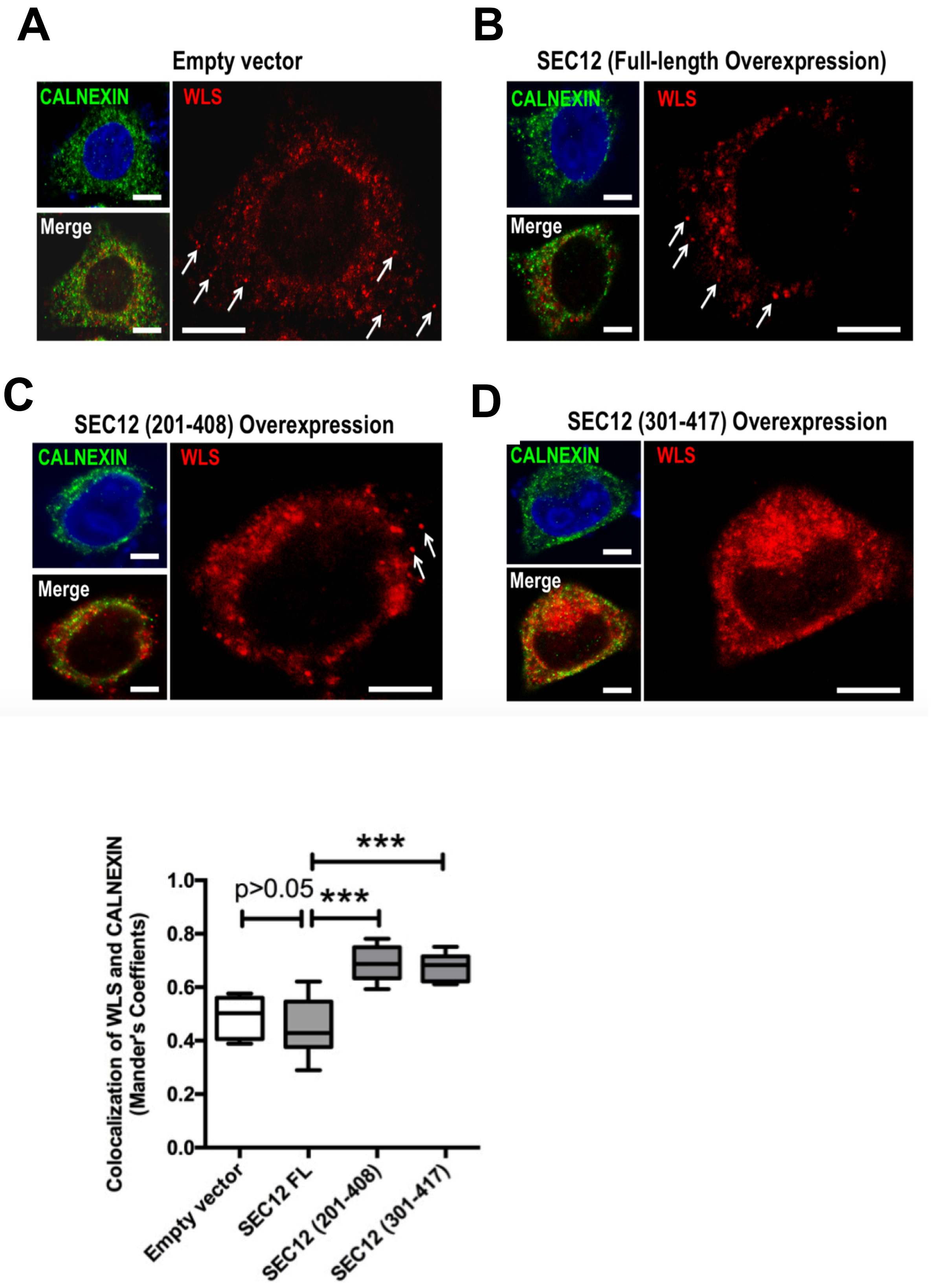
A
Empty vector
CALNEXIN
WLS
Merge
B
SEC12 (Full-length Overexpression)
CALNEXIN
WLS
Merge
C
SEC12 (201-408) Overexpression
CALNEXIN
WLS
Merge
D
SEC12 (301-417) Overexpression
CALNEXIN
WLS
Merge
Colocalization of WLS and CALNEXIN
(Mander's Coeffients)
1.0
0.8
0.6
0.4
0.2
0.0
p>0.05
***
***
Empty vector
SEC12 FL
SEC12 (201-408)
SEC12 (301-417)

Figure 3.14 SEC12 modulates Wls's subcellular distribution

(A-D) HeLa cells were transfected with empty vector (n=6), full-length SEC12 (n-7) or truncated Myc-SEC12 (7 and 9 for SEC12$^{201-408}$ and SEC12$^{301-417}$), fixed, and co-stained for endogenous WLS (red) and CALNEXIN (green). Arrows point to peripheral vesicles.

(E) Co-localization analysis by Manders' coeffieient assay showed a significant increase of WLS-CALNEXIN association in cells transfected with SEC12 truncates (SEC12 $^{201-408}$, $^{301-417}$). ***P<0.001.

Scale bars: 5 μm.

Figure 3.15

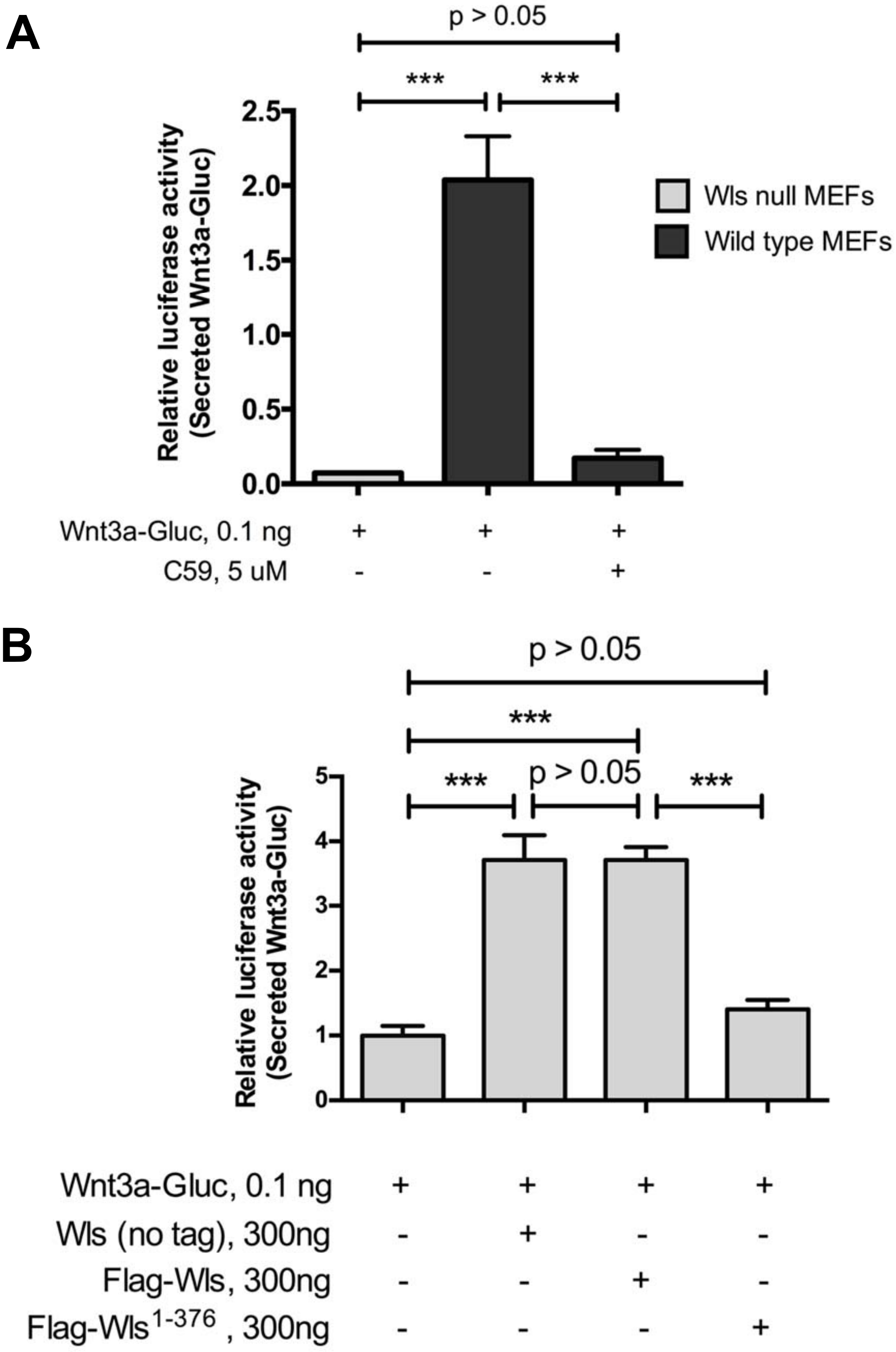
A
p > 0.05
***
***
Relative luciferase activity (Secreted Wnt3a-Gluc)
2.5
2.0
1.5
1.0
0.5
0.0
Wls null MEFs
Wild type MEFs
Wnt3a-Gluc, 0.1 ng + + +
C59, 5 uM - - +
B
p > 0.05
***
***
p > 0.05
***
Relative luciferase activity (Secreted Wnt3a-Gluc)
5
4
3
2
1
0
Wnt3a-Gluc, 0.1 ng + + + +
Wls (no tag), 300ng - + - -
Flag-Wls, 300ng - - + -
Flag-Wls1-376, 300ng - - - +

Figure 3.15 Wls$^{1\text{-}376}$, lacking the defined SEC12-binding domain, fails to support WNT secretion

(A) Wnt3a-Gluc secretion assay showed severe Wnt secretion defect in Wls-deficient MEFs, compared to wild type MEFs. The secretion by wild type MEFs was inhibited by C59 treatment. ***P<0.001. Experiment was repeated three times.

(B) Wnt secretion by Wls-deficient MEFs was increased by transient overexpression of a full-length Wls (non-tagged or Flag-tagged), but not by a SEC12-binding defective Wls$^{1\text{-}376}$. Note that the MEF secretory data were obtained on an approximately 8% transfection efficiency. ***P<0.001. Experiment was repeated six times.

Table 2. Primers for protein recombination

Generating Sequence	Forward primer	Reverse primer
Wls full-length	CCGCTCGAGACCATGGCTGGGGCAATTATAGAAA	GGAATTCATTCCTGTGCTTCTTTACGGGTCAACTTGTAG
Wls 1-497	CCGCTCGAGACCATGGCTGGGGCAATTATAGAAA	CGAATTCCTACTTATGGGATGGTGCATACAAG
Wls 1-491	CCGCTCGAGACCATGGCTGGGGCAATTATAGAAA	GGAATTCGCTTATGGGATGGTGCATACAAG
Wls 1-431	CCGCTCGAGACCATGGCTGGGGCAATTATAGAAA	GGAATTCCCTGAAGATCAGACCCTCATAGTGCA
Wls 1-376	CCGCTCGAGACCATGGCTGGGGCAATTATAGAAA	GGAATTCATTCTGTTCCAACATCTGTAGTCCAGATACTG
Wls ΔWBD	GTACACATTCCTCTCCCTTCTGTATGGTTCGCTATGAAGAC	GTCTTCATAGCGAACCATACAGAAGGGAGAGGAATGTGTAC
Wls Δ233-301	CGGAGGTTTCACTAAGATCCGACAGGGCATC	GAAGATGCCCTGTCGGATCTTAGTGAAACCTCCG
Wls Δ302-377	GCTGTTATTTGGTGACCTGGCTATGGCTTTC	GAAAGCCATAGCCAGGTCACCAAATAACAGC
Wls Y492F	TTCGCACCATCCCATAAGAACTATGGTGAAGACCAGTC	TCTTATGGGATGGTGCGAACAAGAACATCAAAGCAAAG
Wls P494A	TATGCAGCATCCCATAAGAACTATGGTGAAGACCAGTC	TCTTATGGGATGCTGCATACAAGAACATCAAAGCAAA
Wls S495A	TATGCACCAGCCCATAAGAACTATGGGGAAGAC	CTTATGGGCTGGTGCATACAAGAACATCAAAGC
Wls H496V	TATGCACCATCCGTCAAGAACTATGGGGAAGAC	CTTGACGGATGGTGCATACAAGAACATCAAAGC
Wls K497R	TATGCACCATCCCATAGGAACTATGGGGAAGAC	CCTATGGGATGGTGCATACAAGAACATCAAAGC
Sec12 full-length	CCGCTCGAGCGGGGCCGGCGCCGGGCGCCAGAGCTGTACCGGCT	CCGCTCGAGCGGCTAAAGGAAACCTGGAAAGGCACTCTG
Sec12 80-417	GGAATTCCGACATCCTTGCTGCAGGGCAGGATGCCC	CCGCTCGAGCGGCTAAAGGAAACCTGGAAAGGCACTCTG
Sec12 80-408	GGAATTCCGACATCCTTGCTGCAGGGCAGGATGCCC	CCGCTCGAGCGGCTAGAGCAGGATGGTCACAATAATAAG

Sec12 201-408	GGAATTCCGACCTGGCTTTAGGGCCTGATGGCAAGTTG	CCGCTCGAGCGGCTAGAGCAGGATGGTCACAATAATAAG
Sec12 301-417	GGAATTCCGAAGTCGTCTCCTGCCTCGATGTCAGTGAATC	CCGCTCGAGCGGCTAAAGGAAACCTGGAAAGGCACTCTG
Sec12 80-388	GGAATTCCGACATCCTTGCTGCAGGGCAGGATGCCC	CCGCTCGAGCGGCTCTCCGTGAGGGCAAC
EGFP For EGFP-Sec12	GCTCATTTCTGAAGAGGACTTGAATTCGTGAGCAAGGGCGAGGAGCTGT	GAGCAGGAGCCACACAGGAACCTTGTACAGCTCGTCCATGCCGA
VAPA For Sec12-VAPA	CTGTGGCTGTGGACAGTCGTTGCCAGCTGCATCTGTTGCCCTCACGGCGGAGTCTTCCTTCACTTCTTGTTGTAATTGCAGCCATTTTCATTGGATTCTTTCTAGGGAAATTCATCTTGTAGCTCGAG	CTCGAGCTACAAGATGAATTTCCCTAGAAAGAATCCAATGAAAATGGCTGCAATTACAACAAGAAGTGAAGGAAGACTCCGCCGTGAGGGCAACAGATGCAGCTGGCAACGACTGTCCACAGCCACAG
SAR1 H79G	CTTTTGATCTTGGTGGGGGCGAGCAAGCACGTCGC	GCGACGTGCTTGCTCGCCCCCACCAAGATCAAAAG
SAR1 T39N	GATAATGCAGGCAAAAACACTCTTCTTCACATGC	GCATGTGAAGAAGAGTGTTTTTGCCTGCATTATC
WNT3A S209A	CAAGTGCCACGGGCTGGCGGGCAGCTGC	GCAGCTGCCCGCCAGCCCGTGGCACTTG

CHAPTER 4

MULTI-PROTEIN COMPLEX MODULATES ER EXIT OF WNT-WLS FOR SECRETION

Information included in this chapter is partially taken from Sun et al. Journal of Cell Science (2017) 130, 2159-2171.

4.1 Introduction

4.1.1 Sar1 GTPase activity is crucial for the assembly and fission of COPII vesicles

COAT protein II (COPII)-coated vesicles support the protein transportation from the ER to the Golgi. A typical COPII coat consists of small GTPase Sar1 (Nakano and Muramatsu, 1989), the Sec23/24 and the Sec13/31 complex (Barlowe et al., 1994). Crucial for the regulation of COPII coat assembly is Sar1 GTPase activity. Once activated, Sar1-GTP inserts onto the ER membranes (Nishikawa and Nakano, 1993) and initiates the recruitment of the inner COPII coat components (Sec 23/24) by the direct binding to Sec23 of Sar1 (Bi et al., 2002). Sec24 is believed to function as a discriminator in forming the so called pre-budding complex (Kuehn et al., 1998), recognizing the cytosolic exposed ER exiting signaling motif(s) of trans-membrane cargo or adaptors for luminal cargo (Aridor et al., 1998; Miller et al., 2003). Human cells express four Sec24 isoforms, termed Sec24A, Sec24B, Sec24C and Sec24D (Pagano et al., 1999). They selective export of membrane proteins from the ER (Wendeler et al., 2007), possibly regulated by their distinguish distribution in ER exit site (Iwasaki et al., 2015). The formation of the pre-budding complex indeed is a cargo selection step before the coat polymerization, which Sec13/31 are recruited on Sec23/24 to form COPII vesicles (Antonny and Schekman, 2001). After the proper assembly of the

COPII vesicles, the hydrolysis of Sar1-GTP allows the fission of vesicles from the ER membrane (Bielli et al., 2005). Sec23, as a typical GTPase-activating protein (GAP) for Sar1, triggers its GTP hydrolysis (Yoshihisa et al., 1993) and the GAP activity is further stimulated by the recruitment of the outer coat Sec13/31 (Antonny et al., 2001). Above observations suggested the assembly and budding of the COPII vesicles are carefully regulated by Sar1 GTPase activity. Results in prior section have shown that Wls interacts with Sec12 and associates with Sar1. Wls$^{1\text{-}491}$ mutant remains its interaction with Sec12 but losses the Wls-Sar1 association. Thus, question remains in our Wls study regarding its ER export as that how Wls communicates with Sar1 for the secretion.

4.1.2 P24 family proteins are potential regulators of Wnt secretion at ER

The p24 family is comprised by the approximately 24-kDa type I endomembrane protein (emp24) which contains Golgi-Dynamics domain (GOLD) domain binding to cargos within ER lumen, when the carboxyl tail of emp24 protein interacts with vesicular components in cytoplasm (Bonnon et al., 2010). A genome-wide RNAi screen for Wingless (Wg, the *Drosophila* Wnt) secretion in *Drosophila* suggested the potential involvement of two p24 family proteins, Emp24 and Éclair, in ER export of Wg (Port et al., 2011). Another p24 family protein CG9053, known as Opossum in fly, was also proposed to effect the ER-to-Golgi transport of Wg, as Wg accumulated in ER in its absence (Buechling et al., 2011). Biochemical interactions between Wg and Emp24 or Opossum in *Drosophila* suggest that certain degree of regulation exists at the ligand's ER exiting steps (Buechling et al., 2011; Li et al., 2015). In mammal, the transmembrane emp24 domain-containing (TMED) proteins play key roles in regulating the intracellular protein traffic along the secretory pathway. It was important to note that above studies of Wnt and TMED/p24 shed little lights on the functional contribution of TMED/p24 to this particular process of Wg export.

4.1.3 Additional factors might regulate the ER export of Wnt-Wls via modulating Wls-Sec12 complex

Lipidation of Wnts by Porcupine in the ER is required for Wnts/Wls interaction. Wls initially binds to Wnts within the ER **(Figure. 3.2A,** shown as Wls$^{1-491}$, an ER retention mutant interacting with Wnt3a**)**. Since Wnt delivery is the major function of Wls, Wls seems to be "unnecessary" exiting from ER without carrying the important cargo Wnts. Thus, we speculate a mechanism within the cells keeping the cargo-unloaded Wls in ER.

We reported previously that the deletion of the entire C-terminal cytosolic tail of Wls (refers as Wls$^{1-491}$) resulted in its failure in associating with vesicular components (Table 3.1). However, Wls$^{1-491}$ is able to interact with Sec12, forming the Wls-Sec12 complex that is critical for Wnt secretion as we discussed in Chapter 3. We hypothesize that there is an unknown regulatory step in Wls's ER exiting machinery between Wls-Sec12 association and entering COPII vesicles. The regulatory motif of Wls in regulating the unknown mechanism hypothesized above might be located within C-terminus of Wls as $Wls^{1\text{-}491}$ mutant presented a lost-of-vesicle phenotype (Table 3.1). In Chapter 4, we will discuss how Wls-Sar1 complex mediates the incorporation of Wls into COPII vesicles and supports Wnt Secretion via the C-terminus of Wls. On the other hand, we showed TMED10, a homolog of p24delta1, associated with Wls when Wnt3a is overexpressed (Figure 3.2A). These lead to interesting question that what is the role of TMED10 in facilitating Wnt secretion. In this chapter, we will continue to explore if the interaction of Wnt/Wls triggers the ER exit of Wnt/Wls complex and how the Wls communicate with Sar1 for secretion as previously hypothesized in previous section **(4.1.1 Sar1 GTPase activity is crucial for the assembly and fission of COPII vesicles)**.

4.2 Results

4.2.1 Wls-SAR1 association is dependent on the structural integrity of Wls carboxyl terminus

Sequence alignment of Wntless across multiple animal species identified several highly conserved protein motifs **(shown in red, Figure 4.1)** within the carboxyl terminus. These include a terminally located KEAQE motif that has been documented for involvement in Golgi-to-ER retrograde traffic (Yu et al., 2014). As

Wls$^{1\text{-}491}$ that lacked the entire C-terminal cytosolic tail failed to enter COPII compartment **(Figure 4.2C)**, we then assessed the potential contribution of the Wls C-terminal domain for SEC12 and SAR1 binding. Stable cell lines expressing various Flag-tagged Wls truncates that retained (Wls$^{1\text{-}497}$) or lacked (Wls$^{\Delta 492\text{-}497}$) a conserved hexapeptide motif YAPSHK **(Figure 4.2A)** were established and propagated**.** Only full-length Wls, but none of the C-terminally truncated proteins, associated with SAR1 **(Figure 3.3A, 3.1B)**. Consistent with the previous result that the SEC12-binding motif is within the 376-431 aa of Wls, all the C-terminal truncated Wls continued to strongly bind to SEC12 **(Figure 4.2B)**. Live cell imaging (confocal microscope, LSM) showed that unlike the vesicular distributions exhibited by wild type Wls, Wls$^{\Delta 492\text{-}497}$ and Wls$^{1\text{-}491}$ showed ER retention **(**ER marked by GFP-tagged KDEL, **Figure 4.2C, D)** (Dayel et al., 1999). Interestingly, Wls$^{1\text{-}497}$, which preserved the hexapeptide motif, gained some vesicular traffic **(arrows in Figure 4.2C)**. Unlike wild type Wls, Wls$^{\Delta 492\text{-}497}$ failed to travel to plasma membrane **(Figure 4.3)**. These data suggested that Wls-SAR1 association was highly dependent on the integrity and conformation of the Wls C-terminal domain.

4.2.2 The proline-serine motif (494-495) is critical for Wls's Exit from the ER

To further elucidate the molecular function of hexapeptide motif, additional mutant Wls with single amino acid substitutions within the hexapeptide domain were generated using site-directed mutagenesis **(Figure 4.4)**. We found that the Wls^{P494A} mutant, with a proline (494) residue substituted by an alanine, showed a strong ER retention**.** A Wls^{S495A} mutant, with a serine (495) replaced by an alanine, accumulated in large perinuclear puncta and lost their plasma membrane-like localization **(Figure 4.4)**. A Wls$^{P494A/S495P}$ mutant mimicked the endoplasmic reticulum-like localization and resulted in the stronger ER retention, compared to the mutant Wls^{P494A} or Wls^{S495A} carrying single amino acid mutation. Above results suggested proline (494) and serine (495) might have synergic effects in supporting Wls's ER exit **(Figure 4.4)**.

Since proline is conformational restricted by introducing an inherent kink in the polypeptide chain, we suspected that proline 494 conferring a certain conformation to the cytosolic tail of Wls supporting its vesicular delivery. The ER retention phenotype of Wls$^{P494A/S495P}$ suggested switching Proline (494) to the adjacent position (495) couldn't rescue the Wls's vesicular traffic **(Figure 4.4)**. Co-expressing an EGFP-tagged Wls^{P494A} and a mCherry-tagged wild type Wls in the same cells demonstrated a clear blockage of traffic of Wls^{P494A} in ER compartment, compared to the wild type proteins **(Figure 4.5A)**. Same results were obtained with mCherry-tagged Wls^{P494A} and EGFP-tagged wild type Wls **(Figure 4.5B)**. We then investigate the association of Wls^{P494A} mutant with the representative components (SAR1, SEC12 and TMED10) of COPII complex by carrying out co-immunoprecipitation studies. Compared to full-length Wls,

Wls^{P494A} remained the association with SEC12, but not with SAR1 and TMED10, presenting the similar phenotype of Wls$^{\Delta 492\text{-}497}$ **(Figure 4.6)**. We further assessed the cellular compartmentalization of wild type Wls and Wls^{P494A} by using an iodixanol gradient density cell fractionation. Compared with wild type Wls, Wls^{P494A} showed increased co-sedimentation with ER fractions revealed by CALNEXIN **(Figure 4.7)**. This ER retention phenotype of Wls^{P494A} was further supported by a detected association between Wls^{P494A} and CALNEXIN **(Figure 4.7)**. According the above observations, we use Wls^{P494A} as a representative mutant to further explore the role of C-terminus in supporting the ER exit of Wls.

4.2.3 The hexapeptide and proline 494 are critical for Wls-SAR1 interaction

Only full length Wls interacted with endogenous SAR1 in our co-IP assays **(Figure 4.2B)**, thus mapping SAR1-binding sites on Wls using endogenous SAR1 turned out to be challenging. We then overexpressed Myc-tagged SAR1 in HeLa cells transiently expressing Flag-tagged Wls or various mutants. Immunoprecipitating SAR1-Myc by a Myc antibody showed co-precipitations of full length Wls and Wls$^{1\text{-}497}$ (red asterisks), but not Wls$^{\Delta 492\text{-}497}$ or Wls^{P494A} **(Figure 4.8)**. Furthermore, isolating the pre-budding COPII complexes by immunoprecipitating GTP-restricted SAR1^{H79G}-Myc also suggested a failed incorporation of Wls$^{\Delta 492\text{-}497}$ or Wls^{P494A}, compared to Wls$^{1\text{-}497}$ **(Figure 4.8)**. Above data strongly suggested that the hexapeptide, in particular the proline-serine motif

(494-495aa), constitutes a key protein interface for recognition by COPII machinery.

4.2.4 The Gold-domain containing protein TMED10 facilitates Wnt secretion

Early study regarding the molecular regulation of ER-Golgi transport suggests GPI-APs and Wnt proteins are both lipid-modified and transported similarly from the ER (Kinoshita et al., 2013). As Wls associates with TMED10 in our previous study **(Figure 3.2A, 4.6)** and the GOLD domain of TMED10 is involved in the efficient transport of glycosylphosphatidylinositol-anchored proteins (GPI-APs) from the ER (Nagae et al., 2016), we were curious to explore whether TMED10 will play a role in ER exit of Wnt-Wls complex. As shown in **Figure 4.9A**, TMED10 appears to be a negative regulator in modulating Wnt3a secretion as overexpressing TMED10 protein inhibits Wnt3a secretion in cell culture. To our surprise, down-regulation of TMED10 expression did not interfere Wnt3a secretory activities in culturing medium, providing a hint that TMED10 might be functionally redundant to other TMED proteins in supporting Wnt3a secretion in mammal **(Figure 4.9B)**. However, we can’t rule out the possibility that overexpression of TMED10 leads to protein aggregation hence disrupt the intracellular traffic of Wnt ligands, further studies on the subcellular localization of Wnt or Wls proteins responding to the regulation of TMED10 is needed. On the other hand, these observations also unveil the possibility that TMED10 might be supporting secretion of not only Wnt3a molecules, but also other Wnt isoforms.

4.2.5 Wnt-Wls interaction within ER lumen is independent of the COPII vesicles assembly

Like other C-terminally truncated Wls we reported previously (Sun et al., 2017a), Wls^{P494A} failed to bind SAR1 **(Figure 4.6 and 4.8)**, consistent with a blocked ER exit **(Figure 4.4)**. In addition, Wls^{P494A} showed an increased association with ER resident protein CALNEXIN, affirmed its ER retention phenotype **(Figure 4.4).** Interestingly, Wls^{P494A} also showed increased in binding with Wnt ligand, as illustrated by the enhanced interaction between Wls^{P494A} and WNT3A-V5, compared to wild type Wls **(Figure 4.6)**. In the meanwhile, Wls^{P494A} lost its association with COPII adaptor TMED10, which associated with full-length Wls **(Figure 3.2A; Figure 4.10)**. WNT3A molecule binds to Wls^{P494A}, a vesicle-deficient Wls mutant accumulated in ER, suggested that Wnt ligands initially bind to Wls within ER. This Wnt-Wls interaction within the ER lumen occurs before the assembly of COPII vesicles, as knocking down the COPII adaptor TMED10 in HeLa cell has no effect on WNT3A-Wls interaction **(Figure 4.10)**. However, a palmitoylation-deficient mutant WNT3A^{S209A}, which is unlikely secreted (Coombs et al., 2010), showed a weaker binding capacity towards TMED10, compared to wild-type WNT3A **(Figure 4.11)**. Above results suggested

Wnt-Wls interaction in the ER lumen occurs before the recruitment of COPII component by Wls and Wnt-Wls interaction is independent of the COPII vesicles assembly.

4.2.6 WNT7A and ACBD3 are in the same protein complex

The role of TMED10 functions may extend from a Wnt isoform-specific regulator during COPII vesicle assembly to foundational checkpoint that is serving for most of the Wnt isoforms, as the present co-immunoprecipitation analysis has shown that TMED10 is able to associate with various Wnt isoforms (1, 2B2, 3A, 5A, 7A, 9A) **(Figure 4.12)**. Previously we have detected ACBD3 in our proteomic analysis of the interactome profile of Wls (Sun et al., 2017). Here, we found that TMED10 interacts with ACBD3 upon the overexpression of WNT7A ligands **(Figure 4.12)**. The appearance of WNT7A-TMED10-ACBD3 complex lighted up the hypothesis that ACBD3 might be favorable in mediating WNT7A secretory activities and may function as a discriminator selectively support WNT7A secretion.

4.2.7 Wls-SEC12 complex responds to mature Wnt binding to Wls in the ER

Newly synthesized Wnts bind Wls in ER for exocytosis (Yu et al., 2014). We speculated that Wls’s communication with SEC12 and COPII machinery might be used to control export of mature Wnts. To determine whether Wls-Wnt binding in ER might influence Wls-SEC12 association, we first transfected a gradient amount of V5-tagged WNT3A into Flag-Wls expressing HeLa cells, and assessed the ligand effects on Wls's association with SEC12 and SAR1. Compared to the basal level of Wls-SEC12 association in cells transfected with empty-vector, a pronounced increase of Wls-SEC12 association was found in WNT3A transfected cells **(Figure 4.13)**. The level of Wls-SAR1 association was also increased, but to a less extent, by WNT3A overexpression. However, WNT3A transfection did not increase SEC12 association with Wls $^{\Delta WBD}$ lacking Wnt binding motif **(Figure 4.14).** These data suggested that an elevated Wnt synthesis and binding to Wls in ER could enhance association of Wls-COPII machinery.

As Wls transports Wnt molecules that are palmitoylated by Porcupine in ER (Herr and Basler, 2012), we used the Porcupine inhibitor, C59, to abolish Wnt lipidation (Proffitt et al., 2013) and Wnt secretion **(Figure 3.16A)**. C59 treatment drastically reduced Wls-WNT3A interaction at 10 nM, which also diminished Wls-SAR1 association **(Figure 4.15)**. Reduction of Wls-SEC12 interaction was only observed at a higher C59 concentration (50 nM) **(Figure 4.15)**, suggesting that Wls-SEC12 complex was less susceptible to Wnt-Wls dissociation. Of an important note, Wls-SEC12 binding remained readily detectable even at 50 nM C59 treatment when Wls-WNT3A interaction was completely abolished **(Figure 4.15)**. These data suggested that there was a basal level of complex formation between SEC12 and ligand-unbound (free) Wls on ER membrane.

The disrupted Wls-SAR1 association by C59 **(Figure 4.15)** was corroborated by an observed impairment of Wls vesicular pattern in live cells **(**middle panel, **Figure 4.16)**. Likewise, despite of its SEC12-binding capacity **(Figure 4.14)**, Wls$^{\Delta WBD}$ showed strong ER retention **(Figure 4.16)**. In addition, a palmitoylation-defective Wnt3a^{S209A} (Coombs et al., 2010) showed a weaker binding capacity towards Wls, compared to wild type Wnt3a **(Figure 4.17)**. When we transfected Wnt3a^{S209A} to cells, we observed a smaller effect on Wls-SEC12 association comparing to cells transfected with wild type Wnt3a **(Figure 4.17)**. Collectively, these data supported a model where mature Wnt binding to Wls in ER might relay a signal to the pre-formed Wls-SEC12 complex on ER membrane, to facilitate COPII-mediated Wnt vesicle assembly and export. However, ligand-free Wls, despite of its SEC12-binding, had limited access to SAR1 and COPII pre-budding complex, presumably avoiding unnecessary export of ligand-unbound Wls.

4.3 Discussion

4.3.1 The hexapeptide of Wls may contribute to Sar1 activation

In our study, the inhibition of Sar1 activity accumulates Wls at the ER exit site at 24 hours after transfection **(Figure 3.6)**, and the vesicular trafficking of Wls is completely blocked at 36 hours after transfection **(Figure 3.5)**. These observations suggest that the Sar1 GTPase plays a role in ER-exit of Wls. The C-terminal truncation mutant Wls$^{\Delta 492\text{-}497}$ loses its association with Sar1, suggesting the essential requirement of the conserved hexapeptide (YAPSHK) for communicating with and activating Sar1 GTPase. The crystallization and structural determination of Sec12 reveals a region of conserved residues cluster (K Loop), which is catalytically essential for interacting with Sar1. Addition of a single potassium ion stabilizes the K loop and further stimulates Sar1 activity (McMahon et al., 2012). These results suggest that positive charge ion, potassium in specific, helps in catalyzing guanine nucleotide exchange activity of Sec12. In this regard, the PS motif within the conserved hexapeptide contains a potential phosphorylated site and the add-on phosphate might act to attract the positive charge K^+ ion to the K loop. In addition, COSMIC datebase shows a substitution of threonine for lysine at position 497 in human Wls in cancer cells. This missense mutation (Wls^{K497T}) within the conserved hexapeptide of Wls may provide an additional phosphorylation site for recruiting positive charge K^+ ions. If this is the case, Wls^{K497T} might serve as a gain-of-function mutation harboring high Wnt secretion activity in cancer.

4.3.2 A potential role of GOLD-domain containing proteins in supporting Wnt secretion

GOLD-domain containing protein family has been characterized into two categories, according to the protein architecture. Proteins containing a luminal GOLD domains and anchoring in the membrane via the membrane-spanning helix are belong to the p24-like category (category 1). The second category of GOLD domain protein is that the GOLD domain located at the extreme amino or carboxyl terminus and usually with additional lipid membrane-interacting functional domains. ACBD3, encompassing an amino terminal acyl coenzyme A (acyl-CoA) binding domain protein with a carboxyl terminal GOLD domain, specifically associated with WNT7A-TMED10 complex **(Figure 4.12)**. We also showed that overexpression of TMED10 (p24δ1) decreased the Wnt3a secretion **(Figure 4.9)**. This observation is in agreement with a previous study showing that overexpression of a region of protein encompassing the GOLD domain caused disassembly of the Golgi structure and abrogated protein transport from the ER to the Golgi (Sohda et al., 2001). Above observation can be accommodated by the hypothesis regarding the dual-function of TMED10. The TMED10 (category-1) could function as double-headed adaptors that interact with a specific protein (via GOLD domain). TMED 10 could help in the assembly or the delivery of vesicular complexes by tethering specific protein to the membranes, with the GOLD domain binding the protein targets of category-2 proteins, e.g. ACBD3. The hetero-oligomerization of the category-1 and -2 proteins via the GOLD domain seems to help generating combinatorial diversity for their interactions with multiple ligands. If this were the case, TMED10-ACBD3 hetero-dimer may deliver Wnt7a ligands via their GOLD domains. Alternatively, accumulation and homo-oligomerization of category-1 protein could function as a previously unrecognized class of self-inhibition complex that prevents delivery of cargoes.

Wnt3a secretion is unaffected by the RNAi-silencing of TMED10. This result suggests the GOLD domain containing protein family would form some functionally redundant complexes in mammal and such a possibility has been partially unveiled in *Drosophila* study (Hirata et al., 2013). Several p24 protein may escort Wnts in a partially redundant manner (Buechling et al., 2011) and a small portion of Wg (*Drosophila* Wnt) is able to escape from the ER in the absence of two p24 proteins, CHOp24 and Éclair (Port et al., 2011). However, overexpression of Baiser (TMED10 in mammal) cannot rescue defects caused by depleting CHOp24 (TMED2 in mammal) or Éclair (TMED11 in mammal) (Li et al., 2015), arguing that these p24 members may still play their individual roles in the process of escorting Wnt in *Drosophila*. The potential distinguish roles in facilitating Wnts did not allow p24 proteins to be replaced by each other.

4.3.3 A ready-to-go Wls-Sec12 complex on ER membrane supports Wnt secretion

Wnt and Wls have been individually suggested to undergo retrograde Golgi-to-ER transport in COPI vesicles (Yu et al., 2014; Zhang et al., 2016). To our knowledge, this study represents the first to define Wls–SEC12 and Wls–COPII interactions. Activated SAR1 initiates the formation of COPII-coated vesicles and triggers the release of the cargo-bearing vesicles from ER. Wls appears to use the same machinery for ER exit as reported for other growth factors, including collagen type I (Jin et al., 2012), type VII (Saito et al., 2009) and the G-protein-coupled receptors, AT1R, β2-AR, α2B-AR and hCaR (Dong et al., 2008; Zhuang et al., 2010). However, the molecular basis of Wls–COPII communication differs from mechanisms proposed for other cargos. Formation of the Wls–SEC12 complex was detected in cells treated with high concentrations of Porcn inhibitor. Under these conditions, no binding between Wnt3a and Wls was detected, suggesting that there was a basal level of complex formation between Wls that was not bound to ligand (free) and SEC12 on the ER membrane. Increased production of wild-type Wnt ligands in our experiments promoted a substantial Wls–SEC12 association, a change that was not seen with mutant ligands lacking lipidation. Thus, upon receiving a signal of Wls engagement by mature Wnts from the ER lumen, the preformed Wls–SEC12 complex may be used as a ‘ready-to-go’ site for rapid SAR1 docking and activation **(Figure 37)**. In contrast, the preformed complex of collagen type VII and its transporter TANGO1–cTAGE5 (TANGO1 is also known as MIA3) recruits Sec12 to the ER exit site and subsequently triggers packaging of collagen into COPII vesicles (Saito et al., 2014), a mechanism that may not be utilized by Wls. Our data collectively indicate that a pre-formed Wls–SEC12 complex pool can be expanded or stabilized by binding of mature Wnts to

Wls, illustrating an unappreciated ligand dependent ER-exporting mechanism for Wnts. Currently it is not clear how Wnt–Wls binding in the ER influences Wls–SEC12 binding, but a probable alteration of Wls conformation may be induced by ligand engagement, which may stabilize Wls–SEC12 association or expose more SEC12-binding sites. It is noteworthy that on the plasma membrane of Wnt-receiving cells, Wnt-binding to its surface receptors, Frizzled and low-density lipoprotein receptor-related protein 5 and 6 (LRP5/6, a single-pass TM protein), results in a tertiary complex formation (MacDonald et al., 2009), a scenario with some similarities to Wnt–Wls–SEC12 complex at the ER membrane.

Phylogenetic Tree

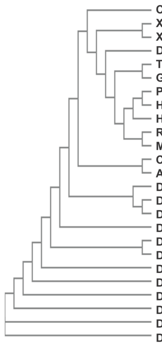

Organism	Uniprot		C-terminus	
Caenorhabditis elegans	Q7YWX7	504	YAPSHKHYRGASQLIDENDDDEIM-EDPSNQHTESNAMTTFLKPSTD-------------	549
Xenopus laevis (African clawed frog)	Q66IZ4	492	YAPSHKHYGDGQSNDGAGMS-------SGEELQLTTTITHIDGPTEVYRLAG---KEAQE	541
Xenopus laevis (African clawed frog)	Q5FWK6	492	YAPSHKHYGDGQSNDGAGMS-------SGEELQLTTTITHIDGPTELYRLAG---KEAQE	541
Danio rerio (Zebrafish) (Brachydanio rerio)	Q7T357	493	YAPSHKRYGDEQSSADQVGN-------SGEDTQLTTTITHVDGPTEIYKMTG---KEAQE	542
Taeniopygia guttata (Zebra finch)	H0ZIX6	491	YAPSHKNYGEDQSNGDLGVN-------SGEELQLTTTITHVDGPTEVYKLAR---KEAQE	540
Gallus gallus (Chicken)	Q5ZLR1	492	YAPSHKNYGEDQSNGDLGVS-------SGEELQLTTTITHVDGPTEVYKLAR---KEAQE	541
Pongo abelii (Sumatran orangutan)	Q5R9R3	492	YAPSHKNYGEDQSNGDLGVH-------SGEELQLTTTITHVDGPTEIYKLTR---KEAQE	541
Homo sapiens (Human)	Q5T9L3	492	YAPSHKNYGEDQSNGDLGVH-------SGEELQLTTTITHVDGPTEIYKLTR---KEAQE	541
Homo sapiens (Human)	Q96IV8	438	YAPSHKNYGEDQSNGDLGVH-------SGEELQLTTTITHVDGPTEIYKLTR---KEAQE	487
Rattus norvegicus (Rat)	Q6P689	492	YAPSHKNYGEDQSNGDLGVH-------SGEELQLTTTITHVDGPTEIYKLTR---KEAQE	541
Mus musculus (Mouse)*	Q6DID7	*492	YAPSHKNYGEDQSNGDLGVH-------SGEELQLTTTITHVDGPTEIYKLTR---KEAQE	541
Culex quinquefasciatus (Southern house mosquito)	B0W515	498	YAPSHKKWPANETTE-----------HIISEEIEFSNLPSDSNPSEISSLTQFARKAALD	546
Anopheles darlingi (Mosquito)	W5J8W3	498	YAPSHKKWPTNETTE-----------NIMSEEIEFSNLPSDSNPSEISSLTQFARKAAQD	546
Drosophila mojavensis	B4L184	503	YAPSHKQWPTMRHSDETTQSNENIVASAASEEIEFSNLPSDSNPSEISSLTSFTRKVAFD	562
Drosophila grimshawi (Idiomyia grimshawi)	B4J2W3	503	YAPSHKQWPTMRHSDETTQSNENIVASAASEEIEFSNLPSDSNPSEISSLTSFTRKVAFD	562
Drosophila virilis	B4LC58	503	YAPSHKQWPTMRHSDETTQSNENIVASAASEEIEFSNLPSDSNPSEISSLTSFTRKVAFD	562
Drosophila willistoni	B4N5D3	503	YAPSHKQWPSMHHSDETTQSNENIVASAASEEIEFSHLPSDSNPSEISSLTSFTRKVAFD	562
Drosophila pseudoobscura pseudoobscura	Q2LZ37	503	YAPSHKQWPTMHHSDETTQSNENIVASAASEEIEFSNLPSDSNPSEISSLTSFTRKVAFE	562
Drosophila persimilis	B4GZN1	503	YAPSHKQWPTMHHSDETTQSNENIVASAASEEIEFSNLPSDSNPSEISSLTSFTRKVAFE	562
Drosophila ananassae	B3M3X7	503	YAPSHKQWPTMHHSDETTQSNENIVASAASEEIEFSHLPSDSNPSEISSLTSFTRKVAFD	562
Drosophila erecta	B3NGS7	503	YAPSHKQWPTMHHSDETTQSNENIVASAASEEIEFSHLPSDSNPSEISSLTSFTRKVAFD	562
Drosophila yakuba	B4PF15	503	YAPSHKQWPTMHHSDETTQSNENIVASAASEEIEFNHLPSDSNPSEISSLTSFTRKVAFD	562
Drosophila sechellia	B4HEB1	503	YAPSHKQWPAMHHSDETTQSNENIVASAASEEIEFSHLPSDSNPSEISSLTSFTRKVAFD	562
Drosophila melanogaster	Q95ST2	535	YAPSHKQWPTMHHSDETTQSNENIVASAASEEIEFSHLPSDSNPSEISSLTSFTRKVAFD	594
Drosophila simulans	B4QPR1	503	YAPSHKQWPTMHHSDETTQSNENIVASAASEEIEFSHLPSDSNPSEISSLTSFTRKVAFD	562

Figure 4.1. Sequence alignment of Wntless across multiple animal species.

The sequences of C-terminal Wntless from *Caenorhabditis Elegans* to *Drosophila* were aligned by the Clustal Omega program and edited in ImageJ software. Residues numbers are labeled from individual start of the C-terminus. The conserved residues are shaded blue or purple and completely identical residues are shaded in red. Mouse Wls that would be mainly used in our study was indicated by star mark. Uniprot database names and accession numbers are as follow: Caenorhabditis elegans, Q7YWX7; Xenopus laevis (African clawed frog), Q66IZ4; Xenopus laevis (African clawed frog), Q5FWK6; Danio rerio (Zebrafish) (Brachydanio rerio), Q7T357; Taeniopygia guttata (Zebra finch), H0ZIX6; Gallus gallus (Chicken), Q5ZLR1; Pongo abelii (Sumatran orangutan), Q5R9R3; Homo sapiens (Human), Q5T9L3; Homo sapiens (Human), Q96IV8; Rattus norvegicus (Rat), Q6P689; Mus musculus (Mouse), Q6DID7; Culex quinquefasciatus (Southern house mosquito), B0W515; Anopheles darlingi (Mosquito), W5J8W3; Drosophila mojavensis, B4L184; Drosophila grimshawi (Idiomyia grimshawi), B4J2W3; Drosophila virilis, B4LC58; Drosophila willistoni, B4N5D3; Drosophila pseudoobscura pseudoobscura, Q2LZ37; Drosophila persimilis, B4GZN1; Drosophila ananassae, B3M3X7; Drosophila erecta, B3NGS7; Drosophila yakuba, B4PF15; Drosophila sechellia, B4HEB1; Drosophila melanogaster, Q95ST2; Drosophila simulans, B4QPR1.

Figure 4.2

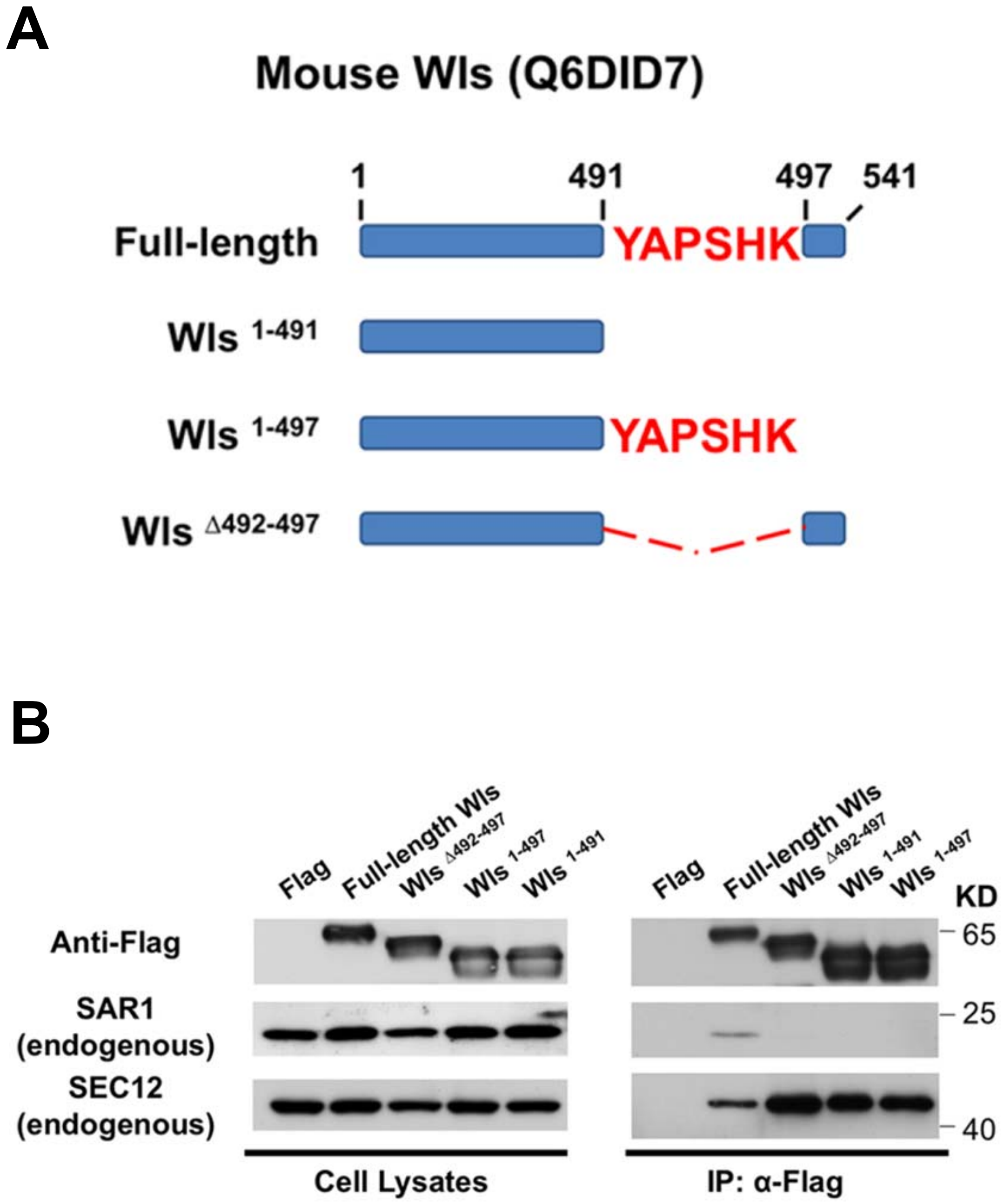
A
Mouse Wls (Q6DID7)
1
491
497
541
Full-length
YAPSHK
Wls 1-491
Wls 1-497
YAPSHK
Wls Δ492-497
B
Flag
Full-length Wls
Wls Δ492-497
Wls 1-497
Wls 1-491
Flag
Full-length Wls
Wls Δ492-497
Wls 1-491
Wls 1-497
KD
Anti-Flag
SAR1 (endogenous)
SEC12 (endogenous)
65
25
40
Cell Lysates
IP: α-Flag

C

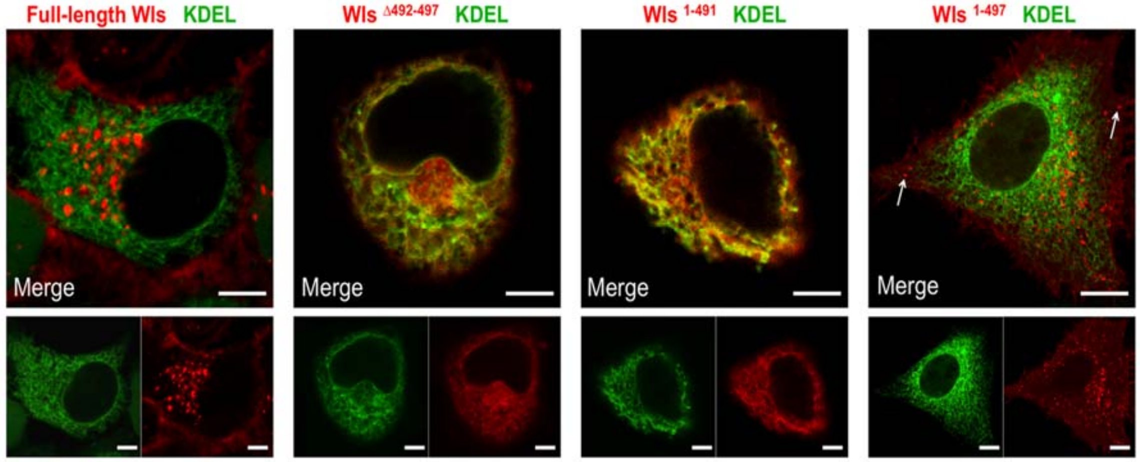
Full-length Wls KDEL
Wls Δ492-497 KDEL
Wls 1-491 KDEL
Wls 1-497 KDEL
Merge
Merge
Merge
Merge

D

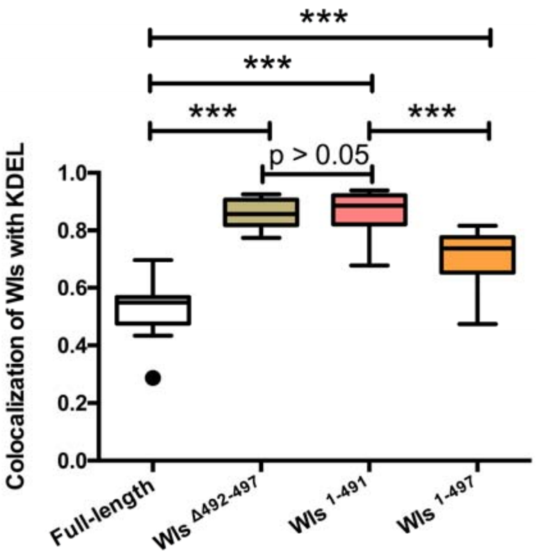
***
***
***
***
p > 0.05
Colocalization of Wls with KDEL
1.0
0.8
0.6
0.4
0.2
0.0
Full-length
Wls Δ492-497
Wls 1-491
Wls 1-497

Figure 4.2 The hexapeptide of Wls are critical for ER exit of Wls

(A) Schematic diagrams showed full-length and various C-terminally truncated Wls proteins: Wls$^{1\text{-}491}$, Wls$^{\Delta 492\text{-}497}$, and Wls$^{1\text{-}497}$.

(B) Co-IP assays using stable HeLa cell lines expressing Flag-tagged wild-type or truncated Wls showing that only wild-type Wls associated with endogenous SAR1, while all truncated Wls associated with SEC12. Data represent more than three independent experiments. Owing to the small size of the Flag peptides, they are not visualized with anti- Flag antibodies in the Flag-only samples.

(C) Live cell confocal fluorescent images of the subcellular localization of mCherry-tagged wild type (n=23) and C-terminally truncated Wls proteins (n=19, 27, and 26 for Wls$^{\Delta 492\text{-}497}$, Wls$^{1\text{-}491}$, Wls$^{1\text{-}497}$). ER was labeled by EGFP-KDEL. Scale bars: 5 μm.

(D) Colocalization analysis between Wls and ER (KDEL) by Manders' coeffieient assay showed a significant increase of WLS-KDEL association Wls$^{\Delta 492\text{-}497}$, Wls$^{1\text{-}491}$ in cells. ***P<0.001

Figure 4.3

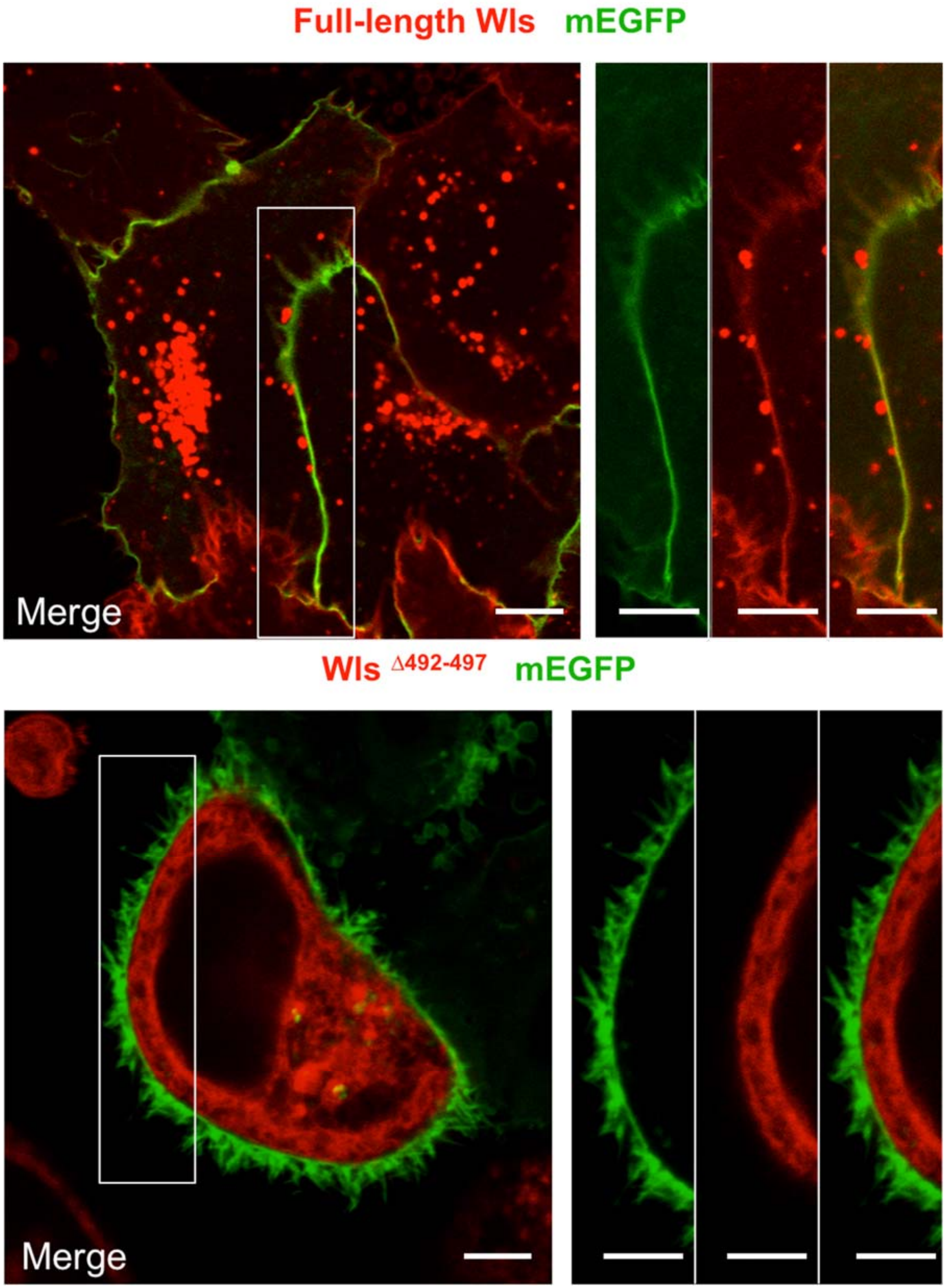
Full-length Wls mEGFP
Merge
Wls $^{\Delta 492\text{-}497}$ mEGFP
Merge

Figure 4.3 Lacking the hexapeptide prevents Wls trafficking to membrane.

Live cell confocal fluorescent images were used to visualize the subcellular localization of plasma membrane (mEGFP) and mCherry-tagged wild type or C-terminally truncated Wls$^{\Delta 492-497}$. Wls$^{\Delta 492-497}$ that lacking the hexapeptide motif showed ER retention and failed to travel to plasma membrane.

Scale bars: 5 μm.

Figure 4.4

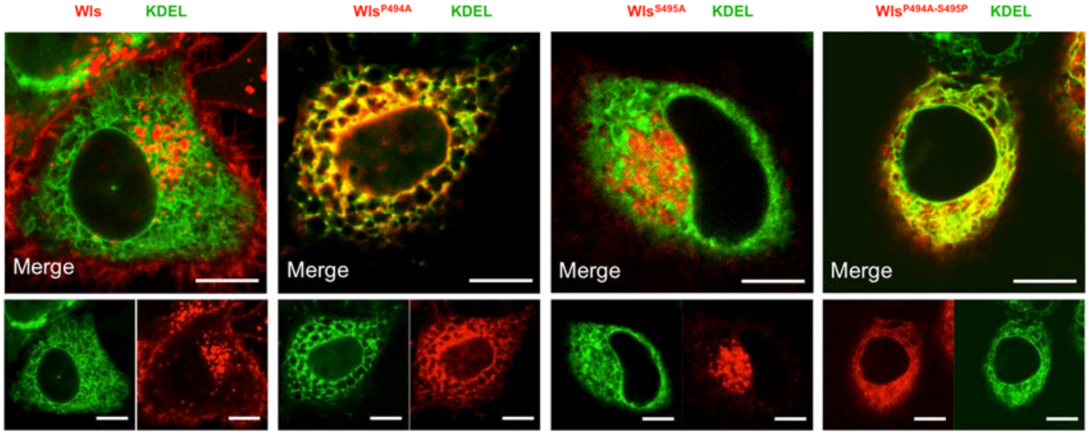
Wls
KDEL
Wls^{P494A}
KDEL
Wls^{S495A}
KDEL
Wls$^{P494A-S495P}$
KDEL
Merge
Merge
Merge
Merge

YAPSHK **(Wild type)**
YAASHK **(P494A)**
YAPAHK **(S495A)**
YAAPVK **(P494A-S495P)**

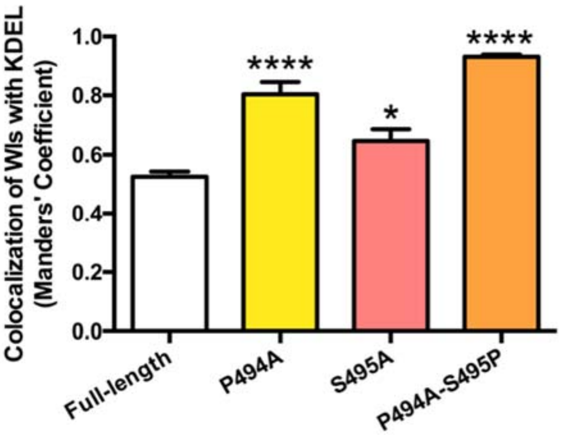

Figure 4.4 The proline 494 and serine 495 of Wls are critical for Wls's vesicular distribution

The intracellular localization of wild type and mutant Wls with single amino acid substitution was determined by confocal live cell imaging. Colocalization analysis between various Wls proteins and ER (KDEL) by Manders' coeffieient assay showed a significant increase of WLS-KDEL association in Wls^{P494A} and Wls^{S495A} cells. *, $P < 0.05$; ****, $P < 0.0001$.

Scale bars: 5 μm.

Figure 4.5

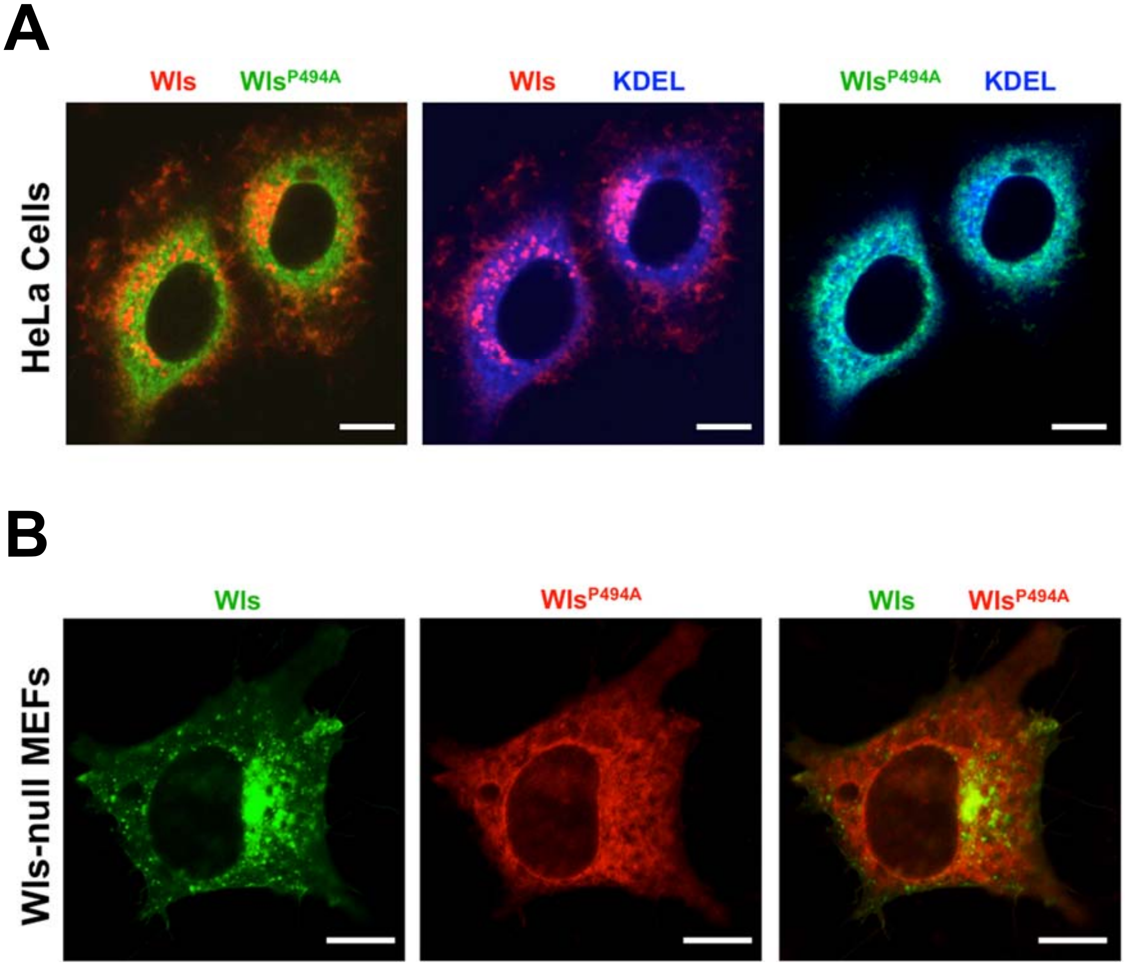
A
Wls
Wls^{P494A}
Wls
KDEL
Wls^{P494A}
KDEL
HeLa Cells
B
Wls
Wls^{P494A}
Wls
Wls^{P494A}
Wls-null MEFs

Figure 4.5 Wls^{P494A} did not affect the vesicular traffic of Wls wild type.

(A) Live cell images of HeLa cells co-expressing a mCherry-tagged wild type Wls (red) and EGFP-tagged Wls^{P494A} (green) showed that wild type Wls was localized to vesicles while Wls^{P494A} was retained in ER (blue).

(B) Live cell images of Wls-deficient MEFs co-expressing an EGFP-tagged wild type Wls (green) and a mCherry-tagged Wls^{P494A} (red) showed distinct intracellular localization patterns.

Scale bars: 5 μm.

Figure 4.6

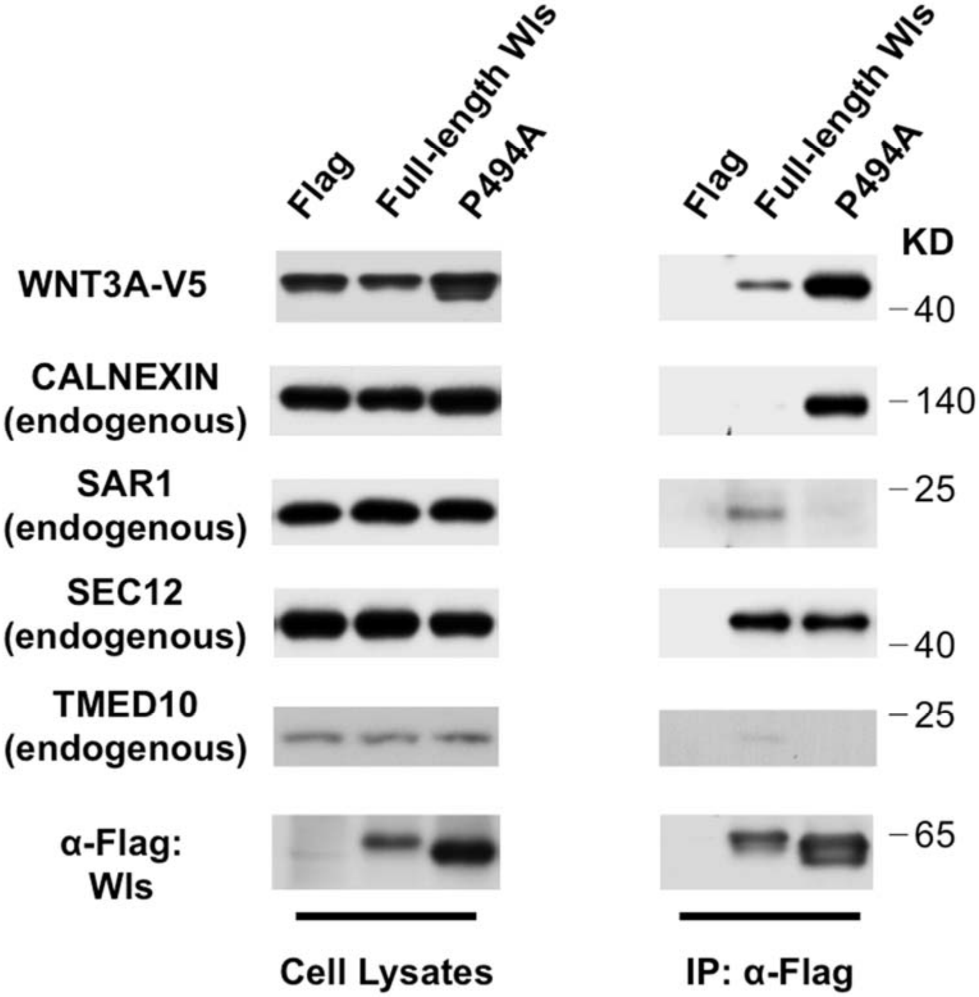
Flag
Full-length Wls
P494A
Flag
Full-length Wls
P494A
KD
WNT3A-V5
40
CALNEXIN
(endogenous)
140
SAR1
(endogenous)
25
SEC12
(endogenous)
40
TMED10
(endogenous)
25
α-Flag:
Wls
65
Cell Lysates
IP: α-Flag

Figure 4.6 Wls^{P494A}, a vesicle-deficient mutant, loses association with COPII vesicle components, but remains interaction to WNT3A and SEC12

Co-IP assays showed that, compared to wild type Wls, Wls^{P494A} lost the association with SAR1 and TMED10, but remained the binding to SEC12. Corresponding to the ER retention phenotype, Wls^{P494A} appeared to associate with CALNEXIN and increased binding to WNT3A as well.

Figure 4.7

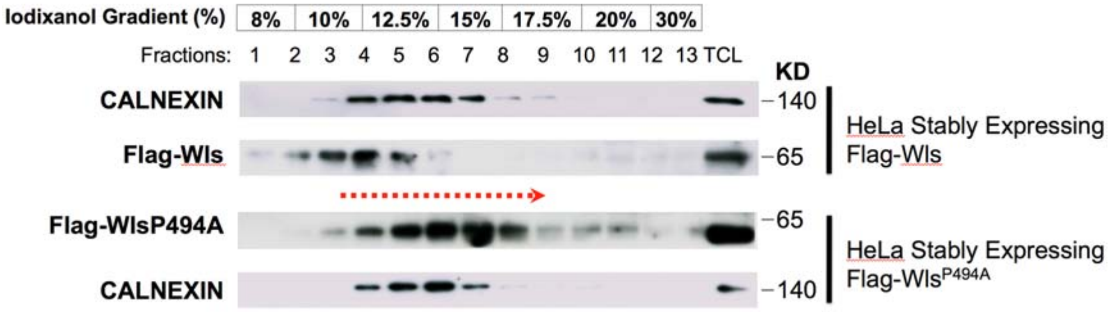
Iodixanol Gradient (%)
8%
10%
12.5%
15%
17.5%
20%
30%
Fractions: 1 2 3 4 5 6 7 8 9 10 11 12 13 TCL
KD
CALNEXIN
-140
Flag-Wls
-65
HeLa Stably Expressing Flag-Wls
Flag-WlsP494A
-65
CALNEXIN
-140
HeLa Stably Expressing Flag-Wls^{P494A}

Figure 4.7 Mutation on the proline 494 accumulates Wls within ER.

ER compartments of HeLa cells, expressing Flag-Wls or Flag-Wls^{P494A}, were isolated by cell fractionation using an iodixanol density gradient. ER fractions were identified by detection of Calnexin. Red dotted arrow indicates a right shift of Flag-Wls^{P494A}, reflecting its co-sedimentation with ER compartment.

Figure 4.8

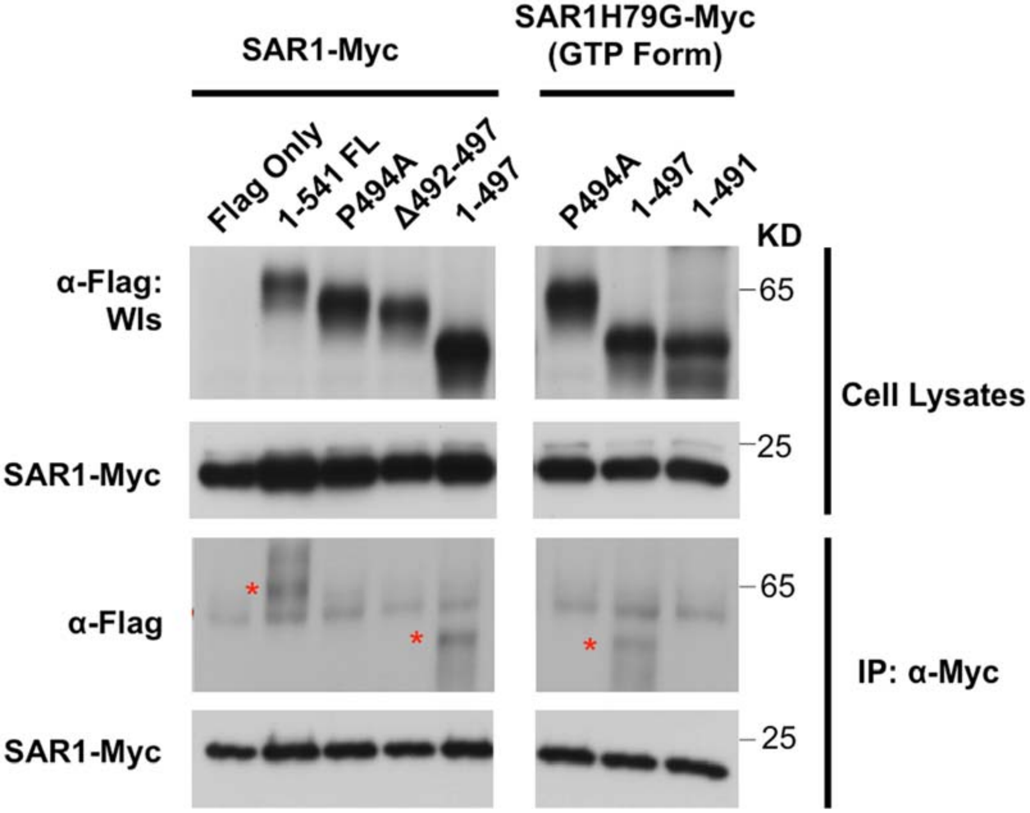
SAR1-Myc
SAR1H79G-Myc
(GTP Form)
Flag Only
1-541 FL
P494A
Δ492-497
1-497
P494A
1-497
1-491
KD
α-Flag:
Wls
65
SAR1-Myc
25
Cell Lysates
α-Flag
*
*
*
65
IP: α-Myc
SAR1-Myc
25

Figure 4.8 The hexapeptide and proline 494 is critical for Wls-SAR1 interaction

Co-IP assays using Myc antibody on HeLa cells overexpressing wild type SAR1-Myc or SAR1^{H79G}-Myc show that Wls^{P494A} and Wls$^{\Delta 492\text{-}497}$ fail to associate with SAR1. Wls^{P494A} and Wls$^{1\text{-}491}$ fail to associate with the GTP-restricted SAR1^{H79G}. In contrast, full length and Wls$^{1\text{-}497}$ show association with SAR1 (denoted by red asterisks).

Figure 4.9

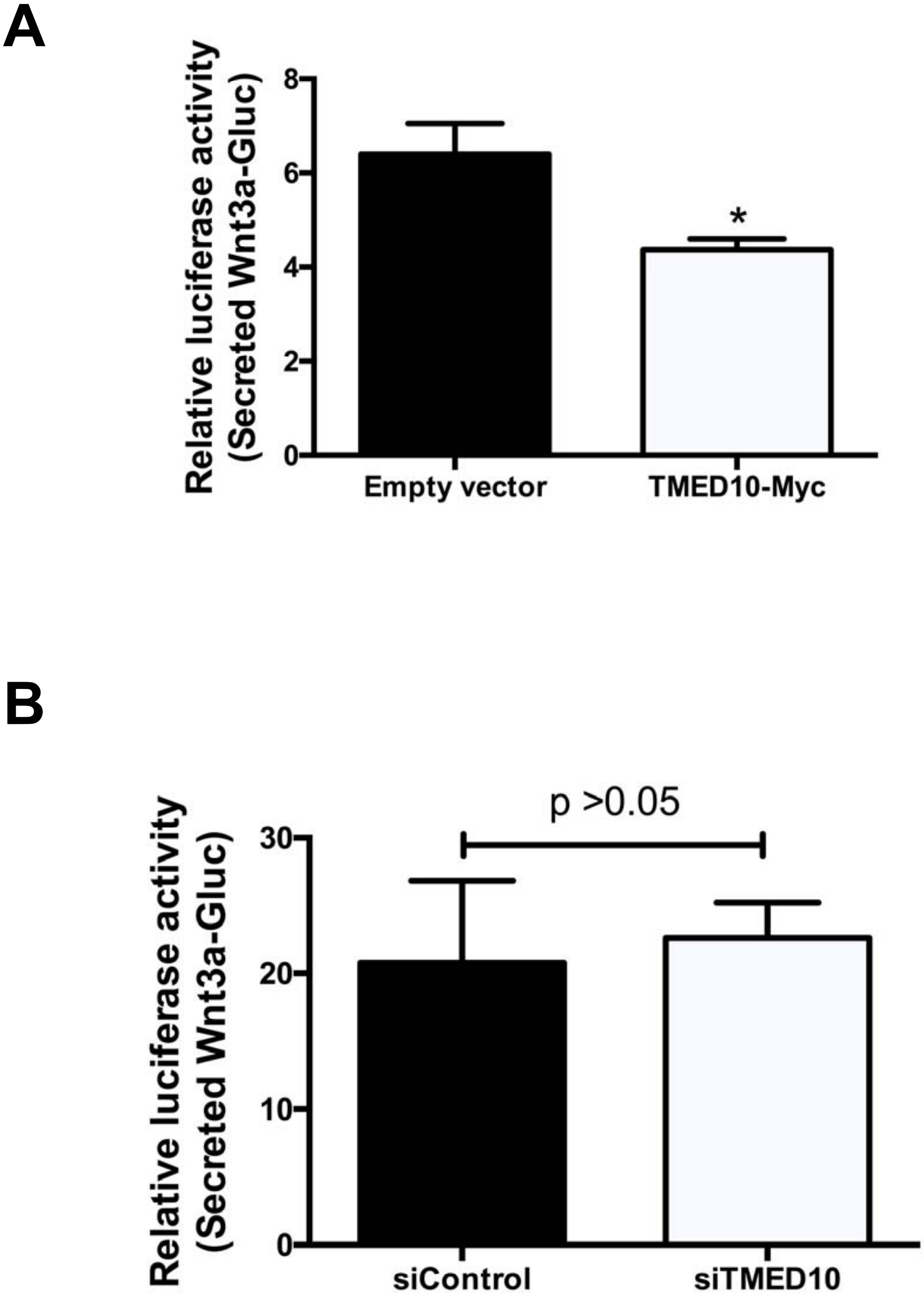
A
Relative luciferase activity
(Secreted Wnt3a-Gluc)
0
2
4
6
8
*
Empty vector
TMED10-Myc
B
Relative luciferase activity
(Secreted Wnt3a-Gluc)
0
10
20
30
p >0.05
siControl
siTMED10

Figure 4.9 TMED10 modulates WNT3A secretion

(A) Wnt3a secretion measured by dual-luciferase methods showed severe Wnt secretion defect in TMED10-overexpressing HEK293T cells, compared to empty vector-transfected cells. *P<0.01; Experiment was repeated twice.

(B) The dual-luciferase assay measuring the Wnt secretion showed Wnt3a secretory activity was not significantly affected knocking down TMED10. Experiment was repeated three times.

Figure 4.10

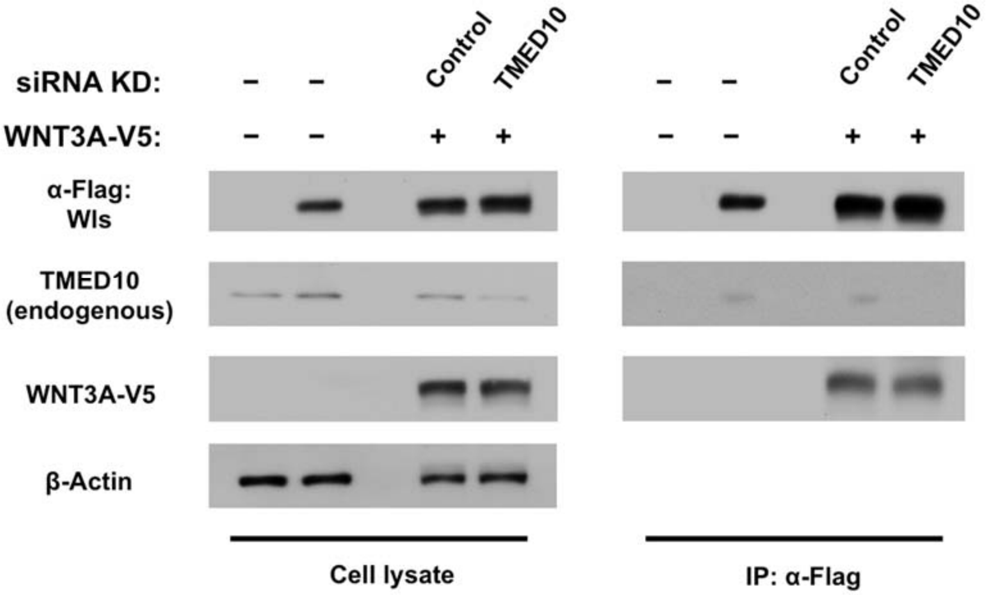
siRNA KD:
– – Control TMED10
– – Control TMED10
WNT3A-V5:
– – + +
– – + +
α-Flag: Wls
TMED10 (endogenous)
WNT3A-V5
β-Actin
Cell lysate
IP: α-Flag

Figure 4.10 TMED10 did not affect the Wnt3a-Wls interaction

Co-IP assays were performed on Flag-Wls-expressing HeLa cells transiently transfected WNT3A plasmids and siRNA targeting scramble sequences or TMED10 sequences. Lysate from 3×Flag peptide-expressing HeLa cell serves as the blank for Co-IP assays and no non-specific binding was detected in 3×Flag peptide-expressing cell lane. TMED10 reduction did not affect Wls-WNT3A interaction. Data represent two independent experiments.

Figure 4.11

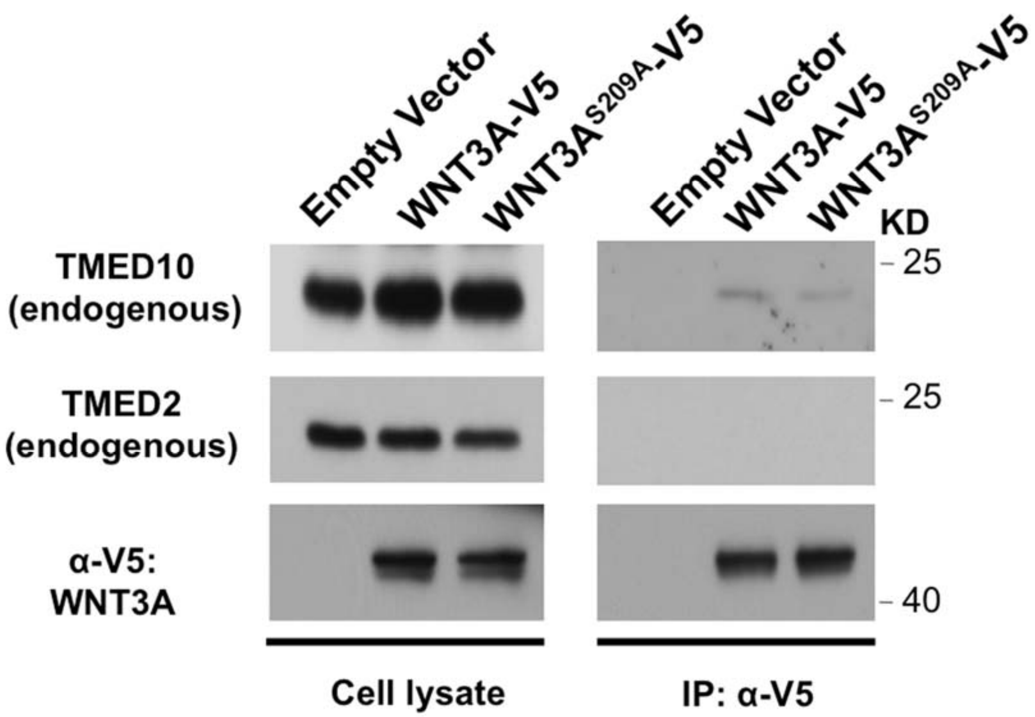
Empty Vector
WNT3A-V5
WNT3A^{S209A}-V5
Empty Vector
WNT3A-V5
WNT3A^{S209A}-V5
KD
TMED10
(endogenous)
25
TMED2
(endogenous)
25
α-V5:
WNT3A
40
Cell lysate
IP: α-V5

Figure 4.11 WNT3A^{S209A}, a lipid-deficient mutant, is less associated TMED10.

Co-IP assays were performed on HEK293T cells transiently transfected wild type WNT3A and WNT3A^{S209A} plasmids. V5-Immunoprecipitates assay showed that, compared to wild type WNT3A-transfected cells, cells that were transfected with WNT3A^{S209A} with less Sec12-binding capacity also showed less Wls-TMED10 association.

Figure 4.12

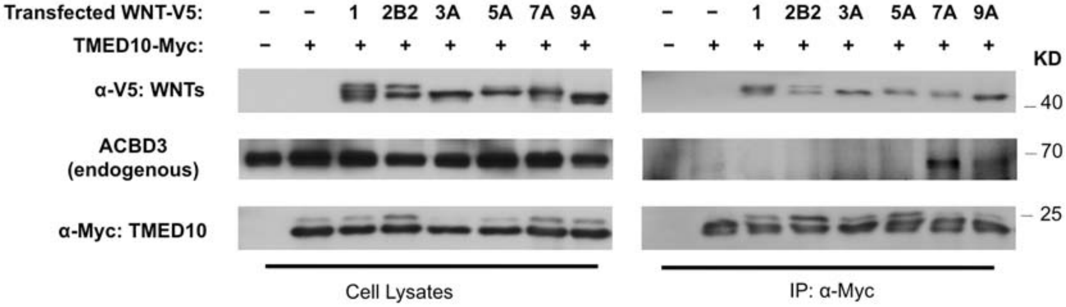
Transfected WNT-V5: − − 1 2B2 3A 5A 7A 9A − − 1 2B2 3A 5A 7A 9A
TMED10-Myc: − + + + + + + + − + + + + + + +
KD
α-V5: WNTs
40
ACBD3 (endogenous)
70
α-Myc: TMED10
25
Cell Lysates
IP: α-Myc

Figure 4.12 The association of TMED10 and ACBD3 is triggered by the over-expression of WNT7A ligand

Co-IP assays were performed on HEK293T cells transiently transfected myc-TMED10 and WNT-V5 (1, B2, 3A, 5A, 7A or 9A) plasmids. Co-IP assays by anti Myc antibody showed that, TMED10 is able to associate with various Wnt ligands (1, B2, 3A, 5A, 7A or 9A). Upon the over-expression of different WNT ligands, TMED10 is specific associated with ACBD3 responding to the overexpression of WNT7A ligands.

Figure 4.13

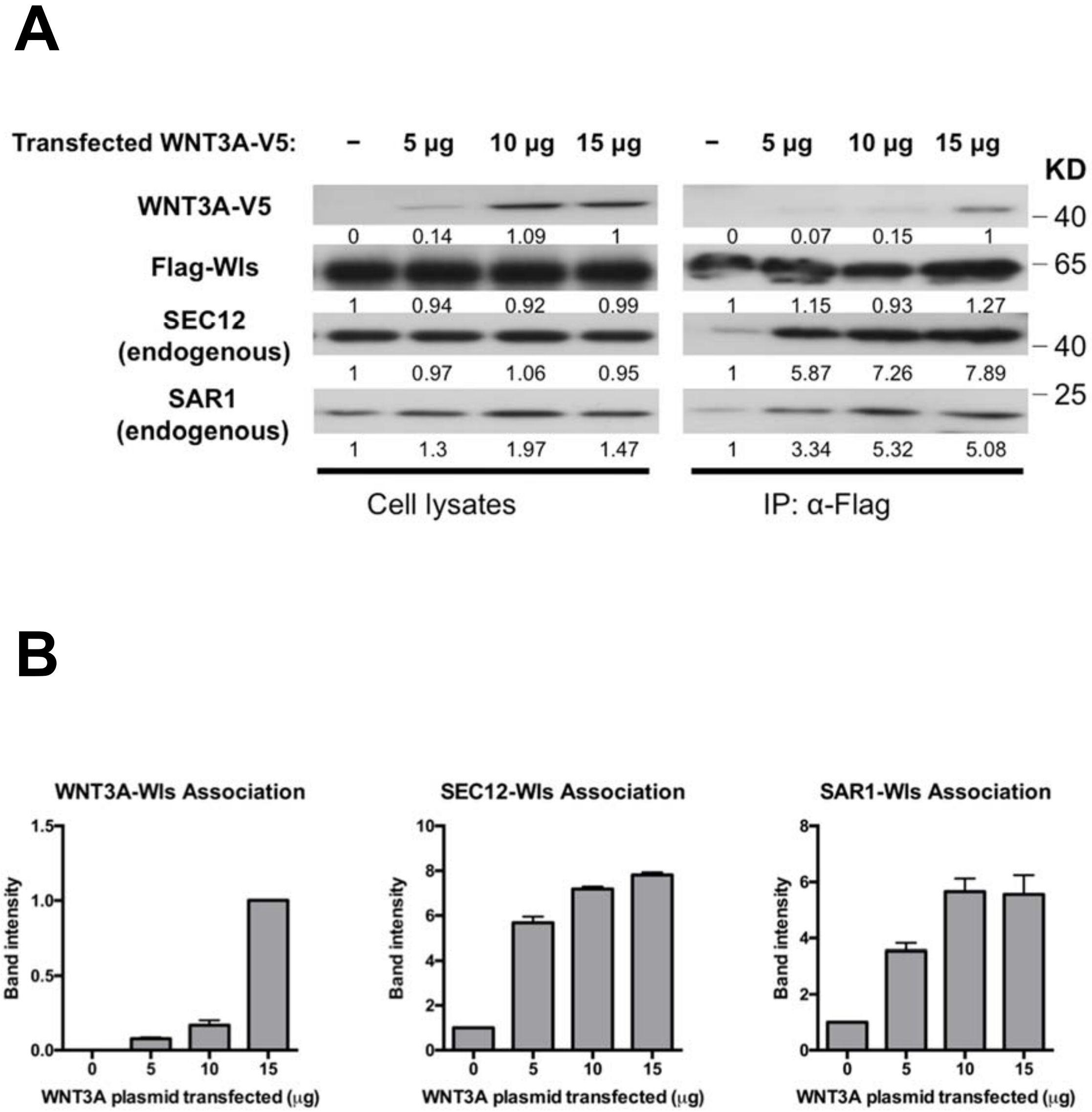
A
Transfected WNT3A-V5:
–
5 μg
10 μg
15 μg
–
5 μg
10 μg
15 μg
KD
WNT3A-V5
0 0.14 1.09 1
0 0.07 0.15 1
40
Flag-Wls
1 0.94 0.92 0.99
1 1.15 0.93 1.27
65
SEC12 (endogenous)
1 0.97 1.06 0.95
1 5.87 7.26 7.89
40
SAR1 (endogenous)
1 1.3 1.97 1.47
1 3.34 5.32 5.08
25
Cell lysates
IP: α-Flag
B
WNT3A-Wls Association
Band intensity
0.0
0.5
1.0
1.5
0
5
10
15
WNT3A plasmid transfected (μg)
SEC12-Wls Association
Band intensity
0
2
4
6
8
10
0
5
10
15
WNT3A plasmid transfected (μg)
SAR1-Wls Association
Band intensity
0
2
4
6
8
0
5
10
15
WNT3A plasmid transfected (μg)

Figure 4.13 Overexpressing WNT3A-V5 increases SEC12 association with Wls.

(A) Co-IP assays were performed on HeLa cells stably expressing Flag-Wls and being transiently transfected 5-15 μg of WNT3A-V5. Co-IP assays by anti Flag antibody showed that overexpressing WNT3A-V5 (5, 10, and 15 μg of plasmids) in HeLa cells increased Wls-SEC12 and Wls-SAR1 associations.

(B) Quantification of band intensity from panel A showed that SEC12-Wls and SAR1-Wls associations are increased because of the induction of Wnt-Wls interaction.

Figure 4.14

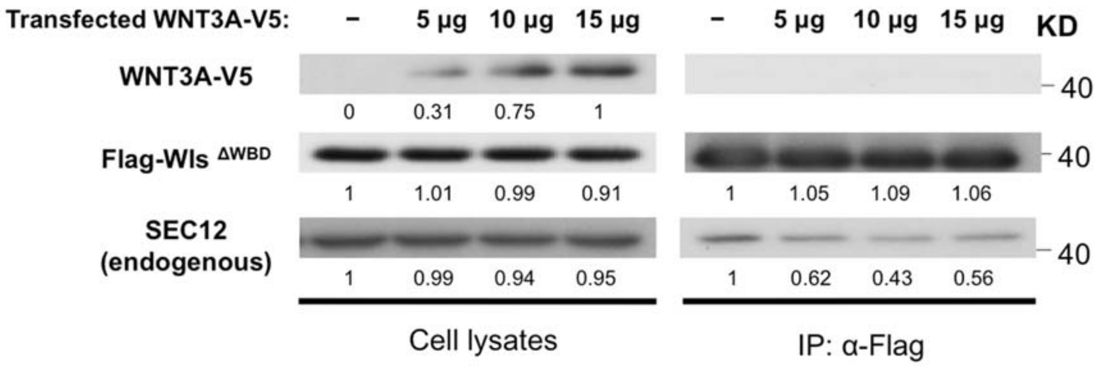
Transfected WNT3A-V5:
–
5 μg
10 μg
15 μg
–
5 μg
10 μg
15 μg
KD
WNT3A-V5
0
0.31
0.75
1
40
Flag-Wls ΔWBD
1
1.01
0.99
0.91
1
1.05
1.09
1.06
40
SEC12 (endogenous)
1
0.99
0.94
0.95
1
0.62
0.43
0.56
40
Cell lysates
IP: α-Flag

Figure 4.14 Overexpressing WNT3A-V5 did not increases SEC12 association with Wls$^{\Delta WBD}$

Co-IP assays were performed on HeLa cells stably expressing Flag-Wls$^{\Delta WBD}$ protein and being transiently transfected 5-15 μg of WNT3A-V5 (same setting of experiment in Figure 4.13). Co-IP assays showed that similar overexpressing WNT3A-V5 in HeLa cells did not increase SEC12 association with Wls$^{\Delta WBD}$ that was deficient in Wnt-binding.

Figure 4.15

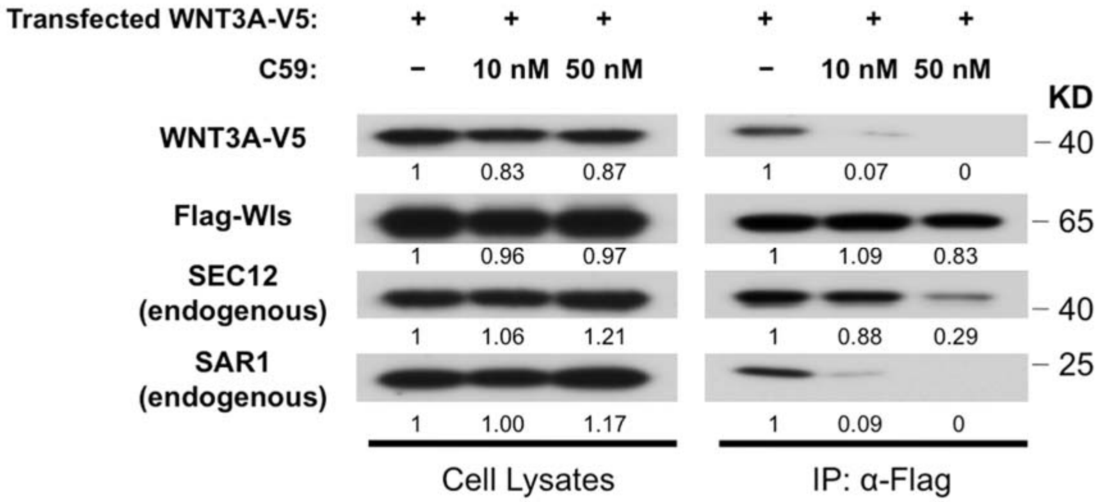
Transfected WNT3A-V5:
+
+
+
+
+
+
C59:
–
10 nM
50 nM
–
10 nM
50 nM
KD
WNT3A-V5
1
0.83
0.87
1
0.07
0
40
Flag-Wls
1
0.96
0.97
1
1.09
0.83
65
SEC12 (endogenous)
1
1.06
1.21
1
0.88
0.29
40
SAR1 (endogenous)
1
1.00
1.17
1
0.09
0
25
Cell Lysates
IP: α-Flag

Figure 4.15 Addition of C59 in cell culture reverses the Wnt-triggered Wls-Sec12 association

Co-IP assays were performed on HeLa cells stably expressing Flag-Wls protein and being incubated with 10 or 50 nM of C59. Cell lysates were collected after 24 hours since the C59 incubation started. Co-IP assays showed that treatment of HeLa cells with porcupine inhibitor C59 (10 or 50 nM) diminished Wls-WNT3A and Wls-SAR1 associations. Note that 50 nM C59 only reduced, but not abolished, Wls-SEC12 complex formation. Vehicle (DMSO) was used on cells that were not treated with C59.

Figure 4.16

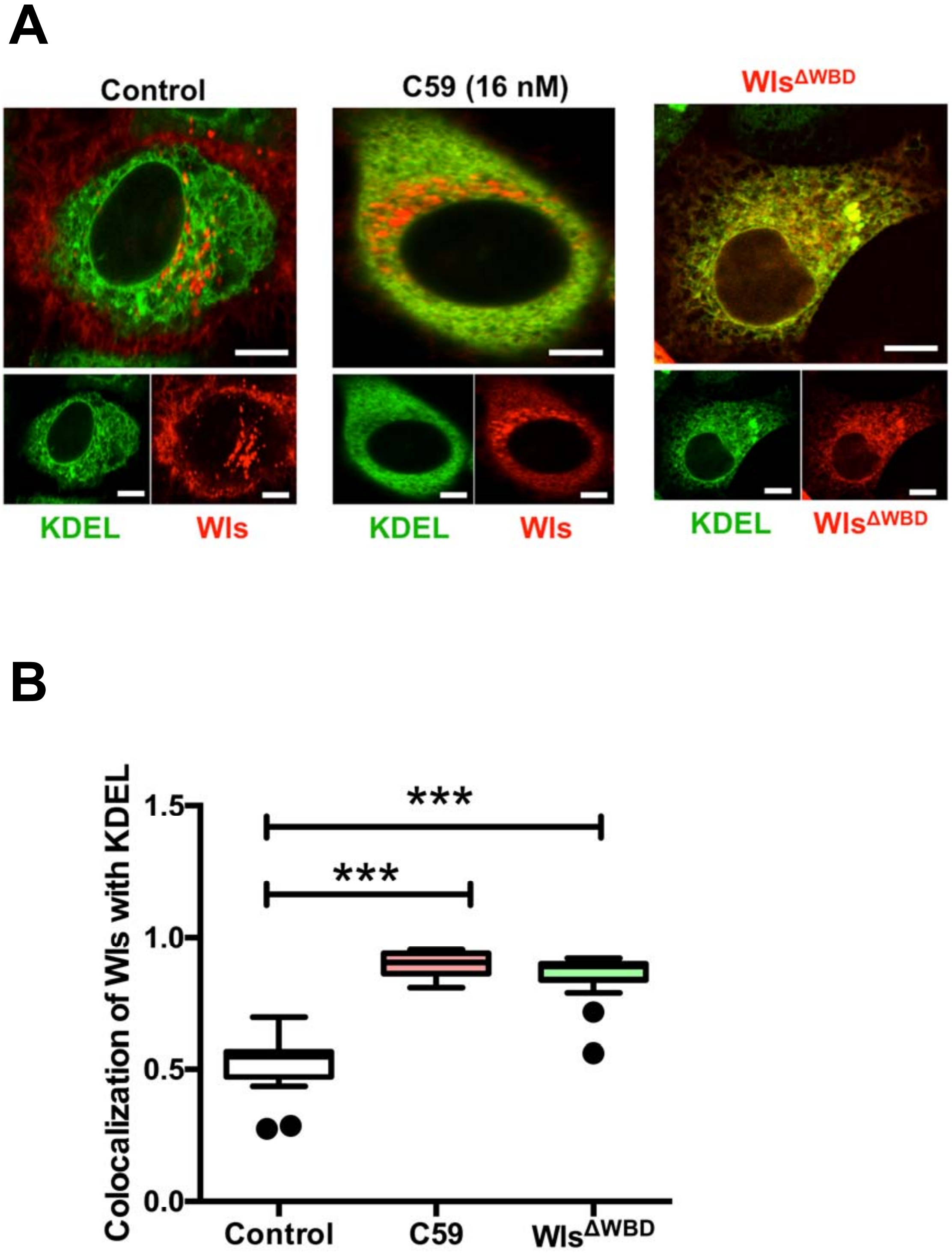
A
Control
C59 (16 nM)
Wls$^{\Delta WBD}$
KDEL
Wls
KDEL
Wls
KDEL
Wls$^{\Delta WBD}$
B
Colocalization of Wls with KDEL
1.5
1.0
0.5
0.0
***
***
Control
C59
Wls$^{\Delta WBD}$

Figure 4.16 Addition of C59 in cell culture causes the ER accumulation of wild type Wls

(A) Live cell confocal fluorescent images of the subcellular localization of mCherry-tagged wild type and truncated Wls proteins Wls$^{\Delta WBD}$. C59 treatment partially increased ER retention of Wls, while Wls$^{\Delta WBD}$ that lacked a Wnt-binding domain showed a severe ER-retention pattern.

(B) Co-localization of Wls and ER (KDEL) is assessed as Manders' coefficient. Inhibiting Wnt-Wls interaction in both cases (C59 treatment and deletion of WBD on WLS) result in a significant increase of Wls-KDEL association. The quantification results are presented as a Tukey box-and-whisker plot. ***P<0.001.

Scale bars: 5 μm.

Figure 4.17

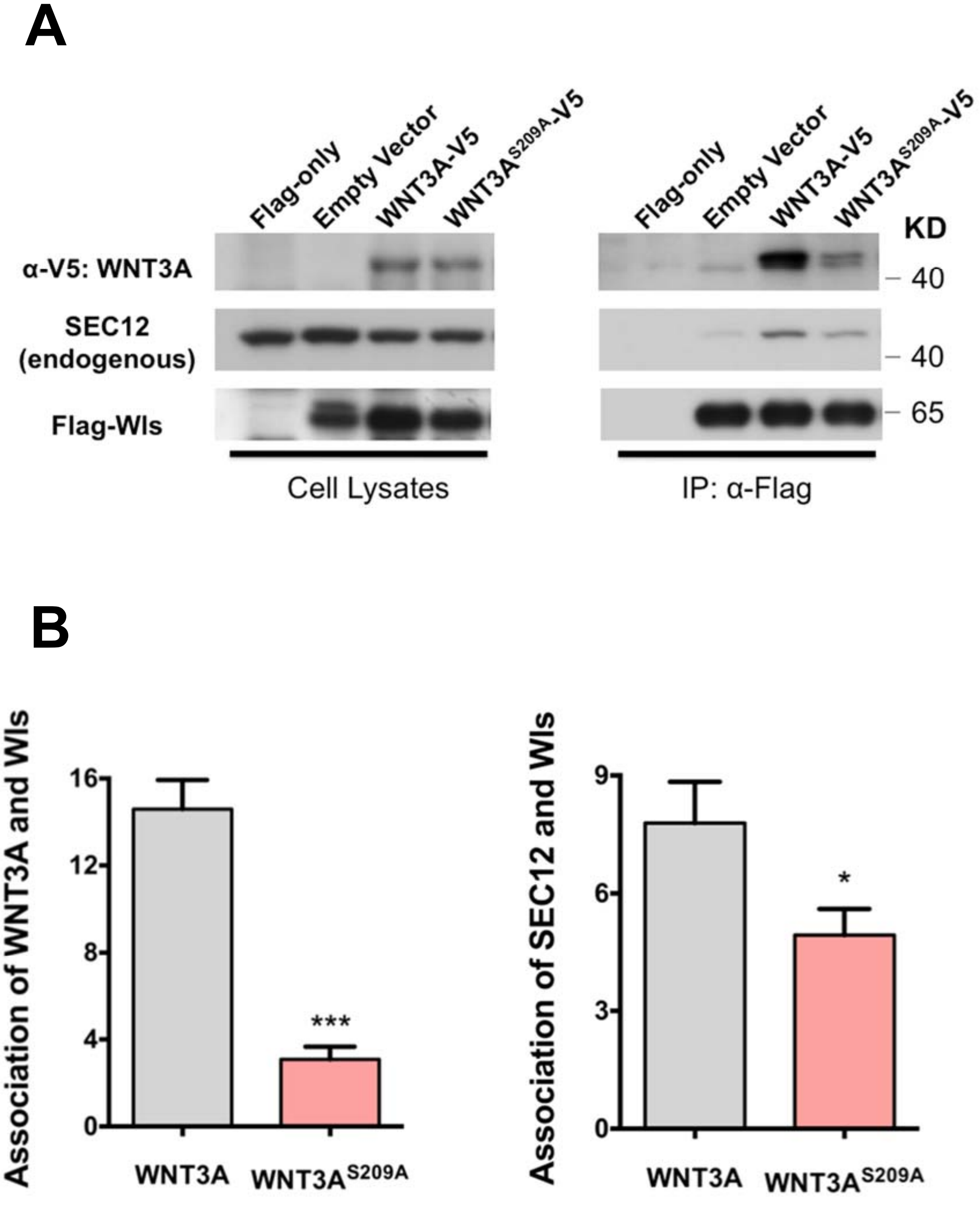
A
Flag-only
Empty Vector
WNT3A-V5
WNT3A^S209A-V5
Flag-only
Empty Vector
WNT3A-V5
WNT3A^S209A-V5
KD
α-V5: WNT3A
SEC12
(endogenous)
Flag-Wls
40
40
65
Cell Lysates
IP: α-Flag
B
Association of WNT3A and Wls
16
12
8
4
0
***
WNT3A
WNT3A^S209A
Association of SEC12 and Wls
9
6
3
0
*
WNT3A
WNT3A^S209A

Figure 4.17 Wnt3A^{S209A} induces less Wls-SEC12 association

(A) Co-IP assays were performed on HeLa cells stably expressing Flag-Wls protein and being transiently transfected with WNT3A or WNT3A^{S209A}. Co-IP assays showed that, compared to wild type WNT3A-transfected cells, cells that were transfected with WNT3A^{S209A} with less Wls-binding capacity also showed less Wls-SEC12 association.

(B) Western blot quantification of panel A. Intensity of individual bands in α-Myc immunoprecipitants was quantified using ImageJ software, and expressed relative to Flag-Wls signal, as a measure of protein relative abundance in different immunoprecipitants samples. $^{*}P<0.05$; $^{***}P<0.001$.

CHAPTER 5

DISCUSSION AND FUTURE PROSPETCTUS

Some information in this chapter is partially taken from Sun et al. Journal of Cell Science (2017) 130, 2159-2171.

5.1 A sophisticated mechanism controlling the entry of Wnt ligands into the early secretory pathway

Although different Wnts regulate diverse signaling pathways in ligand-receiving cells, secretion of virtually all vertebrate Wnts share two remarkably similar features: lipid modification by Porcn in ER and utilization of Wls as the transporter to reach the plasma membrane. Cell fractionation studies demonstrated an ER pool of Wls that interacts with Wnt molecules (Yu et al., 2014). Knocking down *Wls* in Drosophila caused ER stress, a phenotype that was also induced by Porcupine depletion (Zhang et al., 2016), suggesting that defective Wls or Porcn function affect Wnt secretion at the level of ER. However, the exact molecular mechanism that regulates the packaging and export of Wnt secretory vesicles from ER has not been fully understood. Our study provided a direct link between ligand-bound Wls and major molecular components of COPII ER-exiting machinery **(Figure 5.1)**. We affirmed the importance of binding of mature Wnts to Wls within ER, which may serve as a crucial signal to initiate the assembly of the earliest Wnt ER-exiting vesicles for export.

Wnts, after exiting the ER, can reach the cell surface via various routes, such as in exocytic vesicles (Das et al., 2015), exosomes (Gross et al., 2012; Korkut et al., 2009) or through transcytosis (Gallet et al., 2008). Our data pointed to an initial ER-exiting process that is probably common to the secretion of all *de* *novo* synthesized Wnt proteins. It is noteworthy that in addition to the canonical Wls (splicing variant 1) that is conserved across animal species, an alternative splicing variant 2 (widely expressed in primates) that lacks key motifs for retrograde trafficking (Yu et al., 2014) still retains the conserved hexapeptide motif (YAPSHK) described in our study.

At this moment, our data does not support an indispensable role for this motif in Wls–SEC12 interaction. It is plausible that this proline-serine (PS) motif (a.a. 494-495) is critical for Wls to adopt a strict conformation and phosphorylation for recognition by the ER export machinery **(Figure 5.1)**, as loss of this motif alone disrupts Wls–COPII communication. The truncated transporter Wls$^{1-497}$, being capable of SAR1 binding, gained partial vesicular trafficking ability, suggesting that retaining this hexapeptide provided certain structural cues that are required for ER exit and SAR1 association. The precise role of PS motif within the conserved hexapeptide of Wls and a SAR1-dependent Wls export mechanism require further investigations.

In our model, fully modified mature Wnt molecules may be the ultimate drivers for Wls–Wnt export via the COPII machinery. This ER-exiting strategy may ensure economic utilization of Wls for transporting only functional Wnts **(Figure 5.1)**. Taken together, our study supports a sophisticated mechanism controlling Wnt ligand to enter into the early secretory pathway.

5.2 Potential regulation on size of Wnt/Wls-containing COPII vesicle

The size of COPII vesicles is normally 60-80 nm in diameter (Barlowe et al., 1994). The regulation on the size of COPII vesicle has been reported in the study of collagen transport. Collagen fiber has a typical length of 300-400 nm (Fath et al., 2007). Since collagens are too large to be accommodated by the conventional COPII vesicles, they exit from the ER via a modification of the COPII-mediated export system (Jin et al., 2012; Saito et al., 2014). These observations suggest an unknown mechanism in regulating COPII vesicle size, which is essential for incorporating various cargoes of different physical sizes into the vesicular pathway.

Incorporating the cargoes from the ER lumen into COPII vesicles is essential for secretion of luminal proteins, such as the nascent Wnt molecules. Wnts are lipid-modified ~40 kDa proteins and Wls is an eight-pass trans-membrane protein. The size of Wnt/Wls complex is relatively large. Both Wnt and collagen are luminal cargoes that utilize their own trans-membrane transporters to interact with Sec12 for the ER export. A similar mechanism may be involved to allow Wnt and collagen to regulate COPII vesicle size. This mechanism is currently unclear, but it may control the ER export of these large cargos. Transmission Electron microscopy (TEM) and immuno-gold labeling analyses of Wnts, Wls, and COPII markers (such as the coat proteins) can help us elucidate the actual size of Wnt/Wls-containing vesicles and shed light on whether there is a Wnt-dependent size regulation of Wls-containing COPII vesicle.

5.3 Potential strategies to modulate Wnt secretion for cancer therapy

Wnt secretion has been linked to glioma tumorigenesis. Elevated levels of WLS in the glioma cell lines leads to an increased level of canonical WNT signaling. Depletion of WLS in glioma cell reduces its growth *ex vivo* and limits its capacity in forming tumors *in vivo* (Augustin et al., 2012). Certain colon cancer cells also exhibit enhanced Wnt production (Voloshanenko et al., 2013). Most importantly, the increased Wnt secretion is able to modulate the aberrant regulation of the Wnt canonical pathway, even though the presence of the mutations in APC or β-catenin in the experimental human colon cancer cell lines are sufficient to activate the pathway. Cells having enhanced Wnt activities due to mutations in APC or β-catenin remained responsive to Wnt stimulation (Voloshanenko et al., 2013). Above observation opens a door for therapeutic strategies for certain cancers by targeting Wnt secretion. The two major intracellular regulators, Porcupine and Wls, are ideal targets.

Small molecules that target Porcupine in advanced solid tumors showed promising inhibitory effects (Duraiswamy et al., 2015; Liu et al., 2013; Madan et al., 2016). Multiple clinical trials (NCT01351103, NCT02278133, NCT02521844) are ongoing to determine the efficacy and toxicity of these Wnt secretory inhibitors but none of them has completed the phase I clinical trials and proceeded to phase II study yet. There is currently no drug available in clinic to target Wls and to control Wnt secretion. Our results shed lights on a possibility that peptides or small molecules interfering with the Wls-Sec12 interacting interface may be promising targets for future exploration. Specifically, cell-permeable mimetic peptides for the hexapeptide (YAPSHK) of Wls may be pursued for their efficacies in blocking Wnt production in aggressive Wnt-producing cancers.

5.4 The hypothetical contribution of TMED10 and ACBD3 to WNT7A secretion

We found that TMED10 complexes with WNT7A and ACBD3, and may negatively regulate WNT7A secretion. However, the precise contribution of TMED10 and ACBD3 to WNT7A secretion remains not clear at this moment. There is an interesting correlation between ACBD3 and TMED10 during stress response in the brain. The regulatory event mediated by a 5’ splice site (5’SS) consensus sequence is important for both constitutive and alternative splicing (AS) (Wang and Burge, 2008). Although the 5’SS consensus is highly abundant in the mammalian introns, it is not selected for splicing in normal cells and therefore called the latent splicing (Miriami et al., 2002). Stress or glial tumors (French et al., 2007) can trigger the activation of latent splicing, resulting in a pre-maturely terminated aberrant mRNAs (French et al., 2007; Li et al., 2002; Miriami et al., 2002; Nevo et al., 2012). Of our particular interests, both TMED10 and ACBD3 are significantly up-regulated in latent splicing events resulting in down-regulation of protein production under stress conditions (French et al., 2007). Down-regulation of these secretory regulators may be a part of cellular adaptive responses to stress. Since both TMED10 and ACBD3 respond to stress in a similar trend, immediate future study would be to examine the RNA levels of TMED10 and ACBD3 in wild type cells, cells treated by Wnts, and cells deficient in Wnt secretion (e.g., MEFs, mouse intestinal organoids, or human colon cancer cell lines). These studies will help understand whether loss or gain of Wnt production alters cellular TMED10 and ACBD3 levels in response to the environmental Wnt concentrations. If TMED10 or ACBD3 protein level is decreased in cancer condition, these secretory modulators may contribute to negative modulation of Wnt production since Wnt secretory level is up regulated in colon cancer (Voloshanenko et al., 2013). If this is indeed the case, TMED10 or ACBD3 may be explored as tumor-suppressor in future studies.

Nineteen of Wnt mammalian homologs have been discovered (www.stanford.edu/~rnusse/wntwindow.html). No crystal structure for a Wnt protein has yet been reported. However, shared features of all Wnts in the secretory pathway include lipid-modification by Porcupine enzyme and Wls transporter-mediated intracellular traffic. Different Wnt isoforms are secreted by specific cell type. For example, Paneth cells, the major Wnt production cell within the intestinal epithelial crypt, secrete Wnt3 isoform (Sato et al., 2011); Wnt2a and Wnt5b are abundantly detected in the intestinal mesenchymal cells (Valenta et al., 2016). Although ample research into regulatory effects of Wnt signaling that mediated by various Wnt-Frizzled interaction, a great deal still remains unknown regarding the specific Wnt producing cell type in various tissue and mechanisms that control Wnt protein processing in the Wnt production cells. Of our particular interests, how the cells distinguish and secrete a specific Wnt isoform from other Wnt molecules will be investigated in the future. We have previously reported our observation of Wnt7a-TMED10-ACBD3 complex in **Figure 4.12**, and hypothesized that TMED10 and ACBD3 may contribute to modulate secretion of specific Wnt molecules, such as WNT7A. How these proteins distinguish WNT7A from other WNT molecules will be also investigated in the future.

5.5 The potential application and pitfall in utilizing the *ex vivo* organoid culture

Various cell populations in the intestine secrete different Wnt molecules. (Gregorieff and Clevers, 2005). Paneth cells, as the major epithelial Wnt producers, secrete Wnt3 and are the co-resident of stem cell in the crypts (Sato et al., 2011). Since Wnts secreted by sub-epithelial mesenchymal cells can maintain intestinal homeostasis in adult mice, we utilized the *ex vivo* intestinal organoid culture system to eliminate the compensatory effect from non-epithelial cells. Organoid culture system has been a useful tool in elucidating mechanism of Wnt secretion (Das et al., 2015) and stem cell maintenance (Clevers, 2013). In this system, isolated mouse small intestinal crypts can be grown into ever-lasting organoids enbeded in Matrigel supplemented by medium containing EGF, Noggin, and R-Spondin (ENR) (Sato et al., 2009). Due to a lack of Wnt secretion, Wls-deficient organoids failed to grow in such a culture system unless supplemented by exogenous Wnt ligands (Valenta et al., 2016). Thus, organoid maintenance supported by stem cell renewal becomes a useful readout for Wnt secretion and function in the culture system.

We hypothesized that viral infection of Wls-deficient organoids with wild type Wls would rescue organoid growth, whereas mutant Wls with trafficking defects would not have the effect due to their failure to support Wnt secretion. We derived organoids from *Wls*$^{Fl/Fl}$*; Villin-CreERT2* mouse small intestines. These orgnoids had intact Wls expression until exogenous tamoxifen (4-OHT, 500 nM) were added to induce CreER-mediated Wls gene excision. Using a published protocol (Koo et al., 2012), we infected *Wls*$^{Fl/Fl}$*; Villin-CreERT2* organoids with retrovirus expressing mCherry-tagged wild type Wls, Wls$^{\Delta 492\text{-}497}$, and Wls$^{1\text{-}491}$, respectively. Successful infection was verified by mCherry expression in infected organoids **(Figure 5.2)**. Five days after viral infection, tamoxifen was administrated to induce *Wls* deletion. Two days after tamoxifen treatment, all of the non-infected *Wls*$^{Fl/Fl}$*; Villin-CreERT2* organoids were growth-arrested, exemplified by their collapsed structures, whereas 44% of wild type Wls-infected organoids maintained their organoid structure **(Figure 5.3A-B)**. At this time point, organoids infected with Wls$^{\Delta 492\text{-}497}$ (lacking hexapeptide) or Wls$^{1\text{-}491}$ (lack C-terminal tail) showed total growth arrest (**Figure 5.3A-B**). Both gross morphology and EdU labeling of proliferative cells are used to validate the survived organoids **(Figure 5.4)**. These data supported the contribution of hexapeptide-dependent Wls export for Wnt secretion.

The fast-cycling Lgr5+ stem cell is considered as the main source of self-renewal cell in the ex vivo organoid culture system and the proliferation of Lgr5+ stem cell is enhanced via the addition of exogenous Wnt ligands or by co-culturing with Paneth cells (Sato et al., 2011). A shortcoming of our above experiment is that lentiviral infection delivered wild type Wls to all epithelial cells rather than a specific cell population, e.g., the Paneth cells. It would be interesting to test whether Wls-deficient organoids can survive when only Paneth cells are restored for their Wnt secretion activity. In order to explore Paneth cell specific Wnt secretion, future study will have to use Paneth cell specific gene promoters, such as Lyz1 or Defa5 to drive Wls expression in organoids.

5.6 Conclusion

The most important finding of my graduate work is related to the discovery of the multi-protein complex (Wntless-Sec12-Sar1) regulation in the secretion of Wnts, the family of secreted growth factors that are fundamental for embryonic development and adult tissue homeostasis. Once the key regulators (Wntless-Sec12-Sar1) for ER exit of Wnts were determined, I elucidated the signaling pathway triggered by mature Wnt ligands in the early secretory step as well as the specific protein interface (Wntless-Sec12-Sar1) responsible for the exit of mature Wnt ligands from the Endoplasmic Reticulum. The relative defined protein motifs will help in designing peptide or small molecules as promising targets for future pharmaceutical development in the treatment of disease caused by aberrant Wnt signaling, such as cancer. Further study can be expected in developing a model that identifies the determinants, e.g. TMED family and ACBD3, that allow specific Wnts produced in support of certain biological events such as maintaining the homeostasis of intestinal stem niche. Elucidating these determinants can greatly help in the design of specific inhibitors for different Wnt isoforms in translational research.

Figure 5.1

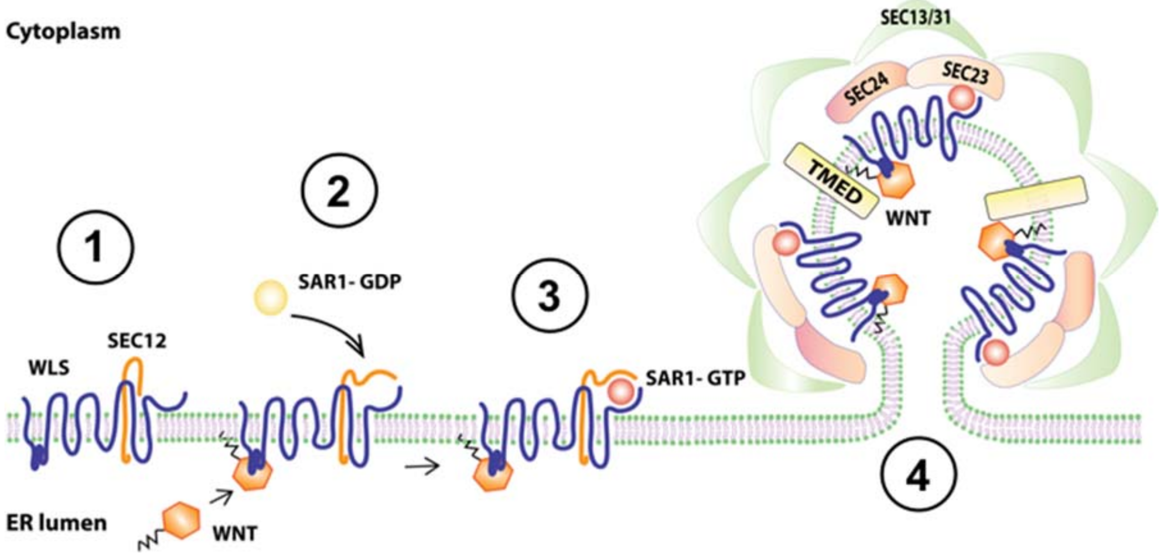
Cytoplasm
SEC13/31
SEC24
SEC23
TMED
WNT
2
1
SAR1- GDP
3
WLS
SEC12
SAR1- GTP
4
ER lumen
WNT

Figure 5.1 A schematic diagram illustrating COPII-dependent ER export of Wls–Wnt.

(1) There is a basal level of pre-formed Wls–SEC12 complex, which is directly mediated by specific cytosolic motifs, on ER membrane. (2) Upon mature Wnt binding to Wls in the ER, the Wls–SEC12 association is enhanced via an unknown mechanism, resulting in increased recruitment of SAR1 to the Wls–SEC12 complex. The C-terminal tail of Wls appears to be required for this process. (3) SEC12 activates SAR1. (4) GTP-bound SAR1 initiates COPII vesicle assembly at ER exit sites, exporting Wls–Wnt from the ER, while leaving SEC12 in the ER membrane.

Figure 5.2

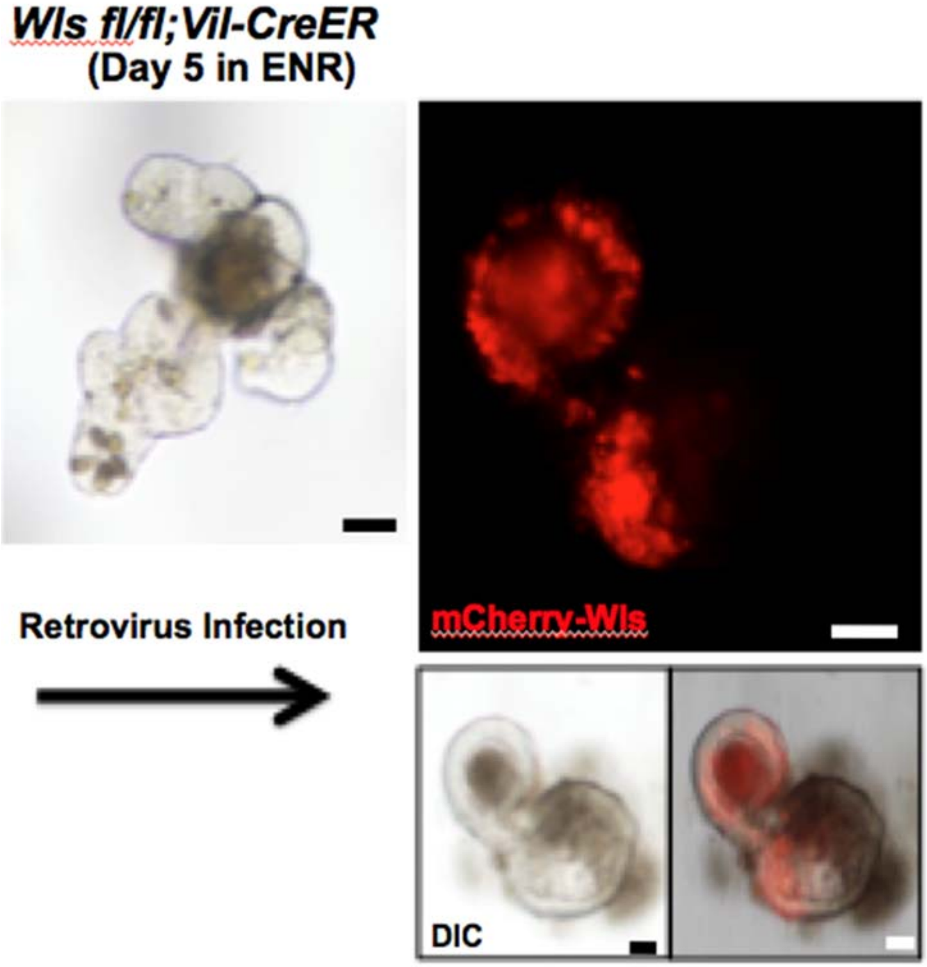
Wls fl/fl;Vil-CreER
(Day 5 in ENR)
Retrovirus Infection
mCherry-Wls
DIC

Figure 5.2 Organoids were infected by lentivirus expression mCherry-Wls

DIC and fluorescent micrographs of live infected organoids. Organoids derived from *Wls$^{Fl/Fl}$; Villin-CreER* mouse small intestines were grown in ENR medium for 5 days (left panel) before retroviral infection. Successful retrovirus infections were affirmed by detection of mCherry expression in organoids (right panel).

Scale bars: 500 µm.

Figure 5.3

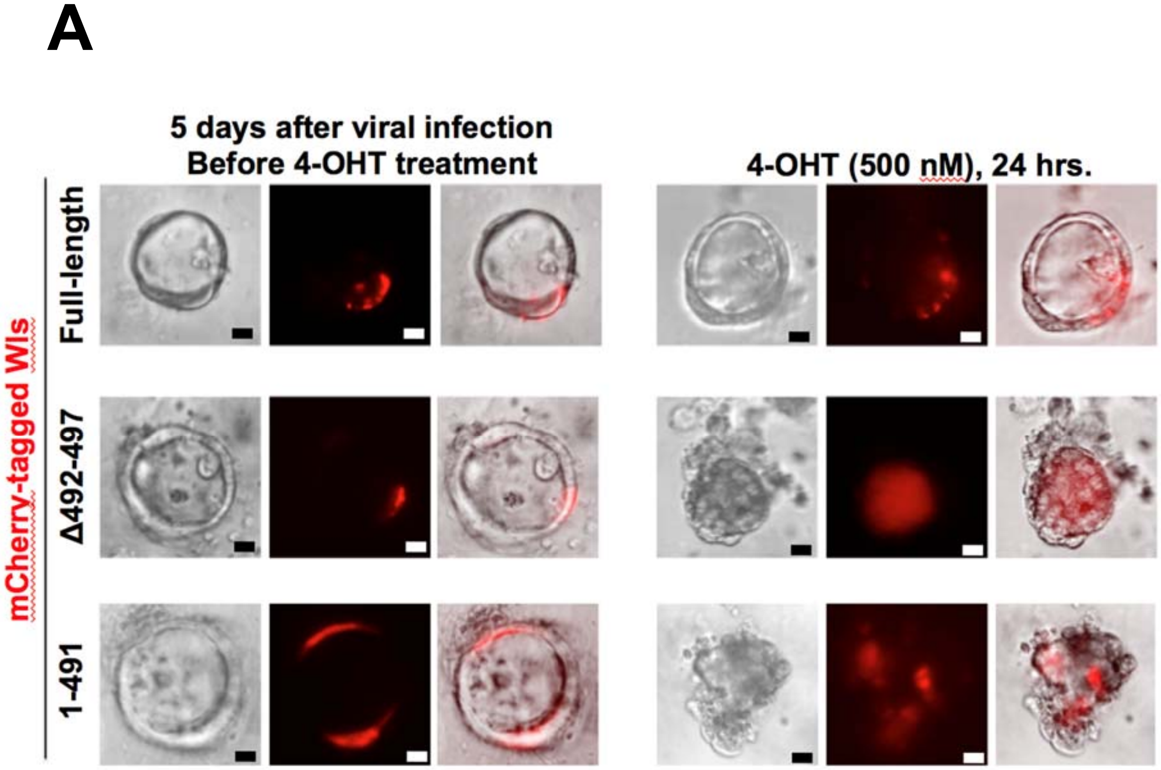
A
5 days after viral infection
Before 4-OHT treatment
4-OHT (500 nM), 24 hrs.
mCherry-tagged Wls
Full-length
Δ492-497
1-491

B

Viral vector	Number of live crypts		
	Before 4-OHT	After 4-OHT	
		24 hrs	**48 hrs**
Full-length	18	12	**8 (44%)**
Δ 492-497	19	17	**0**
1-491	17	9	**0**

Figure 5.3 The hexapeptide-regulated Wls ER export is essential for Wnt secretion and intestinal stem cell maintenance in organoid culture.

(A) DIC and fluorescent micrographs were taken for the live infected organoids with mCherry-tagged wild type Wls, Wls$^{\Delta 492\text{-}497}$, and Wls$^{1\text{-}491}$ following a described protocol. The images were taken before and 24 hours after 4-OHT (500 nM) administration. Scale bars: 500 µm.

(B) A table summarizes the numbers of survived organoids, 24 and 48 hrs after 4-OHT treatments, for each group that was successfully infected by individual Wls-expressing virus. Note that all the non-infected organoids, which did not show mCherry expression, showed growth arrest 2 days after 4-OHT treatments. 44% of mCherry-tagged wild type Wls infected organoids is able to survive in 48 hours 4-OHT (500 nM) administration.

Figure 5.4

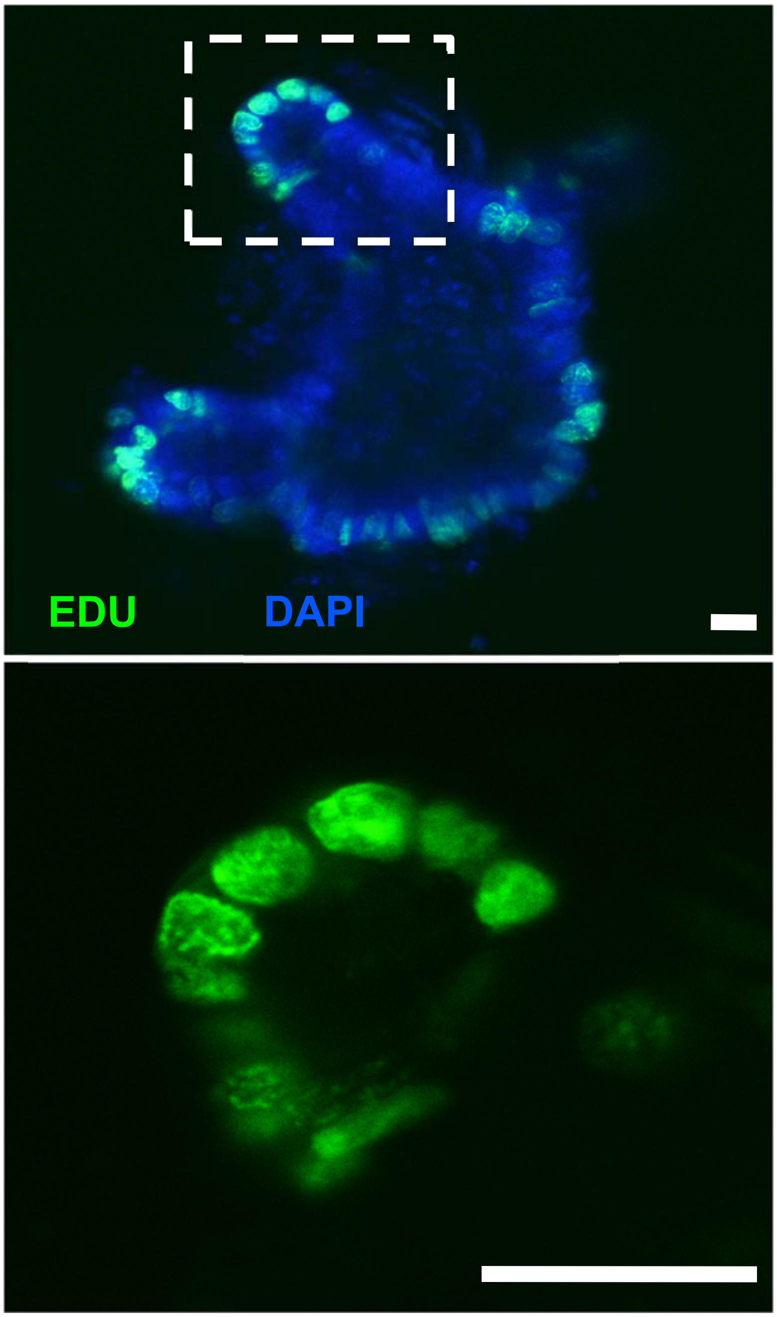

Figure 5.4 Survived Organoids were validated by EdU labeling

Confocal fluorescent detection of EdU labeling (green) in mCherry-Wls infected organoids affirms the viability of organoids. DAPI labels all cell with nuclei staining and EDU only labels the proliferating cells, which sit at the budding of organoids.

Scale bars: 500 µm.

References

Alberts, B. 2002. Molecular biology of the cell. Garland Science, New York. xxxiv, 1548 p. pp.

Amaya, C., R.D. Militello, S.D. Calligaris, and M.I. Colombo. 2016. Rab24 interacts with the Rab7/Rab interacting lysosomal protein complex to regulate endosomal degradation. *Traffic*. 17:1181-1196.

Andres, D.A., I.M. Dickerson, and J.E. Dixon. 1990. Variants of the carboxyl-terminal KDEL sequence direct intracellular retention. *J Biol Chem*. 265:5952-5955.

Ang, A.L., H. Folsch, U.M. Koivisto, M. Pypaert, and I. Mellman. 2003. The Rab8 GTPase selectively regulates AP-1B-dependent basolateral transport in polarized Madin-Darby canine kidney cells. *J Cell Biol*. 163:339-350.

Antonny, B., D. Madden, S. Hamamoto, L. Orci, and R. Schekman. 2001. Dynamics of the COPII coat with GTP and stable analogues. *Nat Cell Biol*. 3:531-537.

Antonny, B., and R. Schekman. 2001. ER export: public transportation by the COPII coach. *Curr Opin Cell Biol*. 13:438-443.

Aridor, M., S.I. Bannykh, T. Rowe, and W.E. Balch. 1995. Sequential coupling between COPII and COPI vesicle coats in endoplasmic reticulum to Golgi transport. *J Cell Biol*. 131:875-893.

Aridor, M., K.N. Fish, S. Bannykh, J. Weissman, T.H. Roberts, J. Lippincott-Schwartz, and W.E. Balch. 2001. The Sar1 GTPase coordinates biosynthetic cargo selection with endoplasmic reticulum export site assembly. *J Cell Biol*. 152:213-229.

Aridor, M., J. Weissman, S. Bannykh, C. Nuoffer, and W.E. Balch. 1998. Cargo selection by the COPII budding machinery during export from the ER. *J Cell Biol*. 141:61-70.

Arvan, P., and D. Castle. 1998. Sorting and storage during secretory granule biogenesis: looking backward and looking forward. *Biochem J*. 332 (Pt 3):593-610.

Augustin, I., D.L. Dewi, J. Hundshammer, G. Erdmann, G. Kerr, and M. Boutros. 2017. Autocrine Wnt regulates the survival and genomic stability of embryonic stem cells. *Sci Signal*. 10.

Augustin, I., V. Goidts, A. Bongers, G. Kerr, G. Vollert, B. Radlwimmer, C. Hartmann, C. Herold-Mende, G. Reifenberger, A. von Deimling, and M. Boutros. 2012. The Wnt secretion protein Evi/Gpr177 promotes glioma tumourigenesis. *EMBO Mol Med*. 4:38-51.

Banziger, C., D. Soldini, C. Schutt, P. Zipperlen, G. Hausmann, and K. Basler.

2006. Wntless, a conserved membrane protein dedicated to the secretion of Wnt proteins from signaling cells. *Cell*. 125:509-522.

Bao, H., R.W. Daniels, G.T. MacLeod, M.P. Charlton, H.L. Atwood, and B. Zhang. 2005. AP180 maintains the distribution of synaptic and vesicle proteins in the nerve terminal and indirectly regulates the efficacy of Ca2+-triggered exocytosis. *J Neurophysiol*. 94:1888-1903.

Barlowe, C., and A. Helenius. 2016. Cargo Capture and Bulk Flow in the Early Secretory Pathway. *Annu Rev Cell Dev Biol*. 32:197-222.

Barlowe, C., L. Orci, T. Yeung, M. Hosobuchi, S. Hamamoto, N. Salama, M.F. Rexach, M. Ravazzola, M. Amherdt, and R. Schekman. 1994. COPII: a membrane coat formed by Sec proteins that drive vesicle budding from the endoplasmic reticulum. *Cell*. 77:895-907.

Barlowe, C., and R. Schekman. 1993. SEC12 encodes a guanine-nucleotide-exchange factor essential for transport vesicle budding from the ER. *Nature*. 365:347-349.

Barrott, J.J., G.M. Cash, A.P. Smith, J.R. Barrow, and L.C. Murtaugh. 2011. Deletion of mouse Porcn blocks Wnt ligand secretion and reveals an ectodermal etiology of human focal dermal hypoplasia/Goltz syndrome. *Proc Natl Acad Sci U S A*. 108:12752-12757.

Bartscherer, K., and M. Boutros. 2008. Regulation of Wnt protein secretion and its role in gradient formation. *EMBO Rep*. 9:977-982.

Bartscherer, K., N. Pelte, D. Ingelfinger, and M. Boutros. 2006. Secretion of Wnt ligands requires Evi, a conserved transmembrane protein. *Cell*. 125:523-533.

Batoko, H., H.Q. Zheng, C. Hawes, and I. Moore. 2000. A rab1 GTPase is required for transport between the endoplasmic reticulum and golgi apparatus and for normal golgi movement in plants. *Plant Cell*. 12:2201-2218.

Beck, K.A., M. Chang, F.M. Brodsky, and J.H. Keen. 1992. Clathrin assembly protein AP-2 induces aggregation of membrane vesicles: a possible role for AP-2 in endosome formation. *J Cell Biol*. 119:787-796.

Beck, R., S. Prinz, P. Diestelkotter-Bachert, S. Rohling, F. Adolf, K. Hoehner, S. Welsch, P. Ronchi, B. Brugger, J.A. Briggs, and F. Wieland. 2011. Coatomer and dimeric ADP ribosylation factor 1 promote distinct steps in membrane scission. *J Cell Biol*. 194:765-777.

Beckett, K., S. Monier, L. Palmer, C. Alexandre, H. Green, E. Bonneil, G. Raposo, P. Thibault, R. Le Borgne, and J.P. Vincent. 2013. Drosophila S2 cells secrete wingless on exosome-like vesicles but the wingless gradient forms independently of exosomes. *Traffic*. 14:82-96.

Belenkaya, T.Y., Y. Wu, X. Tang, B. Zhou, L. Cheng, Y.V. Sharma, D. Yan, E.M. Selva, and X. Lin. 2008a. The retromer complex influences Wnt secretion by recycling wntless from endosomes to the trans-Golgi network. *Dev Cell*. 14:120-131.

Belenkaya, T.Y., Y. Wu, X. Tang, B. Zhou, L. Cheng, Y.V. Sharma, D. Yan, E.M. Selva, and X. Lin. 2008b. The retromer complex influences Wnt secretion by recycling wntless from endosomes to the trans-Golgi network. *Developmental cell*. 14:120-131.

Benedetti, C., M. Fabbri, R. Sitia, and A. Cabibbo. 2000. Aspects of gene regulation during the UPR in human cells. *Biochem Biophys Res Commun*. 278:530-536.

Bhattacharyya, D., and B.S. Glick. 2007. Two mammalian Sec16 homologues have nonredundant functions in endoplasmic reticulum (ER) export and transitional ER organization. *Mol Biol Cell*. 18:839-849.

Bi, X., R.A. Corpina, and J. Goldberg. 2002. Structure of the Sec23/24-Sar1 pre-budding complex of the COPII vesicle coat. *Nature*. 419:271-277.

Bi, X., J.D. Mancias, and J. Goldberg. 2007. Insights into COPII coat nucleation from the structure of Sec23.Sar1 complexed with the active fragment of Sec31. *Dev Cell*. 13:635-645.

Bielli, A., C.J. Haney, G. Gabreski, S.C. Watkins, S.I. Bannykh, and M. Aridor. 2005. Regulation of Sar1 NH2 terminus by GTP binding and hydrolysis promotes membrane deformation to control COPII vesicle fission. *J Cell Biol*. 171:919-924.

Blum, R., F. Pfeiffer, P. Feick, W. Nastainczyk, B. Kohler, K.H. Schafer, and I. Schulz. 1999. Intracellular localization and in vivo trafficking of p24A and p23. *J Cell Sci*. 112 (Pt 4):537-548.

Bonifacino, J.S., and B.S. Glick. 2004. The mechanisms of vesicle budding and fusion. *Cell*. 116:153-166.

Bonnon, C., M.W. Wendeler, J.P. Paccaud, and H.P. Hauri. 2010. Selective export of human GPI-anchored proteins from the endoplasmic reticulum. *J Cell Sci*. 123:1705-1715.

Brandizzi, F., and C. Barlowe. 2013. Organization of the ER-Golgi interface for membrane traffic control. *Nat Rev Mol Cell Biol*. 14:382-392.

Braulke, T., and J.S. Bonifacino. 2009. Sorting of lysosomal proteins. *Biochim Biophys Acta*. 1793:605-614.

Buechling, T., V. Chaudhary, K. Spirohn, M. Weiss, and M. Boutros. 2011. p24 proteins are required for secretion of Wnt ligands. *EMBO Rep*. 12:1265-1272.

Bultema, J.J., J.A. Boyle, P.B. Malenke, F.E. Martin, E.C. Dell'Angelica, R.E. Cheney, and S.M. Di Pietro. 2014. Myosin vc interacts with Rab32 and Rab38 proteins and works in the biogenesis and secretion of melanosomes. *J Biol Chem*. 289:33513-33528.

Burri, L., and T. Lithgow. 2004. A complete set of SNAREs in yeast. *Traffic*.

5:45-52.

Bustos, M.A., O. Lucchesi, M.C. Ruete, L.S. Mayorga, and C.N. Tomes. 2012. Rab27 and Rab3 sequentially regulate human sperm dense-core granule exocytosis. *Proc Natl Acad Sci U S A*. 109:E2057-2066.

Capasso, J.M., C. Abeijon, and C.B. Hirschberg. 1985. Phosphoproteins and protein kinases of the Golgi apparatus membrane. *J Biol Chem*. 260:14879-14884.

Capasso, J.M., and C.B. Hirschberg. 1984. Mechanisms of glycosylation and sulfation in the Golgi apparatus: evidence for nucleotide sugar/nucleoside monophosphate and nucleotide sulfate/nucleoside monophosphate antiports in the Golgi apparatus membrane. *Proc Natl Acad Sci U S A*. 81:7051-7055.

Carmon, K.S., and D.S. Loose. 2008. Secreted frizzled-related protein 4 regulates two Wnt7a signaling pathways and inhibits proliferation in endometrial cancer cells. *Mol Cancer Res*. 6:1017-1028.

Carney, G.E., and N.J. Bowen. 2004. p24 proteins, intracellular trafficking, and behavior: Drosophila melanogaster provides insights and opportunities. *Biol Cell*. 96:271-278.

Carpenter, A.C., S. Rao, J.M. Wells, K. Campbell, and R.A. Lang. 2010. Generation of mice with a conditional null allele for Wntless. *Genesis*. 48:554-558.

Carpentier, J.L., P. Gorden, R.G. Anderson, J.L. Goldstein, M.S. Brown, S. Cohen, and L. Orci. 1982. Co-localization of 125I-epidermal growth factor and ferritin-low density lipoprotein in coated pits: a quantitative electron microscopic study in normal and mutant human fibroblasts. *J Cell Biol*. 95:73-77.

Chardin, P., and I. Callebaut. 2002. The yeast Sar exchange factor Sec12, and its higher organism orthologs, fold as beta-propellers. *FEBS Lett*. 525:171-173.

Chen, B., M.E. Dodge, W. Tang, J. Lu, Z. Ma, C.W. Fan, S. Wei, W. Hao, J. Kilgore, N.S. Williams, M.G. Roth, J.F. Amatruda, C. Chen, and L. Lum. 2009. Small molecule-mediated disruption of Wnt-dependent signaling in tissue regeneration and cancer. *Nat Chem Biol*. 5:100-107.

Chen, S.R., J.X. Tang, J.M. Cheng, X.X. Hao, Y.Q. Wang, X.X. Wang, and Y.X. Liu. 2016. Does murine spermatogenesis require WNT signalling? A lesson from Gpr177 conditional knockout mouse models. *Cell Death Dis*. 7:e2281.

Cheng, C.W., J.C. Yeh, T.P. Fan, S.K. Smith, and D.S. Charnock-Jones. 2008. Wnt5a-mediated non-canonical Wnt signalling regulates human endothelial cell proliferation and migration. *Biochem Biophys Res Commun*. 365:285-290.

Cheung, A.Y., C.Y. Chen, R.H. Glaven, B.H. de Graaf, L. Vidali, P.K. Hepler, and

H.M. Wu. 2002. Rab2 GTPase regulates vesicle trafficking between the endoplasmic reticulum and the Golgi bodies and is important to pollen tube growth. *Plant Cell*. 14:945-962.

Chong, Z.Z., F. Li, and K. Maiese. 2007. Cellular demise and inflammatory microglial activation during beta-amyloid toxicity are governed by Wnt1 and canonical signaling pathways. *Cell Signal*. 19:1150-1162.

Clevers, H. 2013. The intestinal crypt, a prototype stem cell compartment. *Cell*. 154:274-284.

Clevers, H., and R. Nusse. 2012. Wnt/beta-catenin signaling and disease. *Cell*. 149:1192-1205.

Colicelli, J. 2004. Human RAS superfamily proteins and related GTPases. *Sci STKE*. 2004:RE13.

Coombs, G.S., J. Yu, C.A. Canning, C.A. Veltri, T.M. Covey, J.K. Cheong, V. Utomo, N. Banerjee, Z.H. Zhang, R.C. Jadulco, G.P. Concepcion, T.S. Bugni, M.K. Harper, I. Mihalek, C.M. Jones, C.M. Ireland, and D.M. Virshup. 2010. WLS-dependent secretion of WNT3A requires Ser209 acylation and vacuolar acidification. *J Cell Sci*. 123:3357-3367.

Cosson, P., and F. Letourneur. 1997. Coatomer (COPI)-coated vesicles: role in intracellular transport and protein sorting. *Curr Opin Cell Biol*. 9:484-487.

Das, S., S. Yu, R. Sakamori, P. Vedula, Q. Feng, J. Flores, A. Hoffman, J. Fu, E. Stypulkowski, A. Rodriguez, R. Dobrowolski, A. Harada, W. Hsu, E.M. Bonder, M.P. Verzi, and N. Gao. 2015. Rab8a vesicles regulate Wnt ligand delivery and Paneth cell maturation at the intestinal stem cell niche. *Development*. 142:2147-2162.

Day, K.J., L.A. Staehelin, and B.S. Glick. 2013. A three-stage model of Golgi structure and function. *Histochem Cell Biol*. 140:239-249.

Dayel, M.J., E.F. Hom, and A.S. Verkman. 1999. Diffusion of green fluorescent protein in the aqueous-phase lumen of endoplasmic reticulum. *Biophys J*. 76:2843-2851.

de Groot, R.E., H.F. Farin, M. Macurkova, J.H. van Es, H.C. Clevers, and H.C. Korswagen. 2013. Retromer dependent recycling of the Wnt secretion factor Wls is dispensable for stem cell maintenance in the mammalian intestinal epithelium. *PLoS One*. 8:e76971.

Dell'Angelica, E.C., J. Klumperman, W. Stoorvogel, and J.S. Bonifacino. 1998. Association of the AP-3 adaptor complex with clathrin. *Science*. 280:431-434.

Dell'Angelica, E.C., C. Mullins, and J.S. Bonifacino. 1999. AP-4, a novel protein complex related to clathrin adaptors. *J Biol Chem*. 274:7278-7285.

Dong, C., and G. Wu. 2007. Regulation of anterograde transport of adrenergic and angiotensin II receptors by Rab2 and Rab6 GTPases. *Cell Signal*. 19:2388-2399.

Dong, C., F. Zhou, E.K. Fugetta, C.M. Filipeanu, and G. Wu. 2008. Endoplasmic reticulum export of adrenergic and angiotensin II receptors is differentially regulated by Sar1 GTPase. *Cell Signal*. 20:1035-1043.

Dreyer, F., and A. Baur. 2016. Biogenesis and Functions of Exosomes and Extracellular Vesicles. *Methods Mol Biol*. 1448:201-216.

Duraiswamy, A.J., M.A. Lee, B. Madan, S.H. Ang, E.S. Tan, W.W. Cheong, Z. Ke, V. Pendharkar, L.J. Ding, Y.S. Chew, V. Manoharan, K. Sangthongpitag, J. Alam, A. Poulsen, S.Y. Ho, D.M. Virshup, and T.H. Keller. 2015. Discovery and Optimization of a Porcupine Inhibitor. *J Med Chem*. 58:5889-5899.

Egami, Y., S. Kiryu-Seo, T. Yoshimori, and H. Kiyama. 2005. Induced expressions of Rab24 GTPase and LC3 in nerve-injured motor neurons. *Biochem Biophys Res Commun*. 337:1206-1213.

el Marjou, F., K.P. Janssen, B.H. Chang, M. Li, V. Hindie, L. Chan, D. Louvard, P. Chambon, D. Metzger, and S. Robine. 2004. Tissue-specific and inducible Cre-mediated recombination in the gut epithelium. *Genesis*. 39:186-193.

Famili, F., B.A. Naber, S. Vloemans, E.F. de Haas, M.M. Tiemessen, and F.J. Staal. 2015. Discrete roles of canonical and non-canonical Wnt signaling in hematopoiesis and lymphopoiesis. *Cell Death Dis*. 6:e1981.

Fath, S., J.D. Mancias, X. Bi, and J. Goldberg. 2007. Structure and organization of coat proteins in the COPII cage. *Cell*. 129:1325-1336.

Fernandes, P.H., S. Wen, V.R. Sutton, P.A. Ward, I.B. Van den Veyver, and P. Fang. 2010. PORCN mutations and variants identified in patients with focal dermal hypoplasia through diagnostic gene sequencing. *Genet Test Mol Biomarkers*. 14:709-713.

Fine, R.E. 1989. Vesicles without clathrin: intermediates in bulk flow exocytosis. *Cell*. 58:609-610.

Franch-Marro, X., F. Wendler, S. Guidato, J. Griffith, A. Baena-Lopez, N. Itasaki, M.M. Maurice, and J.P. Vincent. 2008. Wingless secretion requires endosome-to-Golgi retrieval of Wntless/Evi/Sprinter by the retromer complex. *Nat Cell Biol*. 10:170-177.

French, P.J., J. Peeters, S. Horsman, E. Duijm, I. Siccama, M.J. van den Bent, T.M. Luider, J.M. Kros, P. van der Spek, and P.A. Sillevis Smitt. 2007. Identification of differentially regulated splice variants and novel exons in glial brain tumors using exon expression arrays. *Cancer Res*. 67:5635-5642.

Friederich, E., K. Vancompernolle, D. Louvard, and J. Vandekerckhove. 1999. Villin function in the organization of the actin cytoskeleton. Correlation of in vivo effects to its biochemical activities in vitro. *J Biol Chem*. 274:26751-26760.

Fu, J., H.M. Ivy Yu, T. Maruyama, A.J. Mirando, and W. Hsu. 2011. Gpr177/mouse Wntless is essential for Wnt-mediated craniofacial and brain development.

Dev Dyn. 240:365-371.

Fu, J., M. Jiang, A.J. Mirando, H.M. Yu, and W. Hsu. 2009. Reciprocal regulation of Wnt and Gpr177/mouse Wntless is required for embryonic axis formation. *Proc Natl Acad Sci U S A*. 106:18598-18603.

Fuerer, C., S.J. Habib, and R. Nusse. 2010. A study on the interactions between heparan sulfate proteoglycans and Wnt proteins. *Dev Dyn*. 239:184-190.

Gaidarov, I., Q. Chen, J.R. Falck, K.K. Reddy, and J.H. Keen. 1996. A functional phosphatidylinositol 3,4,5-trisphosphate/phosphoinositide binding domain in the clathrin adaptor AP-2 alpha subunit. Implications for the endocytic pathway. *J Biol Chem*. 271:20922-20929.

Gallet, A., L. Staccini-Lavenant, and P.P. Therond. 2008. Cellular trafficking of the glypican Dally-like is required for full-strength Hedgehog signaling and wingless transcytosis. *Dev Cell*. 14:712-725.

Galli, L.M., N. Zebarjadi, L. Li, V.R. Lingappa, and L.W. Burrus. 2016. Divergent effects of Porcupine and Wntless on WNT1 trafficking, secretion, and signaling. *Exp Cell Res*. 347:171-183.

Gao, X., and R.N. Hannoush. 2014. Single-cell imaging of Wnt palmitoylation by the acyltransferase porcupine. *Nat Chem Biol*. 10:61-68.

Gasnereau, I., P. Herr, P.Z. Chia, K. Basler, and P.A. Gleeson. 2011. Identification of an endocytosis motif in an intracellular loop of Wntless protein, essential for its recycling and the control of Wnt protein signaling. *J Biol Chem*. 286:43324-43333.

Ghosh, P., N.M. Dahms, and S. Kornfeld. 2003. Mannose 6-phosphate receptors: new twists in the tale. *Nat Rev Mol Cell Biol*. 4:202-212.

Goodman, R.M., S. Thombre, Z. Firtina, D. Gray, D. Betts, J. Roebuck, E.P. Spana, and E.M. Selva. 2006. Sprinter: a novel transmembrane protein required for Wg secretion and signaling. *Development*. 133:4901-4911.

Gordon, M.D., and R. Nusse. 2006. Wnt signaling: multiple pathways, multiple receptors, and multiple transcription factors. *J Biol Chem*. 281:22429-22433.

Gregorieff, A., and H. Clevers. 2005. Wnt signaling in the intestinal epithelium: from endoderm to cancer. *Genes Dev*. 19:877-890.

Gregorieff, A., D. Pinto, H. Begthel, O. Destree, M. Kielman, and H. Clevers. 2005. Expression pattern of Wnt signaling components in the adult intestine. *Gastroenterology*. 129:626-638.

Gregory, M.A., T.L. Phang, P. Neviani, F. Alvarez-Calderon, C.A. Eide, T. O'Hare, V. Zaberezhnyy, R.T. Williams, B.J. Druker, D. Perrotti, and J. Degregori. 2010. Wnt/Ca2+/NFAT signaling maintains survival of Ph+ leukemia cells upon inhibition of Bcr-Abl. *Cancer Cell*. 18:74-87.

Gross, J.C., V. Chaudhary, K. Bartscherer, and M. Boutros. 2012. Active Wnt proteins are secreted on exosomes. *Nat Cell Biol*. 14:1036-1045.

Grzeschik, K.H., D. Bornholdt, F. Oeffner, A. Konig, M. del Carmen Boente, H. Enders, B. Fritz, M. Hertl, U. Grasshoff, K. Hofling, V. Oji, M. Paradisi, C. Schuchardt, Z. Szalai, G. Tadini, H. Traupe, and R. Happle. 2007. Deficiency of PORCN, a regulator of Wnt signaling, is associated with focal dermal hypoplasia. *Nat Genet*. 39:833-835.

Habas, R., Y. Kato, and X. He. 2001. Wnt/Frizzled activation of Rho regulates vertebrate gastrulation and requires a novel Formin homology protein Daam1. *Cell*. 107:843-854.

Hammond, A.T., and B.S. Glick. 2000. Dynamics of transitional endoplasmic reticulum sites in vertebrate cells. *Mol Biol Cell*. 11:3013-3030.

Hampton, R.Y. 2000. ER stress response: getting the UPR hand on misfolded proteins. *Curr Biol*. 10:R518-521.

Han, M.H., A. Kawasaki, J.Y. Wei, and C.J. Barnstable. 2001. Miniature postsynaptic currents depend on Ca2+ released from internal stores via PLC/IP3 pathway. *Neuroreport*. 12:2203-2207.

Hao, W., Z. Luo, L. Zheng, K. Prasad, and E.M. Lafer. 1999. AP180 and AP-2 interact directly in a complex that cooperatively assembles clathrin. *J Biol Chem*. 274:22785-22794.

Hardy, K.M., R.J. Garriock, T.A. Yatskievych, S.L. D'Agostino, P.B. Antin, and P.A. Krieg. 2008. Non-canonical Wnt signaling through Wnt5a/b and a novel Wnt11 gene, Wnt11b, regulates cell migration during avian gastrulation. *Dev Biol*. 320:391-401.

Harterink, M., F. Port, M.J. Lorenowicz, I.J. McGough, M. Silhankova, M.C. Betist, J.R. van Weering, R.G. van Heesbeen, T.C. Middelkoop, K. Basler, P.J. Cullen, and H.C. Korswagen. 2011a. A SNX3-dependent retromer pathway mediates retrograde transport of the Wnt sorting receptor Wntless and is required for Wnt secretion. *Nat Cell Biol*. 13:914-923.

Harterink, M., F. Port, M.J. Lorenowicz, I.J. McGough, M. Silhankova, M.C. Betist, J.R.T. van Weering, R. van Heesbeen, T.C. Middelkoop, K. Basler, P.J. Cullen, and H.C. Korswagen. 2011b. A SNX3-dependent retromer pathway mediates retrograde transport of the Wnt sorting receptor Wntless and is required for Wnt secretion. *Nat Cell Biol*. 13:914-923.

Heller, R.S., D.S. Dichmann, J. Jensen, C. Miller, G. Wong, O.D. Madsen, and P. Serup. 2002. Expression patterns of Wnts, Frizzleds, sFRPs, and misexpression in transgenic mice suggesting a role for Wnts in pancreas and foregut pattern formation. *Dev Dyn*. 225:260-270.

Hemmings, B.A., and P. Cohen. 1983. Glycogen synthase kinase-3 from rabbit skeletal muscle. *Methods Enzymol*. 99:337-345.

Herr, P., and K. Basler. 2012. Porcupine-mediated lipidation is required for Wnt recognition by Wls. *Dev Biol*. 361:392-402.

Herr, P., G. Hausmann, and K. Basler. 2012. WNT secretion and signalling in human disease. *Trends Mol Med*. 18:483-493.

Hirata, R., C. Nihei, and A. Nakano. 2013. Isoform-selective oligomer formation of Saccharomyces cerevisiae p24 family proteins. *J Biol Chem*. 288:37057-37070.

Hofmann, K. 2000. A superfamily of membrane-bound O-acyltransferases with implications for wnt signaling. *Trends Biochem Sci*. 25:111-112.

Huang, S., X. Zhu, Y. Liu, Y. Tao, G. Feng, L. He, X. Guo, and G. Ma. 2012. Wls is expressed in the epidermis and regulates embryonic hair follicle induction in mice. *PLoS One*. 7:e45904.

Huang, S., X. Zhu, Y. Tao, Q. Sun, L. Wang, B. Li, L. He, X. Guo, and G. Ma. 2015. Involvement of epithelial Wntless in the regulation of postnatal hair follicle morphogenesis. *Arch Dermatol Res*. 307:835-839.

Huber, L.A., S. Pimplikar, R.G. Parton, H. Virta, M. Zerial, and K. Simons. 1993. Rab8, a small GTPase involved in vesicular traffic between the TGN and the basolateral plasma membrane. *J Cell Biol*. 123:35-45.

Hughes, H., A. Budnik, K. Schmidt, K.J. Palmer, J. Mantell, C. Noakes, A. Johnson, D.A. Carter, P. Verkade, P. Watson, and D.J. Stephens. 2009. Organisation of human ER-exit sites: requirements for the localisation of Sec16 to transitional ER. *J Cell Sci*. 122:2924-2934.

Hurtley, S.M., and A. Helenius. 1989. Protein oligomerization in the endoplasmic reticulum. *Annu Rev Cell Biol*. 5:277-307.

Ishitani, T., S. Kishida, J. Hyodo-Miura, N. Ueno, J. Yasuda, M. Waterman, H. Shibuya, R.T. Moon, J. Ninomiya-Tsuji, and K. Matsumoto. 2003. The TAK1-NLK mitogen-activated protein kinase cascade functions in the Wnt-5a/Ca(2+) pathway to antagonize Wnt/beta-catenin signaling. *Mol Cell Biol*. 23:131-139.

Iwasaki, H., T. Yorimitsu, and K. Sato. 2015. Distribution of Sec24 isoforms to each ER exit site is dynamically regulated in Saccharomyces cerevisiae. *FEBS Lett*. 589:1234-1239.

Janda, C.Y., D. Waghray, A.M. Levin, C. Thomas, and K.C. Garcia. 2012. Structural basis of Wnt recognition by Frizzled. *Science*. 337:59-64.

Jin, L., K.B. Pahuja, K.E. Wickliffe, A. Gorur, C. Baumgartel, R. Schekman, and M. Rape. 2012. Ubiquitin-dependent regulation of COPII coat size and function. *Nature*. 482:495-500.

Johnson, D.L., J. Wayt, J.M. Wilson, and J.G. Donaldson. 2017. Arf6 and Rab22 mediate T cell conjugate formation by regulating clathrin-independent endosomal membrane trafficking. *J Cell Sci*. 130:2405-2415.

Jones, T.A., H.M. Barker, E.F. da Cruz e Silva, R.E. Mayer-Jaekel, B.A. Hemmings, N.K. Spurr, D. Sheer, and P.T. Cohen. 1993. Localization of the genes encoding the catalytic subunits of protein phosphatase 2A to human chromosome bands 5q23-->q31 and 8p12-->p11.2, respectively.

Cytogenet Cell Genet. 63:35-41.

Juarez, P., R. Sanchez-Lopez, M.A. Ramos, R.P. Stock, and A. Alagon. 2000. Rab8 as a molecular model of vesicular trafficking to investigate the latter steps of the secretory pathway in Entamoeba histolytica. *Arch Med Res*. 31:S157-159.

Kabiri, Z., G. Greicius, B. Madan, S. Biechele, Z. Zhong, H. Zaribafzadeh, Edison, J. Aliyev, Y. Wu, R. Bunte, B.O. Williams, J. Rossant, and D.M. Virshup. 2014. Stroma provides an intestinal stem cell niche in the absence of epithelial Wnts. *Development*. 141:2206-2215.

Kadowaki, T., E. Wilder, J. Klingensmith, K. Zachary, and N. Perrimon. 1996. The segment polarity gene porcupine encodes a putative multitransmembrane protein involved in Wingless processing. *Genes Dev*. 10:3116-3128.

Kauppi, M., A. Simonsen, B. Bremnes, A. Vieira, J. Callaghan, H. Stenmark, and V.M. Olkkonen. 2002. The small GTPase Rab22 interacts with EEA1 and controls endosomal membrane trafficking. *J Cell Sci*. 115:899-911.

Kelleher, D.J., and R. Gilmore. 2006. An evolving view of the eukaryotic oligosaccharyltransferase. *Glycobiology*. 16:47R-62R.

Kim, H.J., J.R. Schleiffarth, J. Jessurun, S. Sumanas, A. Petryk, S. Lin, and S.C. Ekker. 2005. Wnt5 signaling in vertebrate pancreas development. *BMC Biol*. 3:23.

Kim, S.E., H. Huang, M. Zhao, X. Zhang, A. Zhang, M.V. Semonov, B.T. MacDonald, X. Zhang, J. Garcia Abreu, L. Peng, and X. He. 2013. Wnt stabilization of beta-catenin reveals principles for morphogen receptor-scaffold assemblies. *Science*. 340:867-870.

Kinoshita, T., Y. Maeda, and M. Fujita. 2013. Transport of glycosylphosphatidylinositol-anchored proteins from the endoplasmic reticulum. *Biochim Biophys Acta*. 1833:2473-2478.

Kirchhausen, T., and S.C. Harrison. 1981. Protein organization in clathrin trimers. *Cell*. 23:755-761.

Koles, K., J. Nunnari, C. Korkut, R. Barria, C. Brewer, Y. Li, J. Leszyk, B. Zhang, and V. Budnik. 2012. Mechanism of evenness interrupted (Evi)-exosome release at synaptic boutons. *J Biol Chem*. 287:16820-16834.

Komekado, H., H. Yamamoto, T. Chiba, and A. Kikuchi. 2007. Glycosylation and palmitoylation of Wnt-3a are coupled to produce an active form of Wnt-3a. *Genes Cells*. 12:521-534.

Koo, B.K., D.E. Stange, T. Sato, W. Karthaus, H.F. Farin, M. Huch, J.H. van Es, and H. Clevers. 2012. Controlled gene expression in primary Lgr5 organoid cultures. *Nat Methods*. 9:81-83.

Korkut, C., B. Ataman, P. Ramachandran, J. Ashley, R. Barria, N. Gherbesi, and V. Budnik. 2009. Trans-synaptic transmission of vesicular Wnt signals through Evi/Wntless. *Cell*. 139:393-404.

Kroschewski, R., A. Hall, and I. Mellman. 1999. Cdc42 controls secretory and endocytic transport to the basolateral plasma membrane of MDCK cells. *Nat Cell Biol*. 1:8-13.

Kuehn, M.J., J.M. Herrmann, and R. Schekman. 1998. COPII-cargo interactions direct protein sorting into ER-derived transport vesicles. *Nature*. 391:187-190.

Kuhl, M., L.C. Sheldahl, C.C. Malbon, and R.T. Moon. 2000a. Ca(2+)/calmodulin-dependent protein kinase II is stimulated by Wnt and Frizzled homologs and promotes ventral cell fates in Xenopus. *J Biol Chem*. 275:12701-12711.

Kuhl, M., L.C. Sheldahl, M. Park, J.R. Miller, and R.T. Moon. 2000b. The Wnt/Ca2+ pathway: a new vertebrate Wnt signaling pathway takes shape. *Trends Genet*. 16:279-283.

Kurayoshi, M., H. Yamamoto, S. Izumi, and A. Kikuchi. 2007. Post-translational palmitoylation and glycosylation of Wnt-5a are necessary for its signalling. *Biochem J*. 402:515-523.

Lapebie, P., C. Borchiellini, and E. Houliston. 2011. Dissecting the PCP pathway: one or more pathways?: Does a separate Wnt-Fz-Rho pathway drive morphogenesis? *Bioessays*. 33:759-768.

Lee, M.C., L. Orci, S. Hamamoto, E. Futai, M. Ravazzola, and R. Schekman. 2005. Sar1p N-terminal helix initiates membrane curvature and completes the fission of a COPII vesicle. *Cell*. 122:605-617.

Lewalter, K., and V. Muller. 2006. Bioenergetics of archaea: ancient energy conserving mechanisms developed in the early history of life. *Biochim Biophys Acta*. 1757:437-445.

Li, B., C. Wachtel, E. Miriami, G. Yahalom, G. Friedlander, G. Sharon, R. Sperling, and J. Sperling. 2002. Stop codons affect 5' splice site selection by surveillance of splicing. *Proc Natl Acad Sci U S A*. 99:5277-5282.

Li, C., H. Chen, L. Hu, Y. Xing, T. Sasaki, M.F. Villosis, J. Li, M. Nishita, Y. Minami, and P. Minoo. 2008. Ror2 modulates the canonical Wnt signaling in lung epithelial cells through cooperation with Fzd2. *BMC Mol Biol*. 9:11.

Li, Q., J. Wang, Y. Wan, and D. Chen. 2016. Depletion of Rab32 decreases intracellular lipid accumulation and induces lipolysis through enhancing ATGL expression in hepatocytes. *Biochem Biophys Res Commun*. 471:492-496.

Li, X., Y. Wu, C. Shen, T.Y. Belenkaya, L. Ray, and X. Lin. 2015. Drosophila p24 and Sec22 regulate Wingless trafficking in the early secretory pathway. *Biochem Biophys Res Commun*. 463:483-489.

Lim, W.H., B. Liu, D. Cheng, D.J. Hunter, Z. Zhong, D.M. Ramos, B.O. Williams, P.T. Sharpe, C. Bardet, S.J. Mah, and J.A. Helms. 2014a. Wnt signaling regulates pulp volume and dentin thickness. *J Bone Miner Res*.

29:892-901.

Lim, W.H., B. Liu, D. Cheng, B.O. Williams, S.J. Mah, and J.A. Helms. 2014b. Wnt signaling regulates homeostasis of the periodontal ligament. *J Periodontal Res*. 49:751-759.

Lim, W.H., B. Liu, D.J. Hunter, D. Cheng, S.J. Mah, and J.A. Helms. 2014c. Downregulation of Wnt causes root resorption. *Am J Orthod Dentofacial Orthop*. 146:337-345.

Liu, J., S. Pan, M.H. Hsieh, N. Ng, F. Sun, T. Wang, S. Kasibhatla, A.G. Schuller, A.G. Li, D. Cheng, J. Li, C. Tompkins, A. Pferdekamper, A. Steffy, J. Cheng, C. Kowal, V. Phung, G. Guo, Y. Wang, M.P. Graham, S. Flynn, J.C. Brenner, C. Li, M.C. Villarroel, P.G. Schultz, X. Wu, P. McNamara, W.R. Sellers, L. Petruzzelli, A.L. Boral, H.M. Seidel, M.E. McLaughlin, J. Che, T.E. Carey, G. Vanasse, and J.L. Harris. 2013. Targeting Wnt-driven cancer through the inhibition of Porcupine by LGK974. *Proc Natl Acad Sci U S A*. 110:20224-20229.

Liu, M., Z. Feng, H. Ke, Y. Liu, T. Sun, J. Dai, W. Cui, and J.C. Pastor-Pareja. 2017. Tango1 spatially organizes ER exit sites to control ER export. *J Cell Biol*. 216:1035-1049.

Ljubicic, S., P. Bezzi, S. Brajkovic, V. Nesca, C. Guay, N. Ohbayashi, M. Fukuda, A. Abderrhamani, and R. Regazzi. 2013. The GTPase Rab37 Participates in the Control of Insulin Exocytosis. *PLoS One*. 8:e68255.

Logan, C.Y., and R. Nusse. 2004. The Wnt signaling pathway in development and disease. *Annu Rev Cell Dev Biol*. 20:781-810.

Luga, V., L. Zhang, A.M. Viloria-Petit, A.A. Ogunjimi, M.R. Inanlou, E. Chiu, M. Buchanan, A.N. Hosein, M. Basik, and J.L. Wrana. 2012. Exosomes mediate stromal mobilization of autocrine Wnt-PCP signaling in breast cancer cell migration. *Cell*. 151:1542-1556.

MacDonald, B.T., A. Hien, X. Zhang, O. Iranloye, D.M. Virshup, M.L. Waterman, and X. He. 2014. Disulfide bond requirements for active Wnt ligands. *J Biol Chem*. 289:18122-18136.

MacDonald, B.T., K. Tamai, and X. He. 2009. Wnt/beta-catenin signaling: components, mechanisms, and diseases. *Dev Cell*. 17:9-26.

Madan, B., Z. Ke, N. Harmston, S.Y. Ho, A.O. Frois, J. Alam, D.A. Jeyaraj, V. Pendharkar, K. Ghosh, I.H. Virshup, V. Manoharan, E.H. Ong, K. Sangthongpitag, J. Hill, E. Petretto, T.H. Keller, M.A. Lee, A. Matter, and D.M. Virshup. 2016. Wnt addiction of genetically defined cancers reversed by PORCN inhibition. *Oncogene*. 35:2197-2207.

Maldonado-Baez, L., and J.G. Donaldson. 2013. Hook1, microtubules, and Rab22: mediators of selective sorting of clathrin-independent endocytic cargo proteins on endosomes. *Bioarchitecture*. 3:141-146.

Martin, S., K. Driessen, S.J. Nixon, M. Zerial, and R.G. Parton. 2005. Regulated localization of Rab18 to lipid droplets: effects of lipolytic stimulation and inhibition of lipid droplet catabolism. *J Biol Chem*. 280:42325-42335.

Martinez, O., A. Schmidt, J. Salamero, B. Hoflack, M. Roa, and B. Goud. 1994. The small GTP-binding protein rab6 functions in intra-Golgi transport. *J Cell Biol*. 127:1575-1588.

McCrea, P.D., C.W. Turck, and B. Gumbiner. 1991. A homolog of the armadillo protein in Drosophila (plakoglobin) associated with E-cadherin. *Science*. 254:1359-1361.

McMahon, A.P., and A. Bradley. 1990. The Wnt-1 (int-1) proto-oncogene is required for development of a large region of the mouse brain. *Cell*. 62:1073-1085.

McMahon, C., S.M. Studer, C. Clendinen, G.P. Dann, P.D. Jeffrey, and F.M. Hughson. 2012. The structure of Sec12 implicates potassium ion coordination in Sar1 activation. *J Biol Chem*. 287:43599-43606.

Miller, E.A., T.H. Beilharz, P.N. Malkus, M.C. Lee, S. Hamamoto, L. Orci, and R. Schekman. 2003. Multiple cargo binding sites on the COPII subunit Sec24p ensure capture of diverse membrane proteins into transport vesicles. *Cell*. 114:497-509.

Miranda, M., L.M. Galli, M. Enriquez, L.A. Szabo, X. Gao, R.N. Hannoush, and L.W. Burrus. 2014. Identification of the WNT1 residues required for palmitoylation by Porcupine. *FEBS Lett*. 588:4815-4824.

Miriami, E., U. Motro, J. Sperling, and R. Sperling. 2002. Conservation of an open-reading frame as an element affecting 5' splice site selection. *J Struct Biol*. 140:116-122.

Molenaar, M., M. van de Wetering, M. Oosterwegel, J. Peterson-Maduro, S. Godsave, V. Korinek, J. Roose, O. Destree, and H. Clevers. 1996. XTcf-3 transcription factor mediates beta-catenin-induced axis formation in Xenopus embryos. *Cell*. 86:391-399.

Montegna, E.A., M. Bhave, Y. Liu, D. Bhattacharyya, and B.S. Glick. 2012. Sec12 binds to Sec16 at transitional ER sites. *PLoS One*. 7:e31156.

Myung, P.S., M. Takeo, M. Ito, and R.P. Atit. 2013. Epithelial Wnt ligand secretion is required for adult hair follicle growth and regeneration. *J Invest Dermatol*. 133:31-41.

Nagae, M., T. Hirata, K. Morita-Matsumoto, R. Theiler, M. Fujita, T. Kinoshita, and Y. Yamaguchi. 2016. 3D Structure and Interaction of p24beta and p24delta Golgi Dynamics Domains: Implication for p24 Complex Formation and Cargo Transport. *J Mol Biol*. 428:4087-4099.

Nakano, A., and M. Muramatsu. 1989. A novel GTP-binding protein, Sar1p, is involved in transport from the endoplasmic reticulum to the Golgi apparatus. *J Cell Biol*. 109:2677-2691.

Neer, E.J., C.J. Schmidt, R. Nambudripad, and T.F. Smith. 1994. The ancient regulatory-protein family of WD-repeat proteins. *Nature*. 371:297-300.

Neutra, M.R., A. Ciechanover, L.S. Owen, and H.F. Lodish. 1985. Intracellular transport of transferrin- and asialoorosomucoid-colloidal gold conjugates to lysosomes after receptor-mediated endocytosis. *J Histochem Cytochem*. 33:1134-1144.

Nevo, Y., E. Kamhi, J. Jacob-Hirsch, N. Amariglio, G. Rechavi, J. Sperling, and R. Sperling. 2012. Genome-wide activation of latent donor splice sites in stress and disease. *Nucleic Acids Res*. 40:10980-10994.

Ni, X., M. Canuel, and C.R. Morales. 2006. The sorting and trafficking of lysosomal proteins. *Histol Histopathol*. 21:899-913.

Niehrs, C. 2012. The complex world of WNT receptor signalling. *Nat Rev Mol Cell Biol*. 13:767-779.

Nishikawa, S., and A. Nakano. 1993. Identification of a gene required for membrane protein retention in the early secretory pathway. *Proc Natl Acad Sci U S A*. 90:8179-8183.

Nishisho, I., Y. Nakamura, Y. Miyoshi, Y. Miki, H. Ando, A. Horii, K. Koyama, J. Utsunomiya, S. Baba, and P. Hedge. 1991. Mutations of chromosome 5q21 genes in FAP and colorectal cancer patients. *Science*. 253:665-669.

Niu, L.J., R.X. Xu, P. Zhang, M.X. Du, and X.D. Jiang. 2012. Suppression of Frizzled-2-mediated Wnt/Ca(2)(+) signaling significantly attenuates intracellular calcium accumulation in vitro and in a rat model of traumatic brain injury. *Neuroscience*. 213:19-28.

Nolan, C.M., and W.S. Sly. 1987. Intracellular traffic of the mannose 6-phosphate receptor and its ligands. *Adv Exp Med Biol*. 225:199-212.

Nusse, R., A. Brown, J. Papkoff, P. Scambler, G. Shackleford, A. McMahon, R. Moon, and H. Varmus. 1991. A new nomenclature for int-1 and related genes: the Wnt gene family. *Cell*. 64:231.

Nusse, R., A. van Ooyen, D. Cox, Y.K. Fung, and H. Varmus. 1984. Mode of proviral activation of a putative mammary oncogene (int-1) on mouse chromosome 15. *Nature*. 307:131-136.

Nusse, R., and H.E. Varmus. 1992. Wnt genes. *Cell*. 69:1073-1087.

Okamoto, C.T., R. Li, Z. Zhang, Y.Y. Jeng, and C.S. Chew. 2002. Regulation of protein and vesicle trafficking at the apical membrane of epithelial cells. *J Control Release*. 78:35-41.

Pagano, A., F. Letourneur, D. Garcia-Estefania, J.L. Carpentier, L. Orci, and J.P. Paccaud. 1999. Sec24 proteins and sorting at the endoplasmic reticulum. *J Biol Chem*. 274:7833-7840.

Pan, C.L., P.D. Baum, M. Gu, E.M. Jorgensen, S.G. Clark, and G. Garriga. 2008. C. elegans AP-2 and retromer control Wnt signaling by regulating mig-14/Wntless. *Developmental cell*. 14:132-139.

Park, M., A.S. Serpinskaya, N. Papalopulu, and V.I. Gelfand. 2007. Rab32 regulates melanosome transport in Xenopus melanophores by protein kinase a recruitment. *Curr Biol*. 17:2030-2034.

Patrussi, L., and C.T. Baldari. 2016. The Rab GTPase Rab8 as a shared regulator of ciliogenesis and immune synapse assembly: From a conserved pathway to diverse cellular structures. *Small GTPases*. 7:16-20.

Peifer, M., C. Rauskolb, M. Williams, B. Riggleman, and E. Wieschaus. 1991. The segment polarity gene armadillo interacts with the wingless signaling pathway in both embryonic and adult pattern formation. *Development*. 111:1029-1043.

Penton, A., A. Wodarz, and R. Nusse. 2002. A mutational analysis of dishevelled in Drosophila defines novel domains in the dishevelled protein as well as novel suppressing alleles of axin. *Genetics*. 161:747-762.

Pfeiffer, S., S. Ricardo, J.B. Manneville, C. Alexandre, and J.P. Vincent. 2002. Producing cells retain and recycle Wingless in Drosophila embryos. *Curr Biol*. 12:957-962.

Piao, H., J. Kim, S.H. Noh, H.S. Kweon, J.Y. Kim, and M.G. Lee. 2017. Sec16A is critical for both conventional and unconventional secretion of CFTR. *Sci Rep*. 7:39887.

Pind, S.N., C. Nuoffer, J.M. McCaffery, H. Plutner, H.W. Davidson, M.G. Farquhar, and W.E. Balch. 1994. Rab1 and Ca2+ are required for the fusion of carrier vesicles mediating endoplasmic reticulum to Golgi transport. *J Cell Biol*. 125:239-252.

Port, F., and K. Basler. 2010. Wnt trafficking: new insights into Wnt maturation, secretion and spreading. *Traffic*. 11:1265-1271.

Port, F., G. Hausmann, and K. Basler. 2011. A genome-wide RNA interference screen uncovers two p24 proteins as regulators of Wingless secretion. *EMBO Rep*. 12:1144-1152.

Port, F., M. Kuster, P. Herr, E. Furger, C. Banziger, G. Hausmann, and K. Basler. 2008. Wingless secretion promotes and requires retromer-dependent cycling of Wntless. *Nat Cell Biol*. 10:178-185.

Proffitt, K.D., B. Madan, Z. Ke, V. Pendharkar, L. Ding, M.A. Lee, R.N. Hannoush, and D.M. Virshup. 2013. Pharmacological inhibition of the Wnt acyltransferase PORCN prevents growth of WNT-driven mammary cancer. *Cancer Res*. 73:502-507.

Puertollano, R., P.A. Randazzo, J.F. Presley, L.M. Hartnell, and J.S. Bonifacino. 2001. The GGAs promote ARF-dependent recruitment of clathrin to the TGN. *Cell*. 105:93-102.

Qiu, W., L. Chen, and M. Kassem. 2011. Activation of non-canonical Wnt/JNK pathway by Wnt3a is associated with differentiation fate determination of human bone marrow stromal (mesenchymal) stem cells. *Biochem Biophys Res Commun*. 413:98-104.

Reed, S.C. 1937. The Inheritance and Expression of Fused, a New Mutation in the House Mouse. *Genetics*. 22:1-13.

Rein, U., U. Andag, R. Duden, H.D. Schmitt, and A. Spang. 2002. ARF-GAP-mediated interaction between the ER-Golgi v-SNAREs and the COPI coat. *J Cell Biol*. 157:395-404.

Renkin, E.M. 1980. Transport of proteins by diffusion, bulk flow and vesicular mechanisms. *Physiologist*. 23:57-61.

Rios-Esteves, J., and M.D. Resh. 2013. Stearoyl CoA desaturase is required to produce active, lipid-modified Wnt proteins. *Cell Rep*. 4:1072-1081.

Rojas, R., T. van Vlijmen, G.A. Mardones, Y. Prabhu, A.L. Rojas, S. Mohammed, A.J. Heck, G. Raposo, P. van der Sluijs, and J.S. Bonifacino. 2008. Regulation of retromer recruitment to endosomes by sequential action of Rab5 and Rab7. *The Journal of cell biology*. 183:513-526.

Rojo, M., G. Emery, V. Marjomaki, A.W. McDowall, R.G. Parton, and J. Gruenberg. 2000. The transmembrane protein p23 contributes to the organization of the Golgi apparatus. *J Cell Sci*. 113 (Pt 6):1043-1057.

Saito, K., M. Chen, F. Bard, S. Chen, H. Zhou, D. Woodley, R. Polischuk, R. Schekman, and V. Malhotra. 2009. TANGO1 facilitates cargo loading at endoplasmic reticulum exit sites. *Cell*. 136:891-902.

Saito, K., K. Yamashiro, N. Shimazu, T. Tanabe, K. Kontani, and T. Katada. 2014. Concentration of Sec12 at ER exit sites via interaction with cTAGE5 is required for collagen export. *J Cell Biol*. 206:751-762.

Sakamori, R., S. Yu, X. Zhang, A. Hoffman, J. Sun, S. Das, P. Vedula, G. Li, J. Fu, F. Walker, C.S. Yang, Z. Yi, W. Hsu, D.H. Yu, L. Shen, A.J. Rodriguez, M.M. Taketo, E.M. Bonder, M.P. Verzi, and N. Gao. 2014. CDC42 inhibition suppresses progression of incipient intestinal tumors. *Cancer Res*. 74:5480-5492.

Sannerud, R., M. Marie, C. Nizak, H.A. Dale, K. Pernet-Gallay, F. Perez, B. Goud, and J. Saraste. 2006. Rab1 defines a novel pathway connecting the pre-Golgi intermediate compartment with the cell periphery. *Mol Biol Cell*. 17:1514-1526.

Sato, A., D.K. Khadka, W. Liu, R. Bharti, L.W. Runnels, I.B. Dawid, and R. Habas. 2006. Profilin is an effector for Daam1 in non-canonical Wnt signaling and is required for vertebrate gastrulation. *Development*. 133:4219-4231.

Sato, K., and A. Nakano. 2005. Dissection of COPII subunit-cargo assembly and disassembly kinetics during Sar1p-GTP hydrolysis. *Nat Struct Mol Biol*. 12:167-174.

Sato, T., S. Mushiake, Y. Kato, K. Sato, M. Sato, N. Takeda, K. Ozono, K. Miki, Y. Kubo, A. Tsuji, R. Harada, and A. Harada. 2007. The Rab8 GTPase regulates apical protein localization in intestinal cells. *Nature*. 448:366-369.

Sato, T., J.H. van Es, H.J. Snippert, D.E. Stange, R.G. Vries, M. van den Born, N.

Barker, N.F. Shroyer, M. van de Wetering, and H. Clevers. 2011. Paneth cells constitute the niche for Lgr5 stem cells in intestinal crypts. *Nature*. 469:415-418.

Sato, T., R.G. Vries, H.J. Snippert, M. van de Wetering, N. Barker, D.E. Stange, J.H. van Es, A. Abo, P. Kujala, P.J. Peters, and H. Clevers. 2009. Single Lgr5 stem cells build crypt-villus structures in vitro without a mesenchymal niche. *Nature*. 459:262-265.

Schluter, O.M., M. Khvotchev, R. Jahn, and T.C. Sudhof. 2002. Localization versus function of Rab3 proteins. Evidence for a common regulatory role in controlling fusion. *J Biol Chem*. 277:40919-40929.

Schweizer, A., J.A. Fransen, T. Bachi, L. Ginsel, and H.P. Hauri. 1988. Identification, by a monoclonal antibody, of a 53-kD protein associated with a tubulo-vesicular compartment at the cis-side of the Golgi apparatus. *J Cell Biol*. 107:1643-1653.

Segev, N. 2009. Trafficking inside cells : pathways, mechanisms, and regulation. Landes Bioscience ;

Springer Science+Business Media, Austin, Tex.

New York, N.Y. 445 p. pp.

Shindiapina, P., and C. Barlowe. 2010. Requirements for transitional endoplasmic reticulum site structure and function in Saccharomyces cerevisiae. *Mol Biol Cell*. 21:1530-1545.

Shojaie, N., and S.M. Ghaffari. 2016. Simultaneous Analysis of Wnt and NF-kappaB Signaling Pathways in Doxorubicin Sensitive and Methotrexate Resistant PLC/ PRF/5 Cells. *Cell J*. 17:730-739.

Si, W., Q. Kang, H.H. Luu, J.K. Park, Q. Luo, W.X. Song, W. Jiang, X. Luo, X. Li, H. Yin, A.G. Montag, R.C. Haydon, and T.C. He. 2006. CCN1/Cyr61 is regulated by the canonical Wnt signal and plays an important role in Wnt3A-induced osteoblast differentiation of mesenchymal stem cells. *Mol Cell Biol*. 26:2955-2964.

Singleton, P. 1999. Bacteria in biology, biotechnology, and medicine. John Wiley, Chichester ; New York.

Skehel, P.A., R. Fabian-Fine, and E.R. Kandel. 2000. Mouse VAP33 is associated with the endoplasmic reticulum and microtubules. *Proc Natl Acad Sci U S A*. 97:1101-1106.

Soderholm, J., D. Bhattacharyya, D. Strongin, V. Markovitz, P.L. Connerly, C.A. Reinke, and B.S. Glick. 2004. The transitional ER localization mechanism of Pichia pastoris Sec12. *Dev Cell*. 6:649-659.

Sohda, M., Y. Misumi, A. Yamamoto, A. Yano, N. Nakamura, and Y. Ikehara. 2001. Identification and characterization of a novel Golgi protein, GCP60, that interacts with the integral membrane protein giantin. *J Biol Chem*. 276:45298-45306.

Sohn, K., L. Orci, M. Ravazzola, M. Amherdt, M. Bremser, F. Lottspeich, K. Fiedler, J.B. Helms, and F.T. Wieland. 1996. A major transmembrane protein of Golgi-derived COPI-coated vesicles involved in coatomer binding. *J Cell Biol*. 135:1239-1248.

Stamnes, M.A., M.W. Craighead, M.H. Hoe, N. Lampen, S. Geromanos, P. Tempst, and J.E. Rothman. 1995. An integral membrane component of coatomer-coated transport vesicles defines a family of proteins involved in budding. *Proc Natl Acad Sci U S A*. 92:8011-8015.

Stenbeck, G. 1998. Soluble NSF-attachment proteins. *Int J Biochem Cell Biol*. 30:573-577.

Stenmark, H. 2009. Rab GTPases as coordinators of vesicle traffic. *Nat Rev Mol Cell Biol*. 10:513-525.

Stirnimann, C.U., E. Petsalaki, R.B. Russell, and C.W. Muller. 2010. WD40 proteins propel cellular networks. *Trends Biochem Sci*. 35:565-574.

Stoorvogel, W., M.J. Kleijmeer, H.J. Geuze, and G. Raposo. 2002. The biogenesis and functions of exosomes. *Traffic*. 3:321-330.

Strating, J.R., and G.J. Martens. 2009. The p24 family and selective transport processes at the ER-Golgi interface. *Biol Cell*. 101:495-509.

Sun, J., S. Yu, X. Zhang, C. Capac, O. Aligbe, T. Daudelin, E.M. Bonder, and N. Gao. 2017a. Wntless-Sec12 complex on ER membrane regulates early Wnt secretory vesicle assembly and mature ligand export. *J Cell Sci*.

Sun, J., S. Yu, X. Zhang, C. Capac, O. Aligbe, T. Daudelin, E.M. Bonder, and N. Gao. 2017b. A Wntless-SEC12 complex on the ER membrane regulates early Wnt secretory vesicle assembly and mature ligand export. *J Cell Sci*. 130:2159-2171.

Takada, R., Y. Satomi, T. Kurata, N. Ueno, S. Norioka, H. Kondoh, T. Takao, and S. Takada. 2006. Monounsaturated fatty acid modification of Wnt protein: its role in Wnt secretion. *Dev Cell*. 11:791-801.

Tanabe, T., M. Maeda, K. Saito, and T. Katada. 2016. Dual function of cTAGE5 in collagen export from the endoplasmic reticulum. *Mol Biol Cell*. 27:2008-2013.

Tanaka, K., K. Okabayashi, M. Asashima, N. Perrimon, and T. Kadowaki. 2000. The evolutionarily conserved porcupine gene family is involved in the processing of the Wnt family. *Eur J Biochem*. 267:4300-4311.

Thomas, K.R., and M.R. Capecchi. 1990. Targeted disruption of the murine int-1 proto-oncogene resulting in severe abnormalities in midbrain and cerebellar development. *Nature*. 346:847-850.

Tian, X., R.U. Jin, A.J. Bredemeyer, E.J. Oates, K.M. Blazewska, C.E. McKenna, and J.C. Mills. 2010. RAB26 and RAB3D are direct transcriptional targets of MIST1 that regulate exocrine granule maturation. *Mol Cell Biol*. 30:1269-1284.

Tisdale, E.J., and W.E. Balch. 1996. Rab2 is essential for the maturation of pre-Golgi intermediates. *J Biol Chem*. 271:29372-29379.

Tooze, S.A. 1998. Biogenesis of secretory granules in the trans-Golgi network of neuroendocrine and endocrine cells. *Biochim Biophys Acta*. 1404:231-244.

Touchot, N., P. Chardin, and A. Tavitian. 1987. Four additional members of the ras gene superfamily isolated by an oligonucleotide strategy: molecular cloning of YPT-related cDNAs from a rat brain library. *Proc Natl Acad Sci U S A*. 84:8210-8214.

Traub, L.M., S. Kornfeld, and E. Ungewickell. 1995. Different domains of the AP-1 adaptor complex are required for Golgi membrane binding and clathrin recruitment. *J Biol Chem*. 270:4933-4942.

Valenta, T., B. Degirmenci, A.E. Moor, P. Herr, D. Zimmerli, M.B. Moor, G. Hausmann, C. Cantu, M. Aguet, and K. Basler. 2016. Wnt Ligands Secreted by Subepithelial Mesenchymal Cells Are Essential for the Survival of Intestinal Stem Cells and Gut Homeostasis. *Cell Rep*. 15:911-918.

van Amerongen, R., C. Fuerer, M. Mizutani, and R. Nusse. 2012. Wnt5a can both activate and repress Wnt/beta-catenin signaling during mouse embryonic development. *Dev Biol*. 369:101-114.

van den Heuvel, M., C. Harryman-Samos, J. Klingensmith, N. Perrimon, and R. Nusse. 1993. Mutations in the segment polarity genes wingless and porcupine impair secretion of the wingless protein. *EMBO J*. 12:5293-5302.

Voloshanenko, O., G. Erdmann, T.D. Dubash, I. Augustin, M. Metzig, G. Moffa, C. Hundsrucker, G. Kerr, T. Sandmann, B. Anchang, K. Demir, C. Boehm, S. Leible, C.R. Ball, H. Glimm, R. Spang, and M. Boutros. 2013. Wnt secretion is required to maintain high levels of Wnt activity in colon cancer cells. *Nat Commun*. 4:2610.

Vyas, N., A. Walvekar, D. Tate, V. Lakshmanan, D. Bansal, A. Lo Cicero, G. Raposo, D. Palakodeti, and J. Dhawan. 2014. Vertebrate Hedgehog is secreted on two types of extracellular vesicles with different signaling properties. *Sci Rep*. 4:7357.

Wang, C., Z. Liu, and X. Huang. 2012. Rab32 is important for autophagy and lipid storage in Drosophila. *PLoS One*. 7:e32086.

Wang, C.W., and D.J. Klionsky. 2003. The molecular mechanism of autophagy. *Mol Med*. 9:65-76.

Wang, X., V. Reid Sutton, J. Omar Peraza-Llanes, Z. Yu, R. Rosetta, Y.C. Kou, T.N. Eble, A. Patel, C. Thaller, P. Fang, and I.B. Van den Veyver. 2007. Mutations in X-linked PORCN, a putative regulator of Wnt signaling, cause focal dermal hypoplasia. *Nat Genet*. 39:836-838.

Wang, Y., Y.P. Li, C. Paulson, J.Z. Shao, X. Zhang, M. Wu, and W. Chen. 2014. Wnt and the Wnt signaling pathway in bone development and disease.

Front Biosci (Landmark Ed). 19:379-407.

Wang, Z., and C.B. Burge. 2008. Splicing regulation: from a parts list of regulatory elements to an integrated splicing code. *RNA*. 14:802-813.

Wang, Z.H., C. Rabouille, and E.R. Geisbrecht. 2015. Loss of a Clueless-dGRASP complex results in ER stress and blocks Integrin exit from the perinuclear endoplasmic reticulum in Drosophila larval muscle. *Biol Open*. 4:636-648.

Watson, P., A.K. Townley, P. Koka, K.J. Palmer, and D.J. Stephens. 2006. Sec16 defines endoplasmic reticulum exit sites and is required for secretory cargo export in mammalian cells. *Traffic*. 7:1678-1687.

Wendeler, M.W., J.P. Paccaud, and H.P. Hauri. 2007. Role of Sec24 isoforms in selective export of membrane proteins from the endoplasmic reticulum. *EMBO Rep*. 8:258-264.

White, J., L. Johannes, F. Mallard, A. Girod, S. Grill, S. Reinsch, P. Keller, B. Tzschaschel, A. Echard, B. Goud, and E.H. Stelzer. 1999. Rab6 coordinates a novel Golgi to ER retrograde transport pathway in live cells. *J Cell Biol*. 147:743-760.

Wikramanayake, A.H., R. Peterson, J. Chen, L. Huang, J.M. Bince, D.R. McClay, and W.H. Klein. 2004. Nuclear beta-catenin-dependent Wnt8 signaling in vegetal cells of the early sea urchin embryo regulates gastrulation and differentiation of endoderm and mesodermal cell lineages. *Genesis*. 39:194-205.

Wilhelmi, I., R. Kanski, A. Neumann, O. Herdt, F. Hoff, R. Jacob, M. Preussner, and F. Heyd. 2016. Sec16 alternative splicing dynamically controls COPII transport efficiency. *Nat Commun*. 7:12347.

Willert, K., J.D. Brown, E. Danenberg, A.W. Duncan, I.L. Weissman, T. Reya, J.R. Yates, 3rd, and R. Nusse. 2003. Wnt proteins are lipid-modified and can act as stem cell growth factors. *Nature*. 423:448-452.

Williams, B.O., and K.L. Insogna. 2009. Where Wnts went: the exploding field of Lrp5 and Lrp6 signaling in bone. *J Bone Miner Res*. 24:171-178.

Winslow, M.M., M. Pan, M. Starbuck, E.M. Gallo, L. Deng, G. Karsenty, and G.R. Crabtree. 2006. Calcineurin/NFAT signaling in osteoblasts regulates bone mass. *Dev Cell*. 10:771-782.

Wu, G. 2012. Regulation of post-Golgi traffic of G protein-coupled receptors. *Subcell Biochem*. 63:83-95.

Yamamoto, K., R. Fujii, Y. Toyofuku, T. Saito, H. Koseki, V.W. Hsu, and T. Aoe. 2001. The KDEL receptor mediates a retrieval mechanism that contributes to quality control at the endoplasmic reticulum. *EMBO J*. 20:3082-3091.

Yang, P.T., M.J. Lorenowicz, M. Silhankova, D.Y. Coudreuse, M.C. Betist, and H.C. Korswagen. 2008. Wnt signaling requires retromer-dependent recycling of MIG-14/Wntless in Wnt-producing cells. *Developmental cell*. 14:140-147.

Yeung, J., and D. Goldowitz. 2017. Wls expression in the rhombic lip orchestrates the embryonic development of the mouse cerebellum. *Neuroscience*. 354:30-42.

Yeung, J., T.J. Ha, D.J. Swanson, K. Choi, Y. Tong, and D. Goldowitz. 2014. Wls provides a new compartmental view of the rhombic lip in mouse cerebellar development. *J Neurosci*. 34:12527-12537.

Yin, X., J. Li, B. Salmon, L. Huang, W.H. Lim, B. Liu, D.J. Hunter, R.C. Ransom, G. Singh, M. Gillette, S. Zou, and J.A. Helms. 2015. Wnt Signaling and Its Contribution to Craniofacial Tissue Homeostasis. *J Dent Res*. 94:1487-1494.

Yla-Anttila, P., E. Mikkonen, K.E. Happonen, P. Holland, T. Ueno, A. Simonsen, and E.L. Eskelinen. 2015. RAB24 facilitates clearance of autophagic compartments during basal conditions. *Autophagy*. 11:1833-1848.

Yoshihisa, T., C. Barlowe, and R. Schekman. 1993. Requirement for a GTPase-activating protein in vesicle budding from the endoplasmic reticulum. *Science*. 259:1466-1468.

Yu, H.M., Y. Jin, J. Fu, and W. Hsu. 2010. Expression of Gpr177, a Wnt trafficking regulator, in mouse embryogenesis. *Dev Dyn*. 239:2102-2109.

Yu, J., J. Chia, C.A. Canning, C.M. Jones, F.A. Bard, and D.M. Virshup. 2014. WLS retrograde transport to the endoplasmic reticulum during Wnt secretion. *Dev Cell*. 29:277-291.

Zanetti, G., K.B. Pahuja, S. Studer, S. Shim, and R. Schekman. 2012. COPII and the regulation of protein sorting in mammals. *Nat Cell Biol*. 14:20-28.

Zhang, P., L. Zhou, C. Pei, X. Lin, and Z. Yuan. 2016. Dysfunction of Wntless triggers the retrograde Golgi-to-ER transport of Wingless and induces ER stress. *Sci Rep*. 6:19418.

Zhang, Y., C. Tu, D. Zhang, Y. Zheng, Z. Peng, Y. Feng, S. Xiao, and Z. Li. 2015. Wnt/beta-Catenin and Wnt5a/Ca Pathways Regulate Proliferation and Apoptosis of Keratinocytes in Psoriasis Lesions. *Cell Physiol Biochem*. 36:1890-1902.

Zhu, X., H. Zhu, L. Zhang, S. Huang, J. Cao, G. Ma, G. Feng, L. He, Y. Yang, and X. Guo. 2012. Wls-mediated Wnts differentially regulate distal limb patterning and tissue morphogenesis. *Dev Biol*. 365:328-338.

Zhuang, X., S. Chowdhury, J.K. Northup, and K. Ray. 2010. Sar1-dependent trafficking of the human calcium receptor to the cell surface. *Biochem Biophys Res Commun*. 396:874-880.